NASA Technical Memorandum 84513

Supercritical Maneuvering Fighter Configuration

Wind-Tunnel Investigation at Mach Numbers of 0.60 to 0.95

Michael J. Mann, Charles E. Mercer,
and Richard L. Campbell
Langley Research Center
Hampton, Virginia

NASA
National Aeronautics
and Space Administration
Scientific and Technical
Information Branch
1982

SUMMARY

A wind-tunnel investigation has been conducted to study the application of supercritical technology to highly maneuverable combat aircraft. The configuration studied has a leading-edge sweep of 45° and an aspect ratio of 3.28. Two supercritical-wing shapes were tested at Mach numbers from 0.60 to 0.95 with angles of attack from -2° to 17°. One supercritical wing was designed to achieve a high level of transonic maneuver performance at a Mach number of 0.90; however, excessive flow separation developed on this wing at a Mach number of 0.85. A second supercritical wing was tested which had significantly reduced flow separation and improved drag characteristics at a Mach number of 0.85 and maintained the performance of the original wing at the higher Mach numbers. Leading-edge vortex generators did not improve the performance of the second wing; however, a sharp leading-edge flap produced sizable drag reductions at Mach numbers from 0.60 to 0.90.

INTRODUCTION

Extensive research is currently underway at the NASA Langley Research Center to improve the maneuver capability of fighter aircraft. Two general types of wings are included in this research. One type includes the slender wings which provide high levels of supersonic performance and which utilize the high levels of vortex lift available to provide subsonic and transonic maneuver capability. Research on the maneuver performance of slender-wing aircraft includes the development of design concepts for reducing drag by the effective recovery of the leading-edge thrust (ref. 1). The other general type of wing under study is the higher-aspect-ratio, moderately swept wing based on a compromise between optimum subsonic and supersonic performance. These wings require the development of large areas of supercritical flow with minimum shock-induced separation effects in order to achieve good transonic maneuver performance.

The purpose of this paper is to investigate the level of performance that might be achieved for the second type of wing by utilizing the design procedures of reference 2. Supercritical technology has been applied in an effort to reduce the shock-induced flow separation at transonic maneuver conditions. Recognizing that significant flow separation eventually will develop at the higher lift coefficients, the attached-flow design has been supplemented with leading-edge devices. The devices studied were an underwing or pylon-type vortex generator (VG) and a sharp leading-edge flap (SLEF).

The current study has focused solely on the warped wing geometry required at maneuver conditions. It is recognized, of course, that some form of variable geometry would be required to provide the desired maneuver and the cruise wing shapes. This type of variable geometry has not been addressed in this study.

This report presents experimental results on a supercritical maneuvering fighter which has been tested with two supercritical-wing configurations and leading-edge devices. The tests were conducted in the Langley 16-Foot Transonic Tunnel at Mach numbers of 0.60 to 0.95 and for lift coefficients up to about one. Additional

information relative to these tests is presented in a "Supplement to NASA Technical Memorandum 84513," which is available upon request.[1]

SYMBOLS AND ABBREVIATIONS

All forces and moments are referred to the wind-axis system. The moments are presented with respect to a center-of-gravity location at 50.34 percent of the mean aerodynamic chord. (See fig. 1.) Force and moment coefficients are based on the geometry of the basic trapezoidal wing extended to the model centerline. (See table I.) Dimensions are given in the International System of Units (SI) with the U.S. Customary Units in parentheses. The measurements and calculations were made in U.S. Customary Units. Symbols in parentheses are computer symbols.

b		wing span, cm (in.)
C_D		drag coefficient, $\frac{\text{Drag}}{qS}$
C_L		lift coefficient, $\frac{\text{Lift}}{qS}$
C_m		pitching-moment coefficient, $\frac{\text{Pitching moment}}{qS\bar{c}}$
C_p		pressure coefficient, $\frac{p_\ell - p}{q}$
c	(C)	local wing chord, cm (in.)
$\bar{c}$		mean aerodynamic chord, cm (in.)
	(FS)	fuselage station of local wing leading edge, measured from model nose, cm (in.)
L/D		lift-drag ratio
M		free-stream Mach number
p		free-stream static pressure, Pa (lbf/ft^2)
p_ℓ		local static pressure, Pa (lbf/ft^2)
q		free-stream dynamic pressure, Pa (lbf/ft^2)
S		wing reference area, m^2 (ft^2)
SLEF		sharp leading-edge flap
VG		vortex generator

[1]Available from the NASA Scientific and Technical Information Facility, Baltimore/Washington International Airport, Maryland 21240.

x	(X)	local distance from wing leading edge, parallel to model center-line and horizontal reference line in figure 1, cm (in.)
y		spanwise distance from plane of symmetry, cm (in.)
	(Z)	perpendicular distance from horizontal reference line in figure 1, measured parallel to plane of symmetry, cm (in.)
α		angle of attack, referenced to horizontal reference line in figure 1, deg
η	(ETA)	semispan location, y/(b/2)

Subscript:

i	internal (flow-through nacelle)

APPARATUS AND TEST

Model Description

Drawings of the wind-tunnel model are shown in figures 1 to 5. Several photographs are shown in figure 6 and the general geometric characteristics are given in table I. The configuration represents a high-performance combat aircraft with a wing leading-edge sweep of 45° and an aspect ratio of 3.28. The model is a midwing configuration with the upper surface of the wing blended into the fuselage (fig. 2). The wing root incidence is approximately 1° and there is approximately 10° of twist (washout) between the root and tip.

Two supercritical-wing configurations have been tested. The SMF-2 (supercritical maneuvering fighter) wing developed in reference 2 provides the basis for the configuration-1 wing of the current study. Configuration 1 has been designed to reduce the shock-induced flow separation at a Mach number of 0.90 for lift coefficients up to 0.86. In order to accomplish this, a target pressure distribution was selected which involves a large region of supercritical flow and a moderate shock strength. The flow expands to low pressures at the leading edge and isentropically compresses as it proceeds toward the trailing edge. The isentropic compression reduces the Mach number ahead of the shock and, therefore, reduces the shock strength.

The wing geometry of reference 2 was designed by the use of the FLO-22 transonic isolated-wing computer code (ref. 3) and, therefore, does not include the effects of the fuselage on the transonic flow. Configuration 1 of the current study includes a correction to the SMF-2 geometry of reference 2 which accounts for the fuselage effects. This correction has been made by use of the FLO-27 code which computes the transonic flow over a wing in the presence of a cylindrical fuselage (ref. 4).

The second supercritical-wing configuration of the current study was developed from configuration 1. The objectives for configuration 2 were to reduce the shock-induced flow separation and the attendant maneuver drag penalties which occurred for configuration 1, at a Mach number of 0.85 and to still maintain the performance of configuration 1 at the higher Mach numbers examined in this study. Because the wind-

tunnel model for the configuration-2 wing was to be obtained by the addition of a filler material to the upper surface of the configuration-1 wing, a restriction in the design of configuration 2 was that the new upper-surface contour lie entirely outside the old contour. The FLO-27 code and the design procedure of reference 2 were utilized to develop the configuration-2 wing geometry.

The airfoil sections for the two wing configurations are compared in figure 5. The modifications to the wind-tunnel model to obtain configuration 2 resulted in a wing with increased thickness. The maximum thickness ratio for configuration 1 varied from 8.2 percent at $\eta = 0.2$ to 5.4 percent at $\eta = 0.9$. The maximum thickness ratio for configuration 2 varied from 8.4 percent at $\eta = 0.2$ to 7.1 percent at $\eta = 0.9$, with most of the increase occurring in the outboard sections.

The geometric details and wing locations of the vortex generators (VG) are shown in figure 3. The design of the vortex generators is based on the work reported in references 5 and 6.

The sharp leading-edge flap (SLEF) is an adaptation of the vortex-flap concept of Rao (ref. 7). However, the intended purpose of the SLEF was to influence the flow over the entire chord length, in contrast to the purpose of reference 7 which was to increase the leading-edge thrust by means of a vortex situated on the flap itself. The SLEF is shown in figure 4.

Test and Corrections

The investigation was conducted in the Langley 16-Foot Transonic Tunnel. This is a continuous-flow, single-return atmospheric tunnel with a slotted, octagonal test section. A description of the tunnel is given in reference 8.

The tests were run at Mach numbers from 0.60 to 0.95 with angles of attack from -2° to 17°. The Reynolds number, based on the wing mean aerodynamic chord, varied from 2.55×10^6 at $M = 0.60$ to 3.09×10^6 at $M = 0.95$.

Boundary-layer transition strips 0.32 cm (1/8 in.) wide were applied to the model. No. 120 carborundum grains were applied 1 cm (0.4 in.) streamwise behind the leading edges of the wings and the vertical tail. No. 100 grains were applied 2.8 cm (1.1 in.) behind the nose and 1 cm (0.4 in.) behind the inlet of the nacelle (outside only).

Aerodynamic forces and moments were measured by an internal, six-component strain-gage balance. Model angle of attack was obtained by correcting the angle of the model support system for deflections of the sting and balance under aerodynamic load and for tunnel flow angularity. The force data have been corrected to a condition of free-stream static pressure over the fuselage base. The internal drag of the flow-through nacelle was measured and subtracted from the total measured drag. The values of internal drag are given in table II.

The wing was instrumented with flush-surface static presssure orifices. The orifices were distributed in streamwise rows over the upper-right and lower-left wing panels. The orifices were located at semispan stations of 0.30, 0.45, 0.80, and 0.90. All surface pressures were recorded by the use of differential-pressure-scanning valves mounted in the nose section of the model.

PRESENTATION OF RESULTS

The results of this study are presented in the following figures:

DISCUSSION OF RESULTS

The purpose of this study has been the application of supercritical technology to combat aircraft in order to improve the transonic maneuver performance and to either maintain or improve the subsonic maneuver performance. The longitudinal aerodynamic characteristics of the supercritical configurations 1 and 2 (shown in fig. 5) are compared in figure 7. Figure 10 is a comparison of selected chordwise pressure distributions at lift coefficients ranging from 0.78 to 0.97. These pressure distributions will be discussed first because they illustrate the application of the design method of reference 2 and because they help to explain the differences in drag characteristics at high lift between configurations 1 and 2.

The pressure distributions on configuration 1 at a Mach number of 0.90 (figs. 10(e) and 10(f)) generally exhibit a chordwise isentropic compression as intended. Some wing-tip separation at 14° angle of attack is indicated by the flattened pressure distribution and the loss of flow compression near the wing trailing edge. Aside from this tip separation, the flow separation appears to be primarily confined to the trailing-edge region.

As the Mach number is reduced below the design value of 0.90, however, the situation is markedly different. At a Mach number of 0.85 (see figs. 10(c) and 10(d)), configuration 1 is developing a strong shock wave which is producing extensive shock-induced flow separation. As the angle of attack is increased from 13° to 15°, the flow at the semispan locations of 0.45 and 0.90 becomes almost completely separated.

Since high levels of maneuver drag are associated with extensive regions of separated flow, configuration 2 was designed in an effort to reduce the flow separation at a Mach number of 0.85 and still maintain the lift and drag characteristics of configuration 1 at the higher Mach numbers. At a Mach number of 0.85 and a lift coefficient of 0.92 (fig. 10(c)), configuration 2 seems to have a reduced shock strength at the outboard span stations. As the lift coefficient is increased to 0.97 (fig. 10(d)), the flow separation on configuration 2 has been significantly reduced relative to the separation which occurred on configuration 1. At a Mach number of 0.90 (figs. 10(e) and 10(f)), the pressure distributions on configuration 2 do not seem to indicate very great differences from configuration 1. At a lift coefficient of 0.96, configuration 2 has less separation at the tip.

The reduced flow separation on configuration 2 at a Mach number of 0.85 has resulted in a significant improvement in the lift and drag characteristics as illustrated in figure 7. In fact, the drag at high lift for configuration 2 has been reduced well below the drag levels for configuration 1 at Mach numbers of 0.60 and 0.85. The reduced wing-tip separation on configuration 2 at a Mach number of 0.90 and a lift coefficient of 0.96 (fig. 10(f)) correlates with a drag improvement at these conditions. Configuration 2 has higher drag at the low lift coefficients. It is assumed, however, that variable geometry in the form of conventional leading- and trailing-edge flaps would improve the low lift characteristics. Figure 7(c) shows that the improvements of configuration 2 at Mach numbers of 0.60 and 0.85 occur at lift coefficients which are greater than the lift coefficients corresponding to maximum L/D.

As indicated in the Apparatus and Test section, configurations 1 and 2 have the same lower-surface coordinates. If configuration 2 had maintained the original thickness distribution, it may have been possible to have achieved additional drag benefits.

Figure 10 illustrates that configuration 2 still has significant flow separation in the tip region at the higher lift coefficients. As the angle of attack is increased, the region of separation spreads from the trailing edge forward and from the tip inboard. It does not appear that, for these higher lift coefficients, any further significant reductions in flow separation could be achieved solely through modification of the airfoil sections. It was therefore decided to supplement the supercritical-flow design (an "attached-flow" concept) with the leading-edge devices shown in figures 3 and 4. Although flow visualization techniques were not used in the present series of tests to study the exact flow mechanism of these devices, it was hoped, based on the previous work of references 5 to 7, that vortices would be produced which would reduce the drag at high lift coefficients and yet have a negligible adverse effect at low lift coefficients. Both devices were tested on configuration 2.

Figure 8 shows that the vortex generators selected for this study did not produce any significant benefits for configuration 2.

Figures 9 and 11 show the effect of the sharp leading-edge flap on configuration 2. In the Mach number range from 0.60 to 0.90, the SLEF produced sizable drag reductions at the higher lift coefficients, with some small penalty at the low lift coefficients (fig. 9(a)). Presumably, such a device could be retracted to eliminate any drag penalty at low lift coefficients. The SLEF produced somewhat higher lift coefficients at the highest angles of attack (fig. 9(b)) and caused only a slight reduction in longitudinal stability (fig. 9(c)). At $M = 0.95$ the SLEF did not improve the lift and drag characteristics within the lift range of these tests. The wing pressure distributions shown in figure 11 indicate that there is less flow separation at the lower Mach numbers with the SLEF attached. This reduced separation correlates with the improved drag characteristics for these conditions.

SUMMARY OF RESULTS

Wind-tunnel tests have been conducted to study improvements in the supercritical maneuver performance of fighter aircraft through the use of supercritical technology. The results of this study may be summarized as follows:

1. A supercritical wing has been tested which produces a region of isentropic compression ahead of the shock wave at a Mach number of 0.90 and maneuver lift coefficients. This wing produced a moderate degree of flow separation at these conditions. At speeds below the design Mach number, a strong shock wave developed and resulted in extensive shock-induced flow separation.

2. A second supercritical configuration was tested which significantly reduced the degree of flow separation and the drag at high lift for Mach numbers of 0.85 and 0.60. The higher Mach number performance of the original wing was maintained.

3. Vortex generators mounted under the wing leading edge did not improve the performance of the second wing.

4. A sharp leading-edge flap on the outboard half of the wing semispan produced significant drag reductions on the second wing at Mach numbers of 0.60 to 0.90. This flap had a very minor effect on the longitudinal stability.

Langley Research Center
National Aeronautics and Space Administration
Hampton, VA 23665
July 16, 1982

REFERENCES

1. Lamar, John E.; Schemensky, Roy T.; and Reddy, C. Subba: Development of a Vortex-Lift Design Procedure and Application to a Slender Maneuver-Wing Configuration. J. Aircr., vol. 18, no. 4, Apr. 1981, pp. 259-266. (Available as AIAA 80-0327R.)

2. Mann, Michael J.: The Design of Supercritical Wings by the Use of Three-Dimensional Transonic Theory. NASA TP-1400, 1979.

3. Jameson, Antony: Transonic Flow Calculations. Numerical Methods in Fluid Dynamics, H. J. Wirz and J. J. Smolderen, eds., Hemisphere Pub. Corp., 1978, pp. 1-87.

4. Jameson, Antony; and Caughey, D. A.: A Finite Volume Method for Transonic Potential Flow Calculations. A Collection of Technical Papers - AIAA 3rd Computational Fluid Dynamics Conference, June 1977, pp. 35-54. (Available as AIAA Paper 77-635.)

5. Johnson, Thomas D.; and Rao, Dhanvada M.: Experimental Study of Delta Wing Leading-Edge Devices for Drag Reduction at High Lift. NASA CR-165846, 1982.

6. Bartlett, Dennis W.; Harris, Charles D.; and Kelly, Thomas C.: Wind-Tunnel Development of Underwing Leading-Edge Vortex Generators on an NASA Supercritical-Wing Research Airplane Configuration. NASA TM X-2808, 1973.

7. Rao, Dhanvada M.: Leading-Edge 'Vortex Flaps' for Enhanced Subsonic Aerodynamics of Slender Wings. ICAS-80-13.5, Oct. 1980.

8. Corson, Blake W., Jr.; Runckel, Jack F.; and Igoe, William B.: Calibration of the Langley 16-Foot Transonic Tunnel With Test Section Air Removal. NASA TR R-423, 1974.

TABLE I.- GENERAL GEOMETRIC CHARACTERISTICS OF MODEL

Wing (reference trapezoid extended to centerline):	
Sweepback of leading edge, deg	45
Aspect ratio	3.28
Taper ratio	0.2142
Area, m^2 (ft^2)	0.139 (1.50)
Span, cm (in.)	67.686 (26.648)
Mean aerodynamic chord, cm (in.)	23.518 (9.259)
Wing station of mean aerodynamic chord, cm (in.)	13.272 (5.225)
Fuselage station of 25-percent wing mean aerodynamic chord, cm (in.)	52.425 (20.640)
Root chord, cm (in.)	33.993 (13.383)
Tip chord, cm (in.)	7.282 (2.867)
Dihedral, deg	0
Twist (washout from root to tip), deg	10
Incidence (root), deg	1
Vertical tail (exposed trapezoid):	
Sweepback of leading edge, deg	61
Aspect ratio	0.856
Taper ratio	0.2854
Tail area/Wing area	0.168
Span, cm (in.)	14.145 (5.569)
Root chord, cm (in.)	25.718 (10.125)
Tip chord, cm (in.)	7.341 (2.890)
Airfoil section	4% circular-arc biconvex
Vortex generator (one of four):	
Aspect ratio	0.778
Taper ratio	1
Area, cm^2 (in^2)	4.06 (0.63)
Area of two vortex generators/Wing semiarea	0.012
Span, cm (in.)	1.78 (0.70)
Root chord, cm (in.)	2.29 (0.90)
Tip chord, cm (in.)	2.29 (0.90)
Airfoil section (streamwise)	NACA 64A006
Sharp leading-edge flap (one of two):	
Flap area/Wing semiarea	0.032
Span, cm (in.)	14.892 (5.863)
Root chord, cm (in.)	1.5 (0.6)
Tip chord, cm (in.)	1.5 (0.6)
Fuselage:	
Flow-through inlet area, cm^2 (in^2)	23.020 (3.568)
Flow-through exit area, cm^2 (in^2)	18.872 (2.925)
Base/cavity area, cm^2 (in^2)	28.852 (4.472)

TABLE II.- INTERNAL DRAG CHARACTERISTICS

α, deg	$C_{D,i}$ for -				
	M = 0.60	M = 0.80	M = 0.85	M = 0.90	M = 0.95
-4.0	0.00242	0.00253	0.00258	0.00247	0.00236
0	.00242	.00253	.00258	.00247	.00236
2.0	.00243	.00254	.00259	.00248	.00235
4.0	.00245	.00258	.00262	.00252	.00239
6.0	.00251	.00264	.00267	.00258	.00246
8.0	.00259	.00273	.00275	.00267	.00257
10.0	.00270	.00285	.00287	.00279	.00267
12.0	.00286	.00299	.00302	.00295	.00278
14.0	.00307	.00318	.00320	.00315	.00298
16.0		.00340	.00340	.00338	.00325

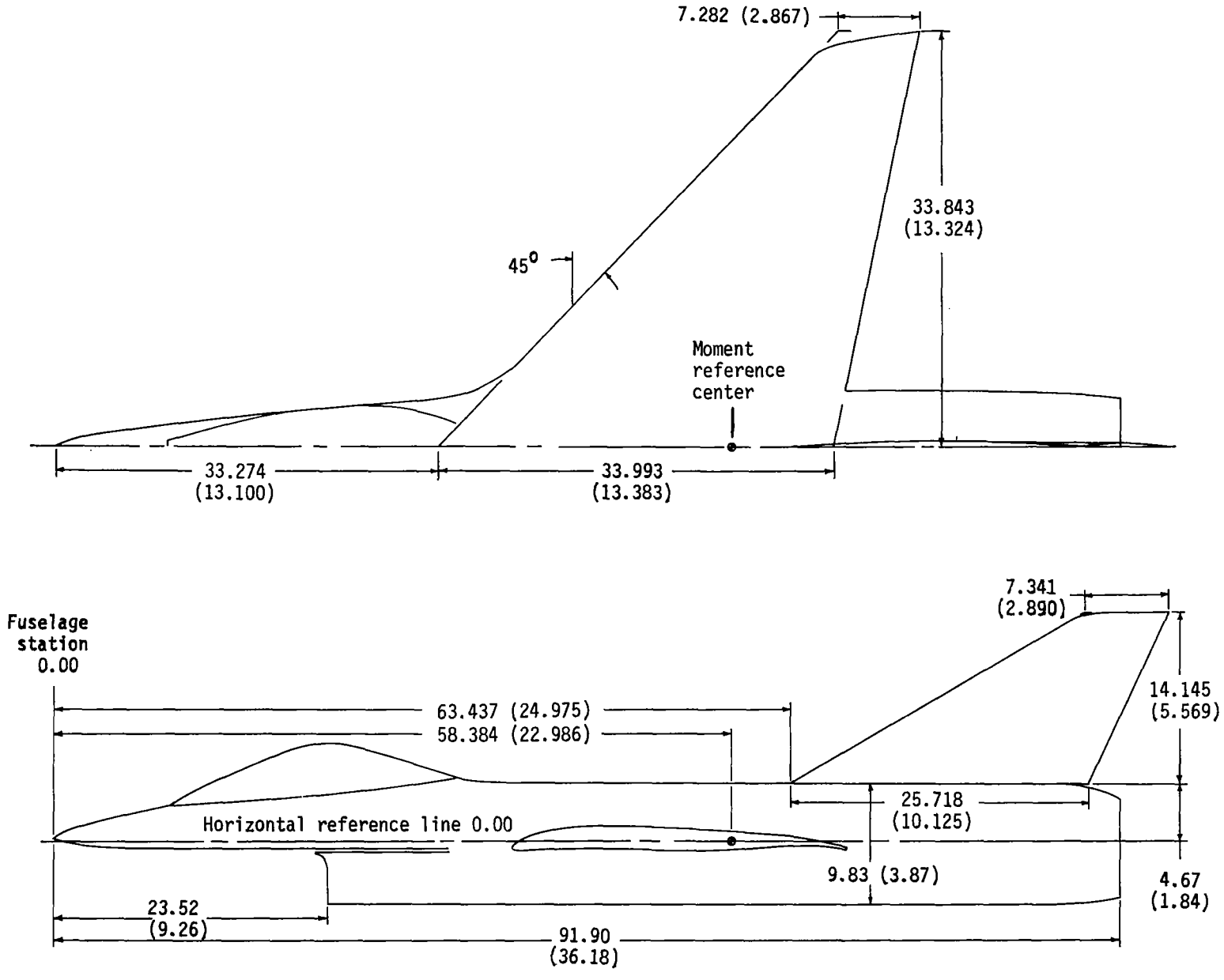

Figure 1.- General arrangement of model. Dimensions are given in centimeters (inches).

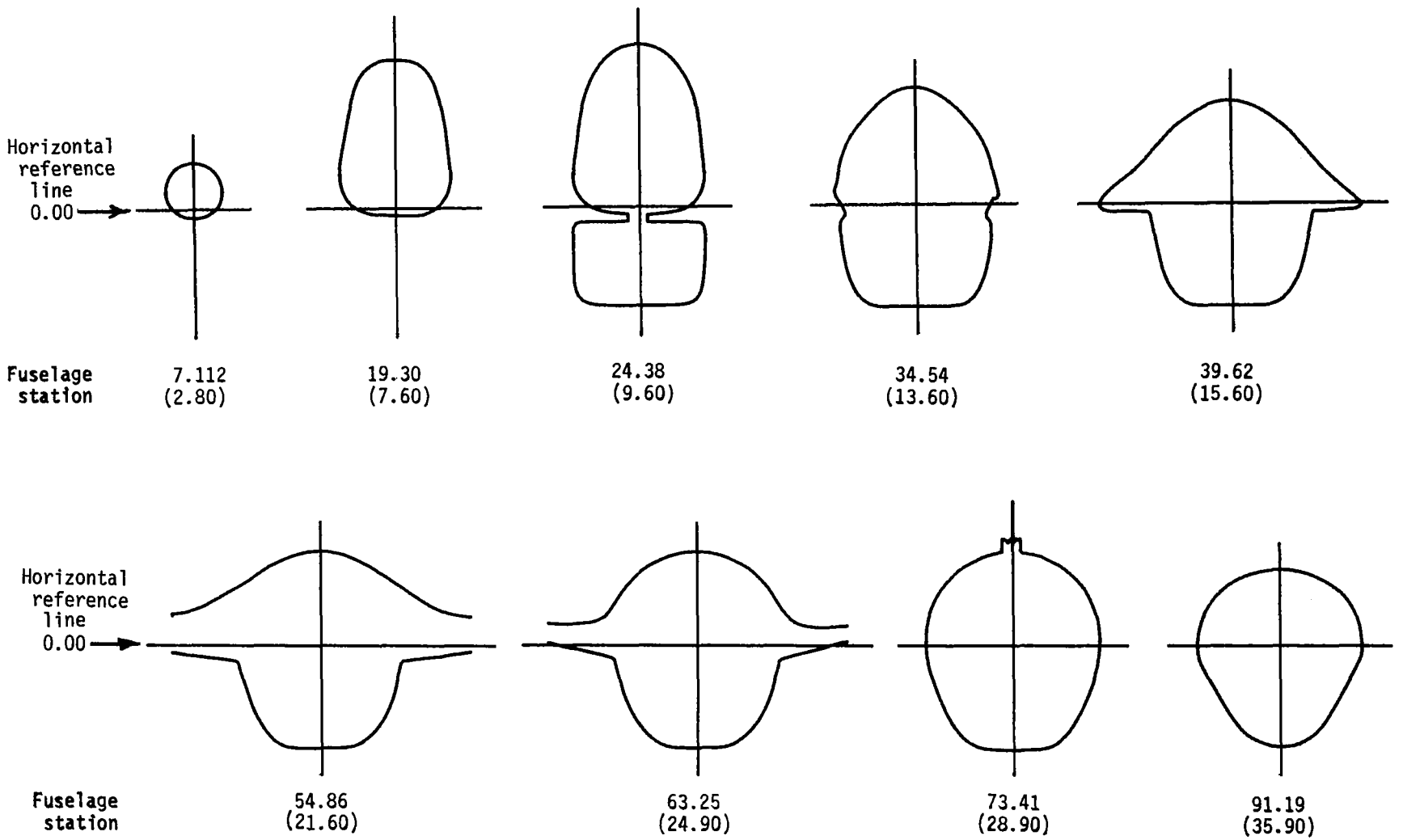

Figure 2.- External contours of fuselage. Stations are in centimeters (inches).

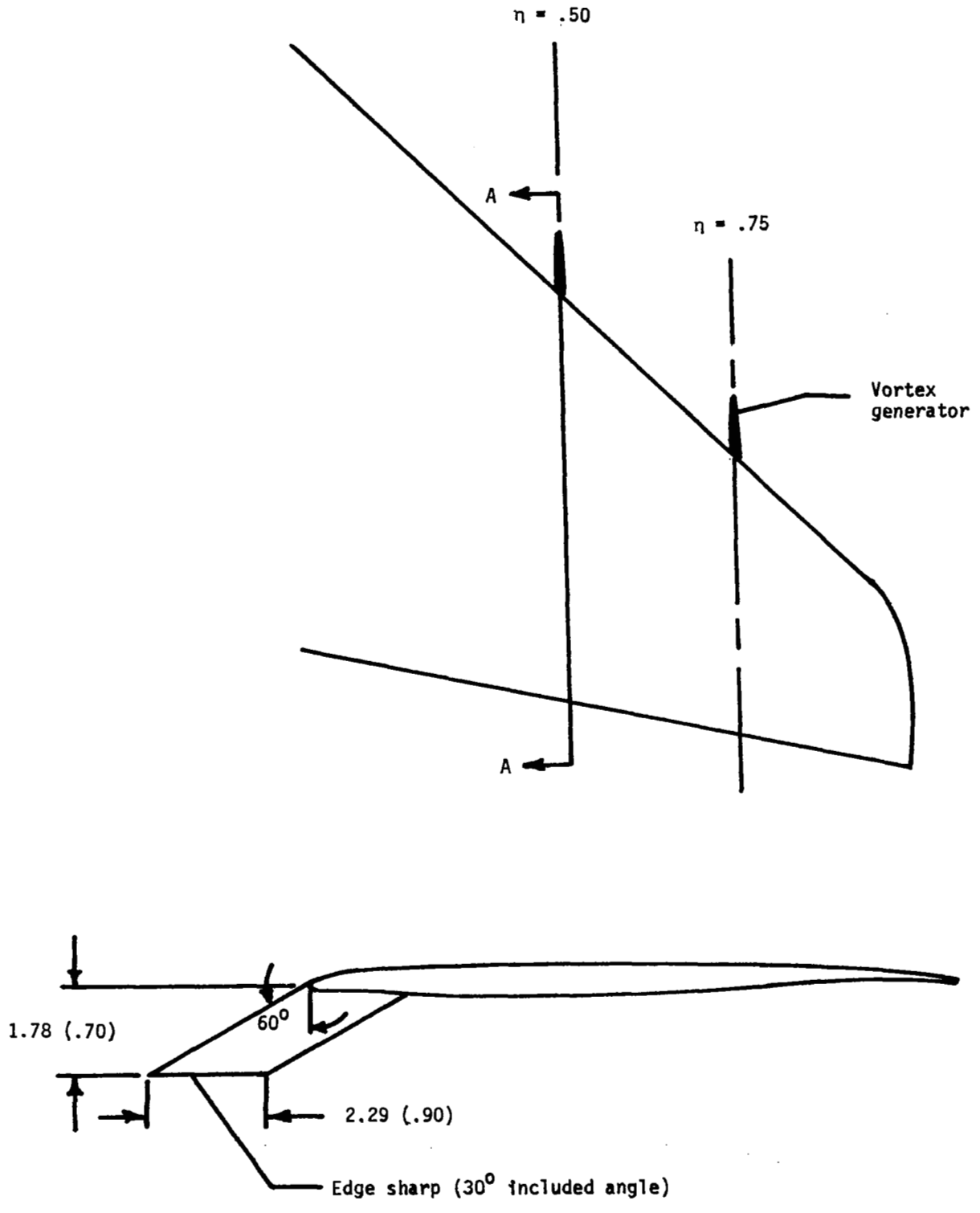

Details of vortex generator (section A-A)

Figure 3.- Vortex generators. Dimensions in centimeters (inches).

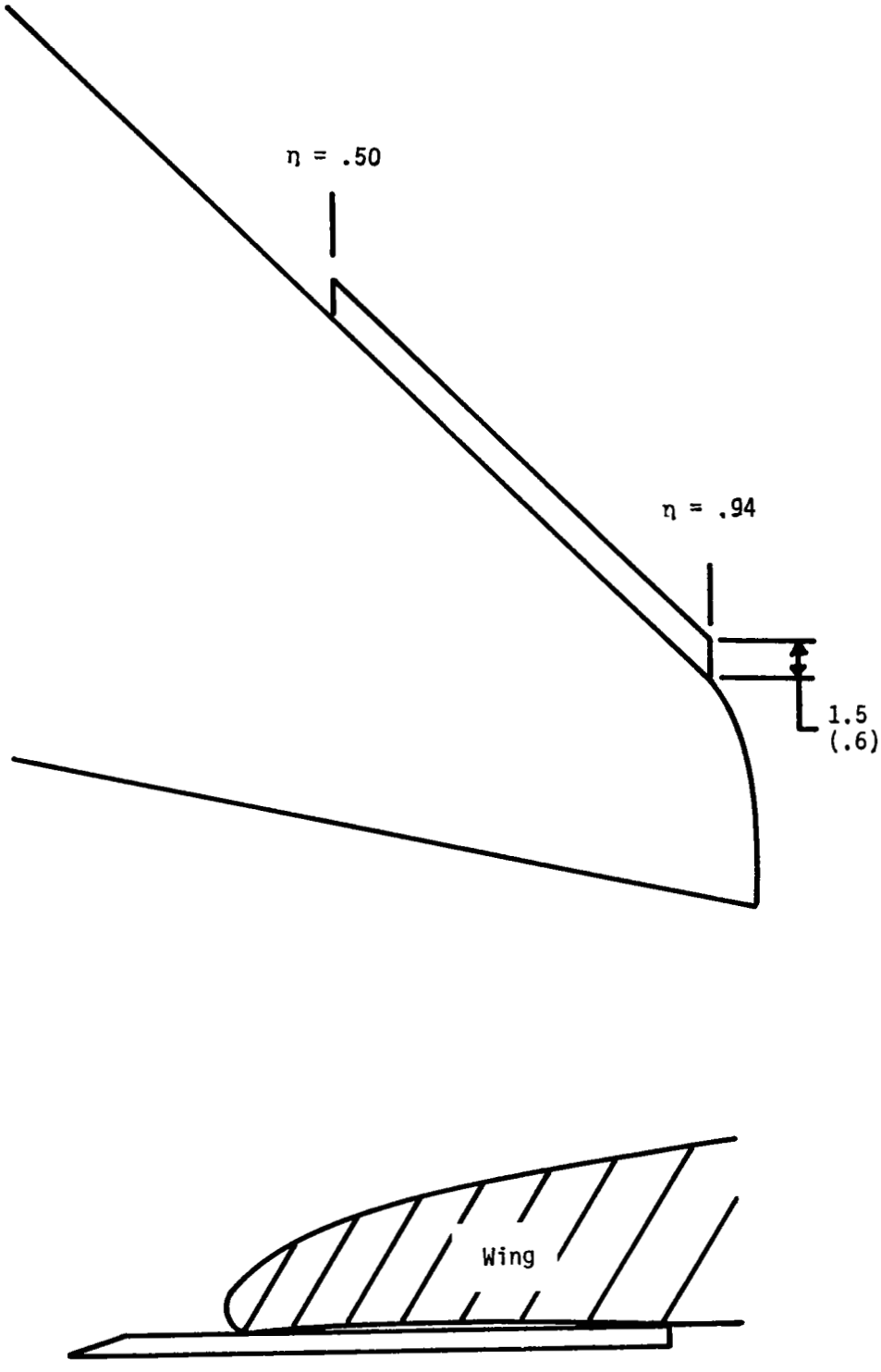

Sketch of flap

Figure 4.- Sharp leading-edge flap. Dimensions in centimeters (inches).

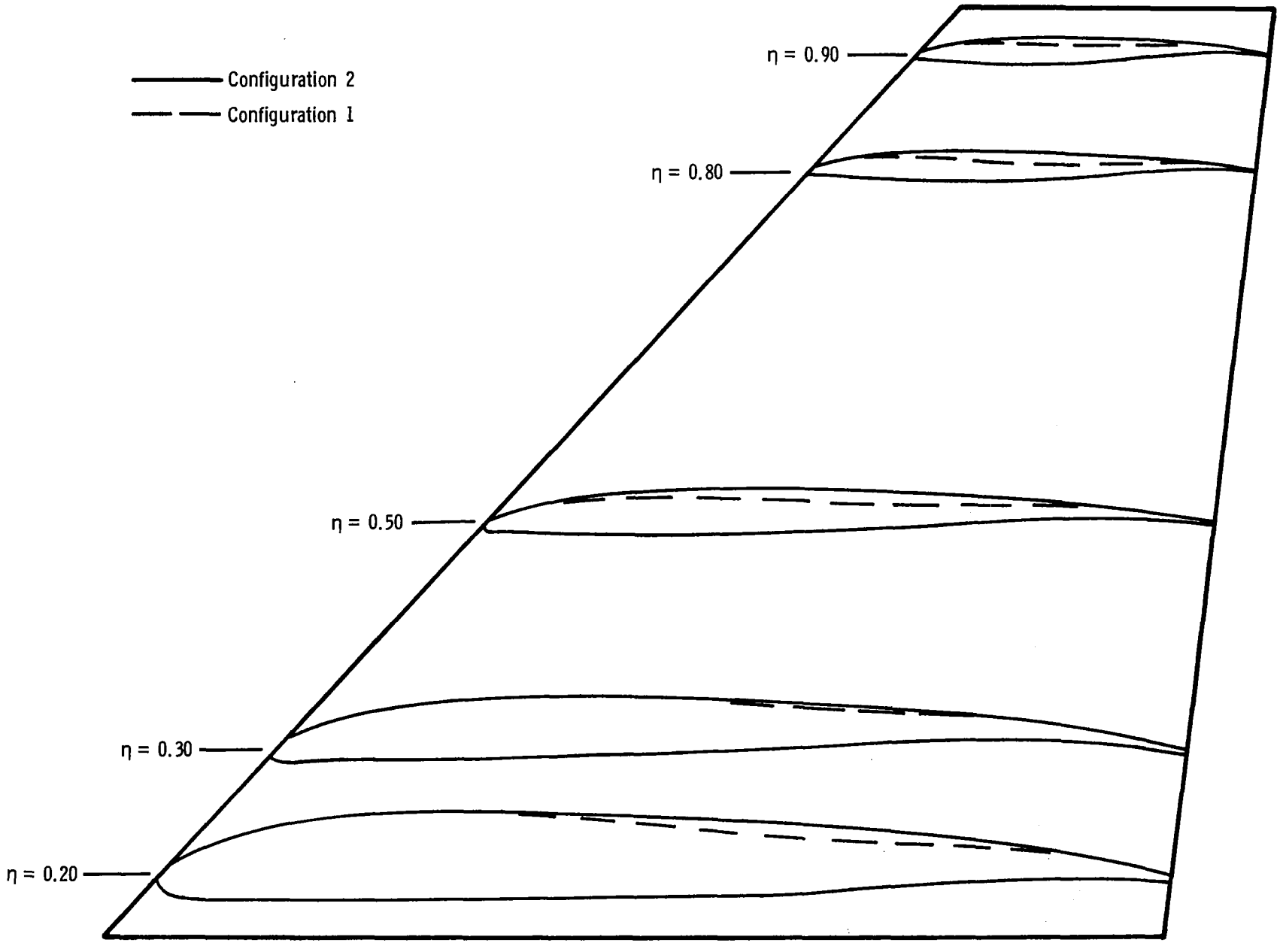

Figure 5.- Comparison of wing airfoils for configurations 1 and 2.

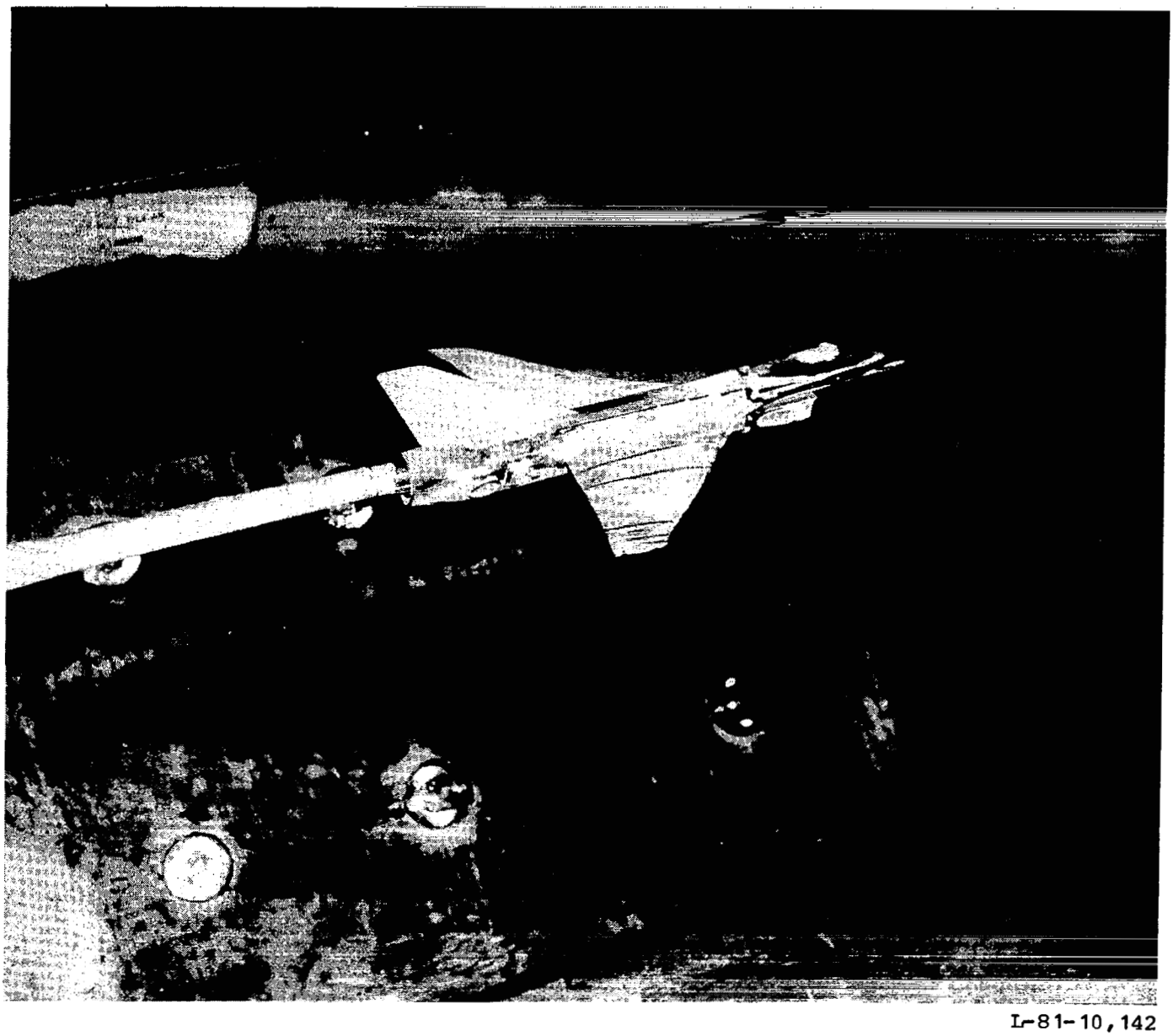

L-81-10,142

(a) Configuration 2, side view.

Figure 6.- SMF-2 model mounted in Langley 16-Foot Transonic Tunnel.

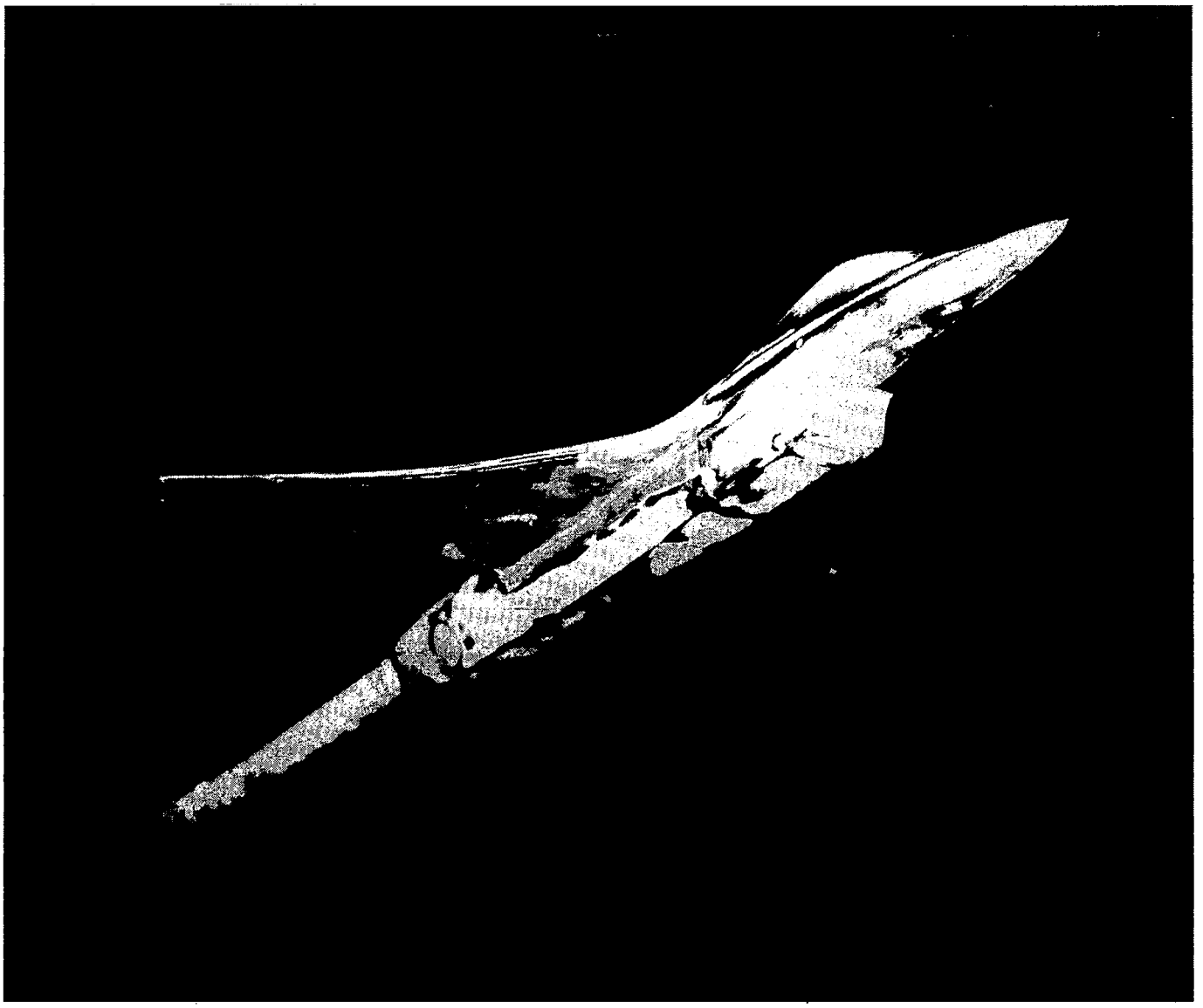

L-80-10,877

(b) Configuration 2, three-quarter front bottom view.

Figure 6.- Continued.

L-81-10,252

(c) Configuration 2 with SLEF, side view.

Figure 6.- Continued.

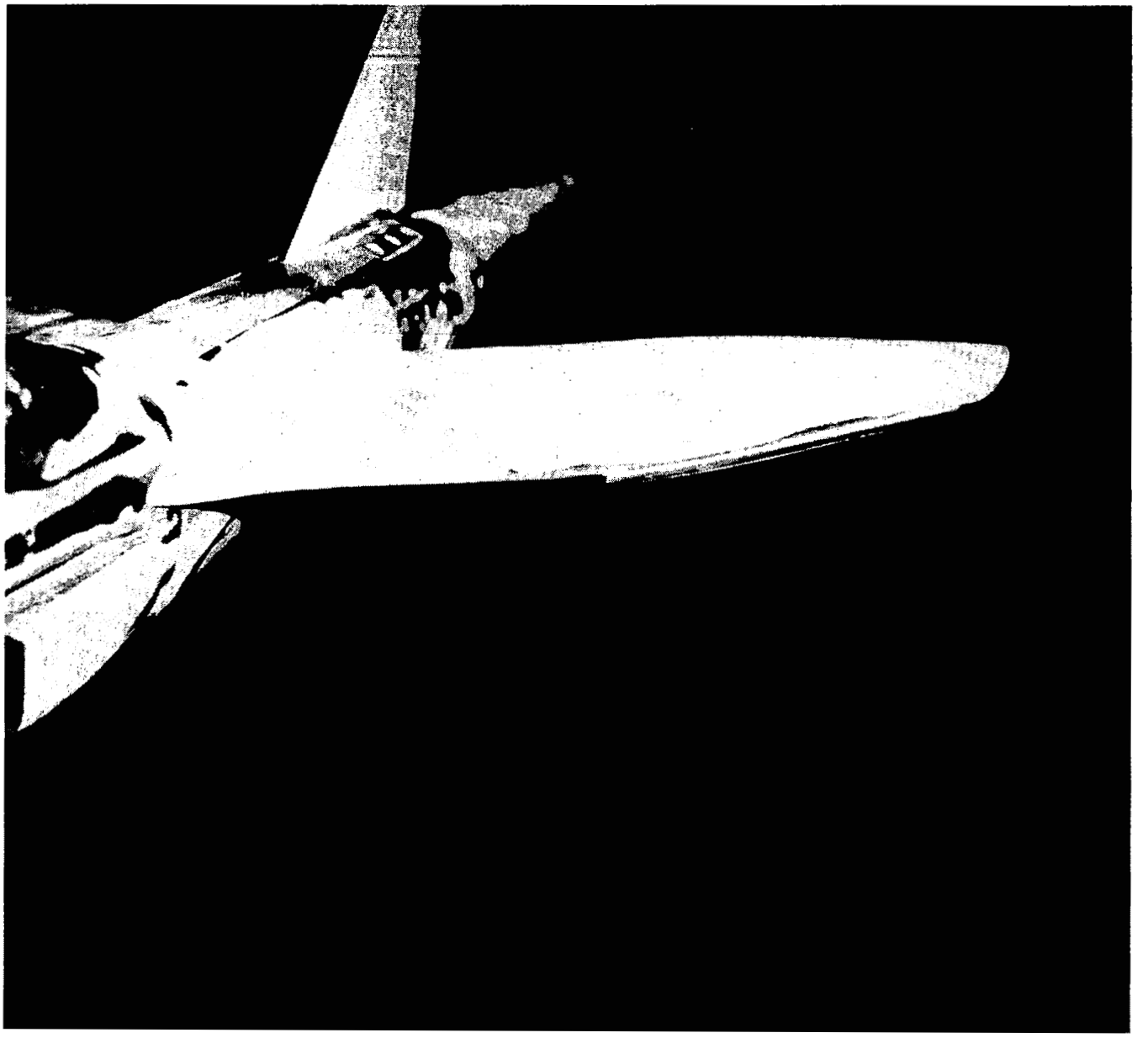

L-81-10,258

(d) Configuration 2 with SLEF, front view left wing.

Figure 6.- Continued.

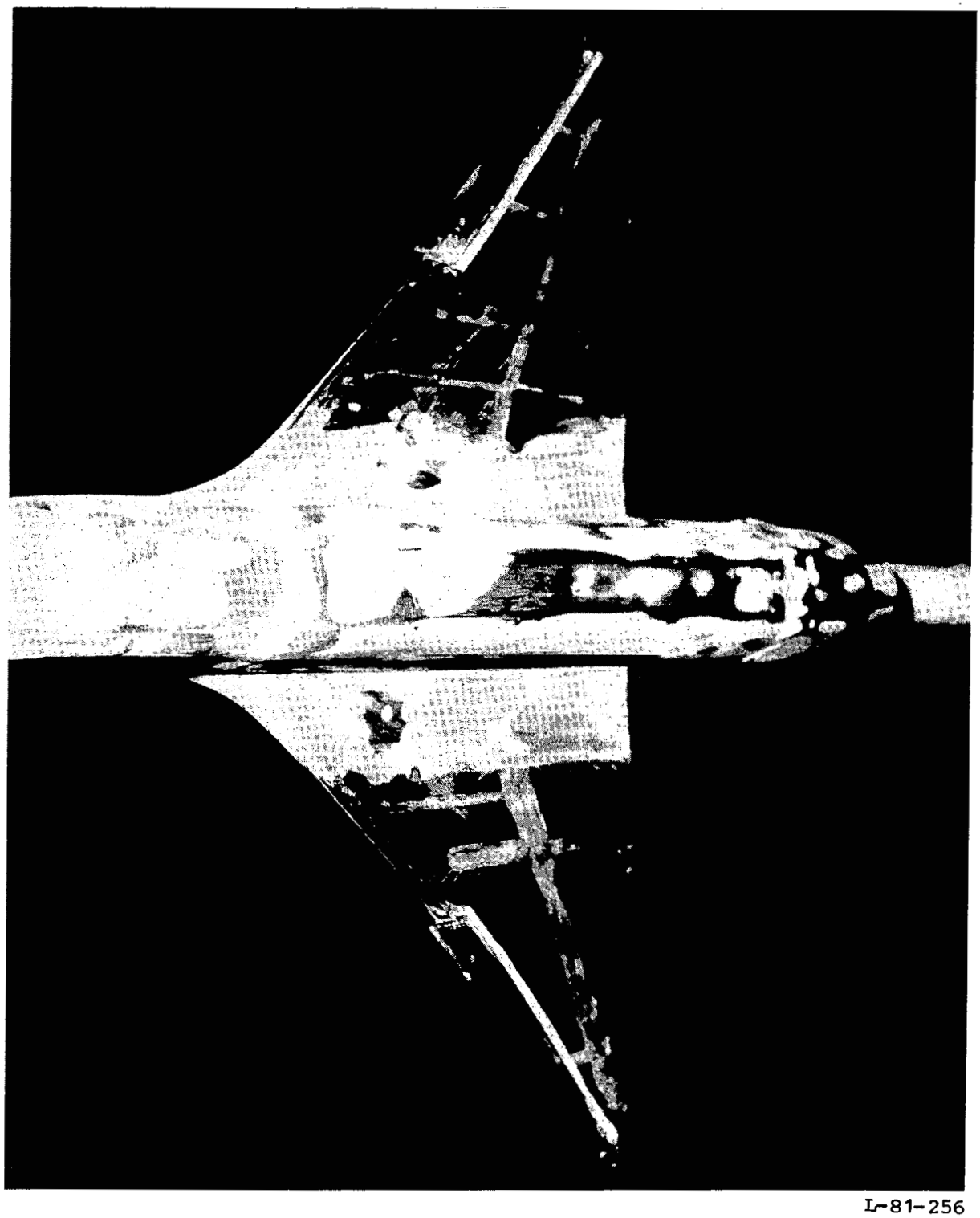

L-81-256

(e) Configuration 2 with SLEF, bottom view.

Figure 6.- Concluded.

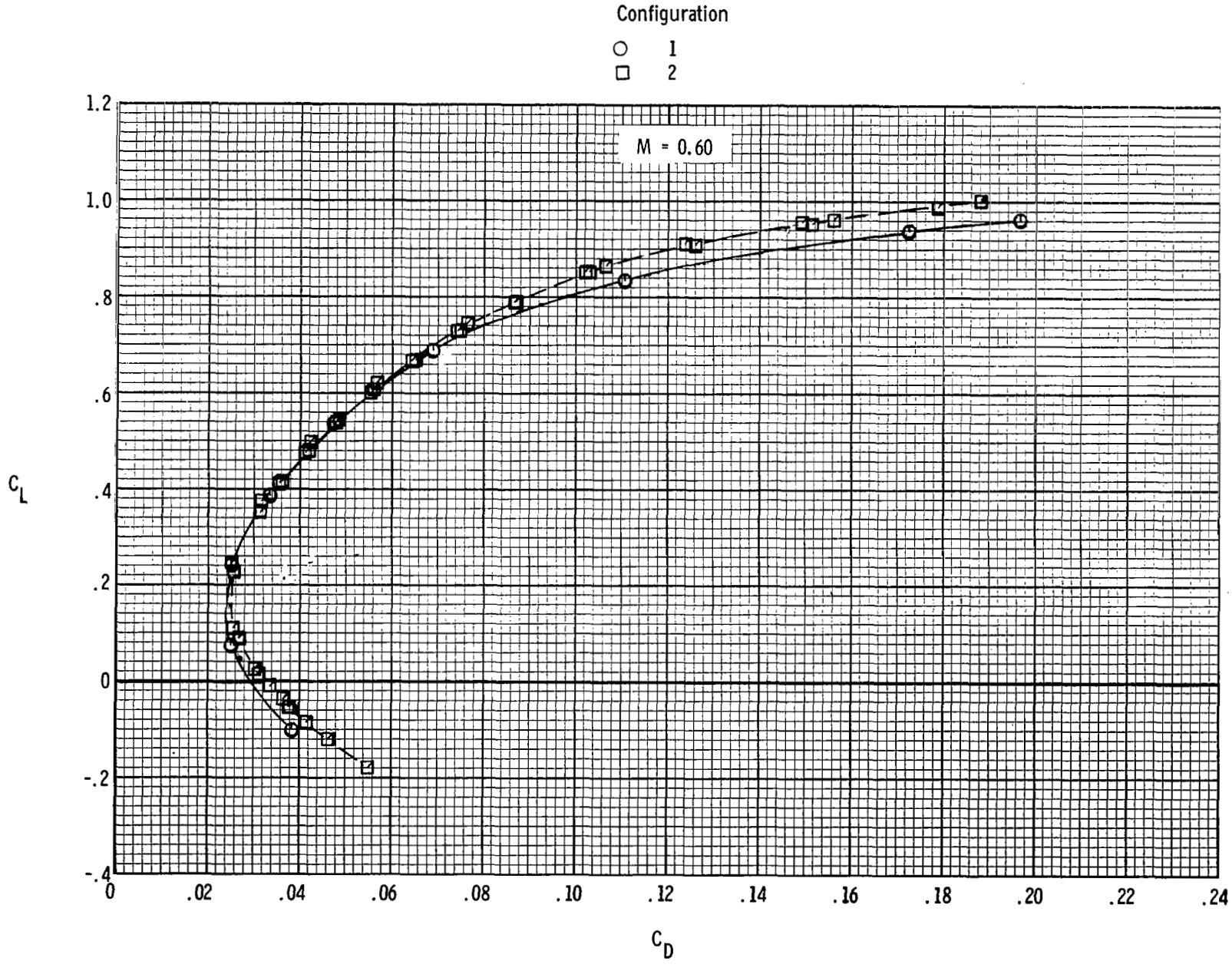

(a) Lift vs drag.

Figure 7.- Effect of wing contouring on longitudinal aerodynamic characteristics.

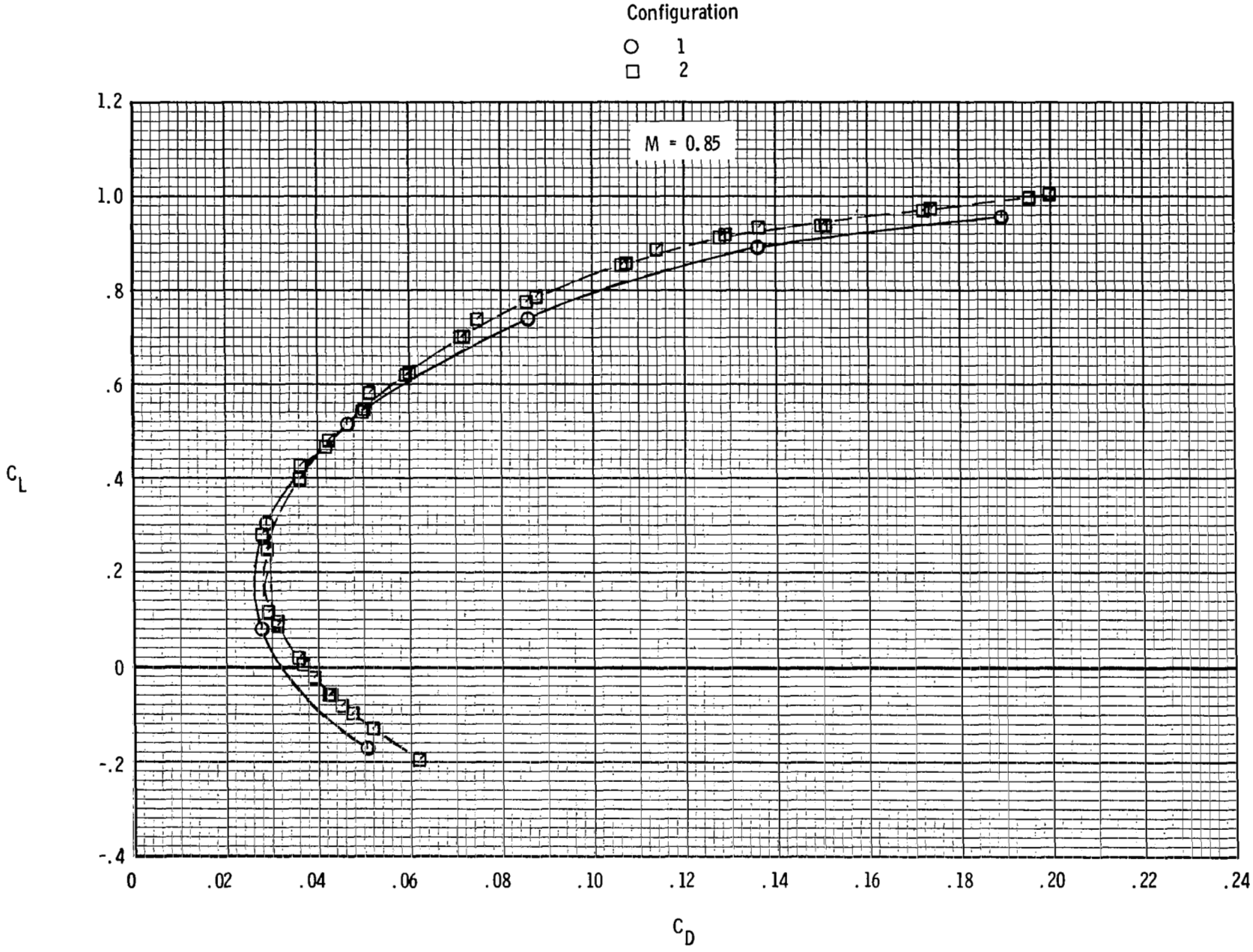

(a) Continued.

Figure 7.- Continued.

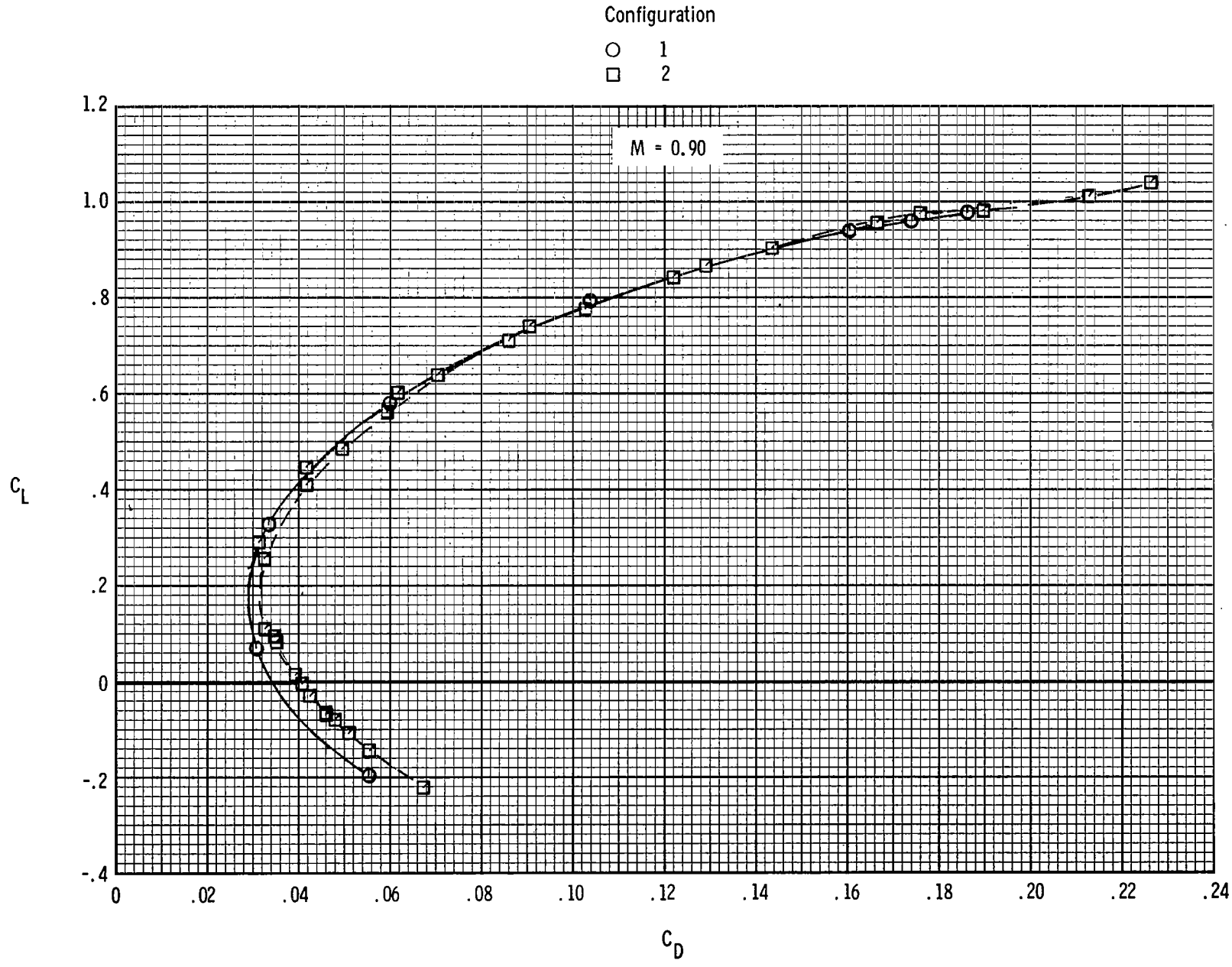

(a) Continued.

Figure 7.- Continued.

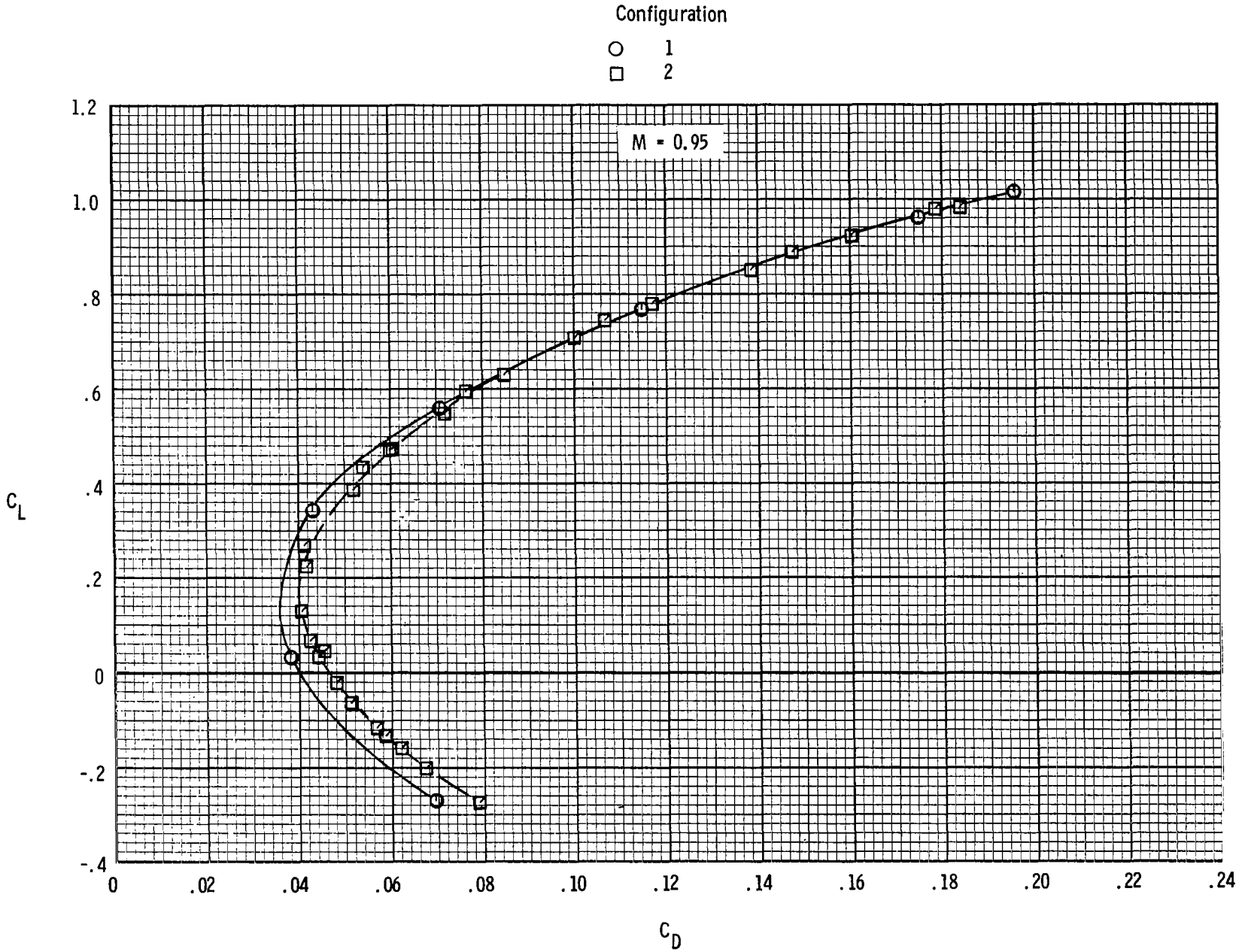

(a) Concluded.

Figure 7.- Continued.

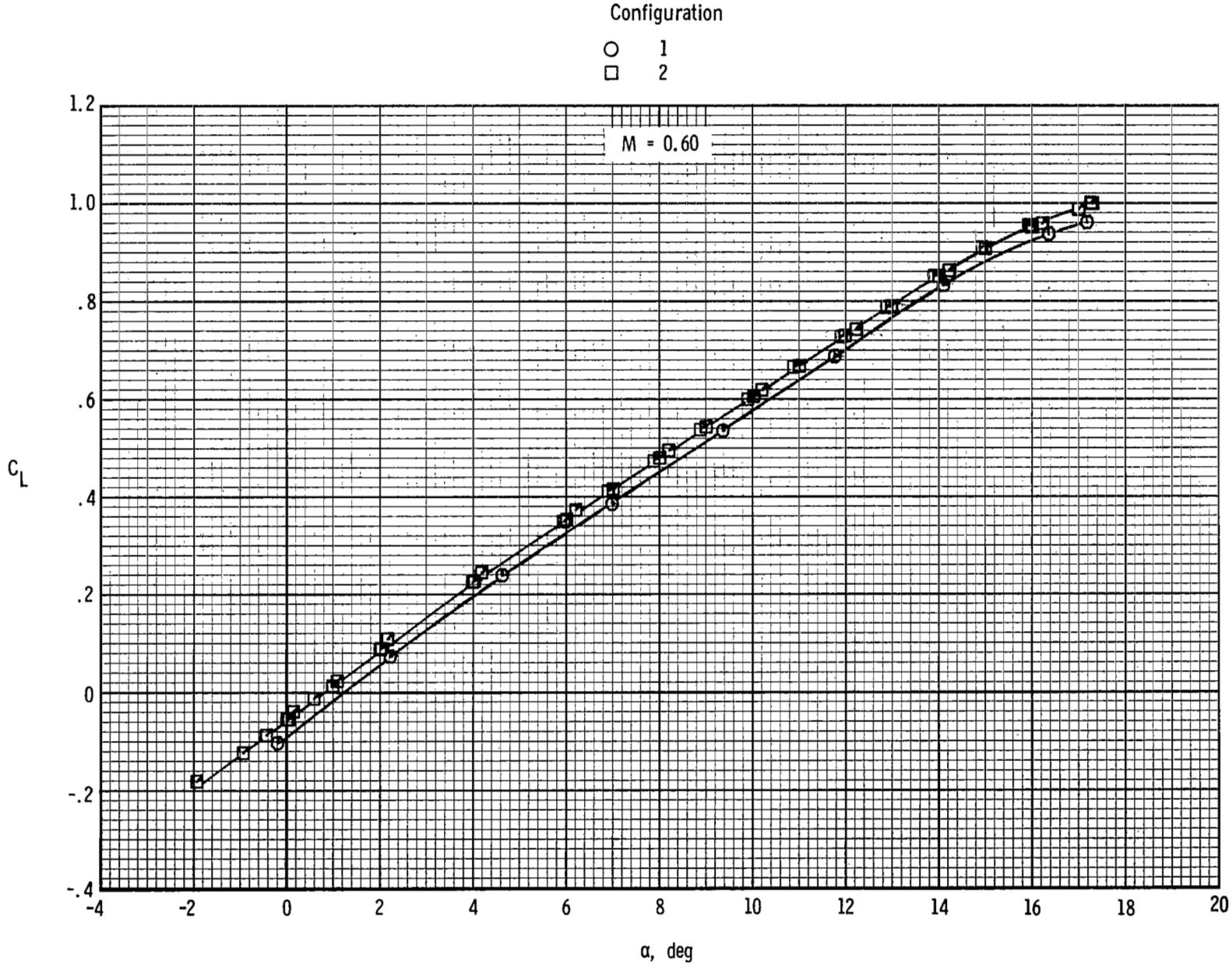

(b) Lift vs angle of attack.

Figure 7.- Continued.

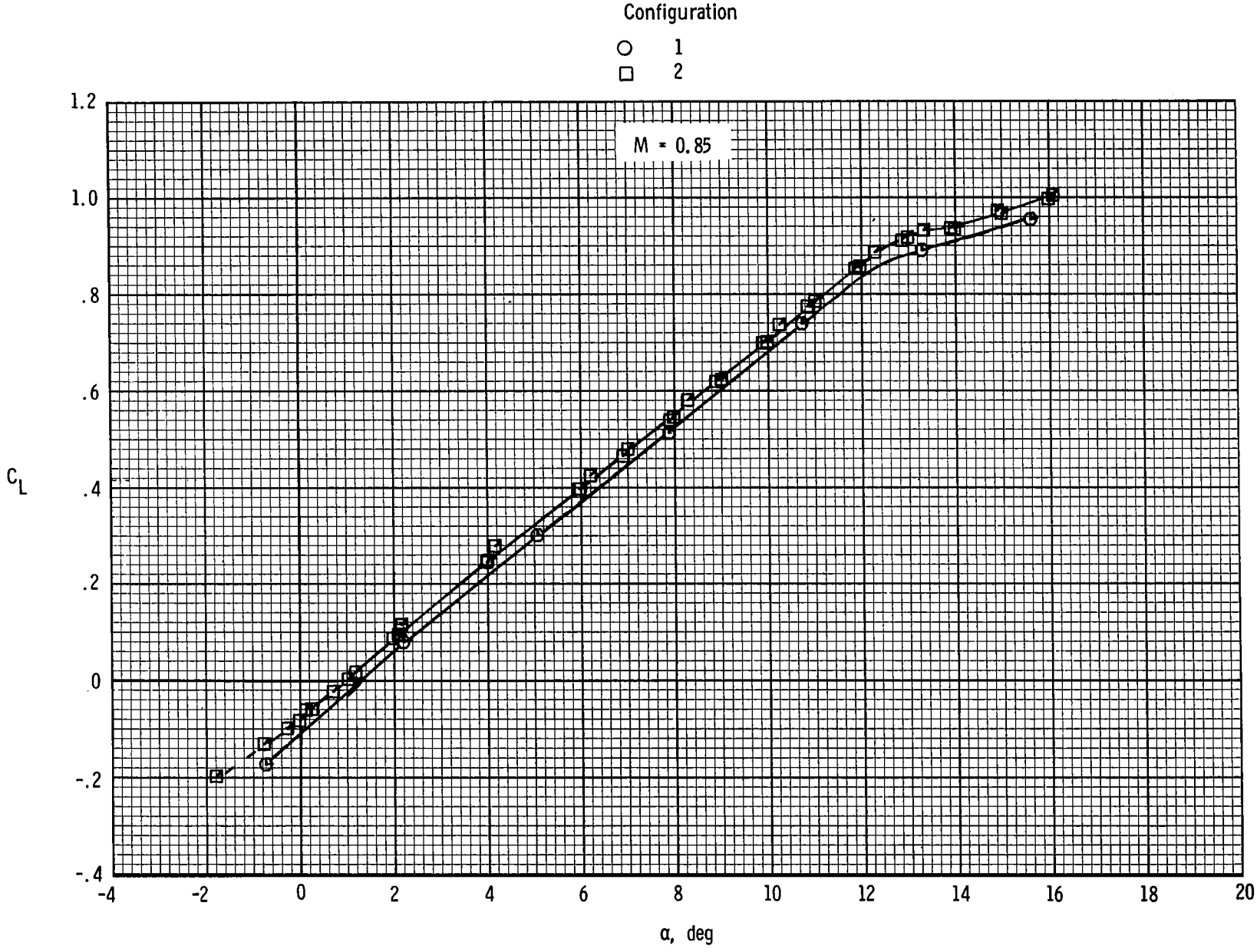

(b) Continued.

Figure 7.- Continued.

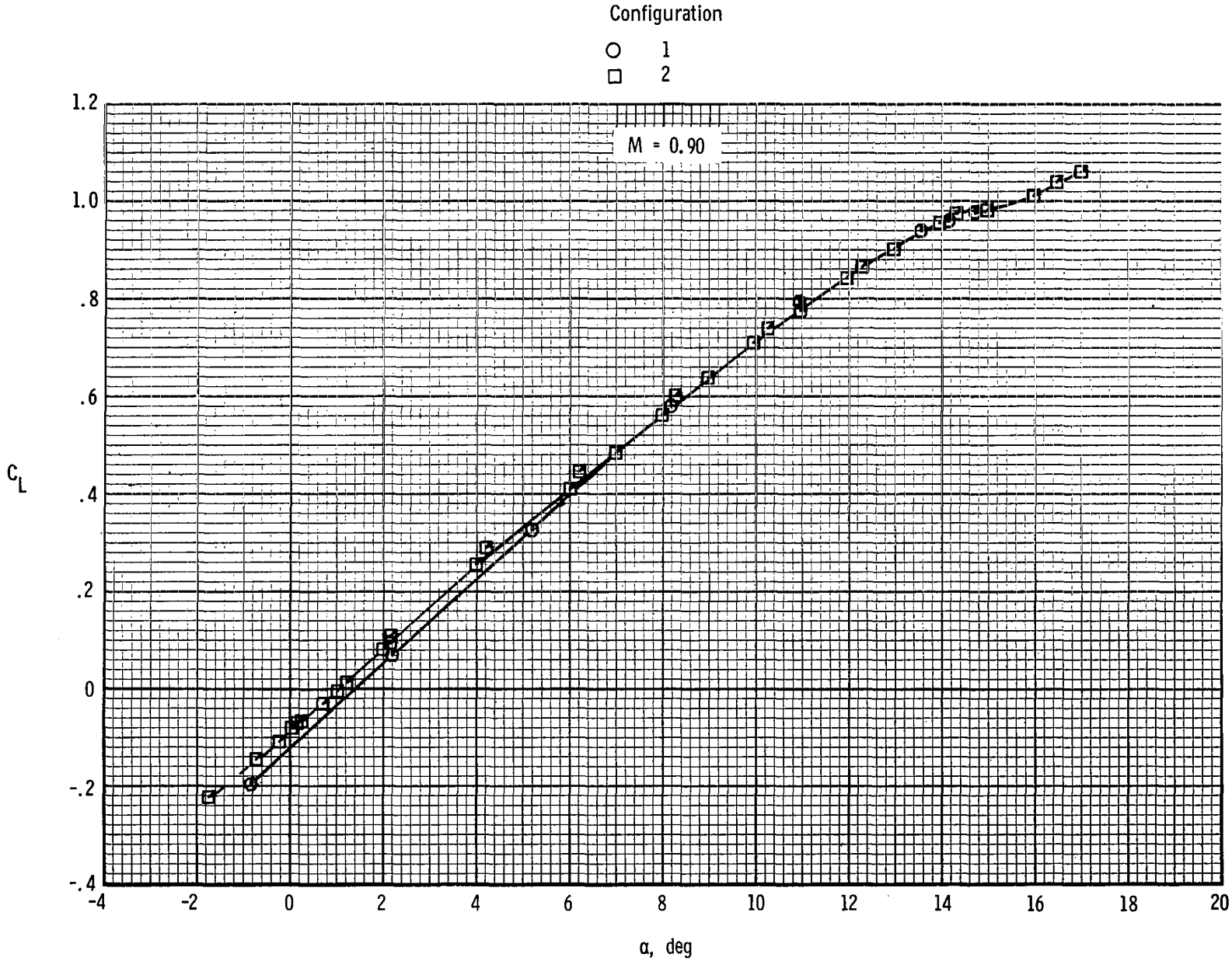

(b) Continued.

Figure 7.- Continued.

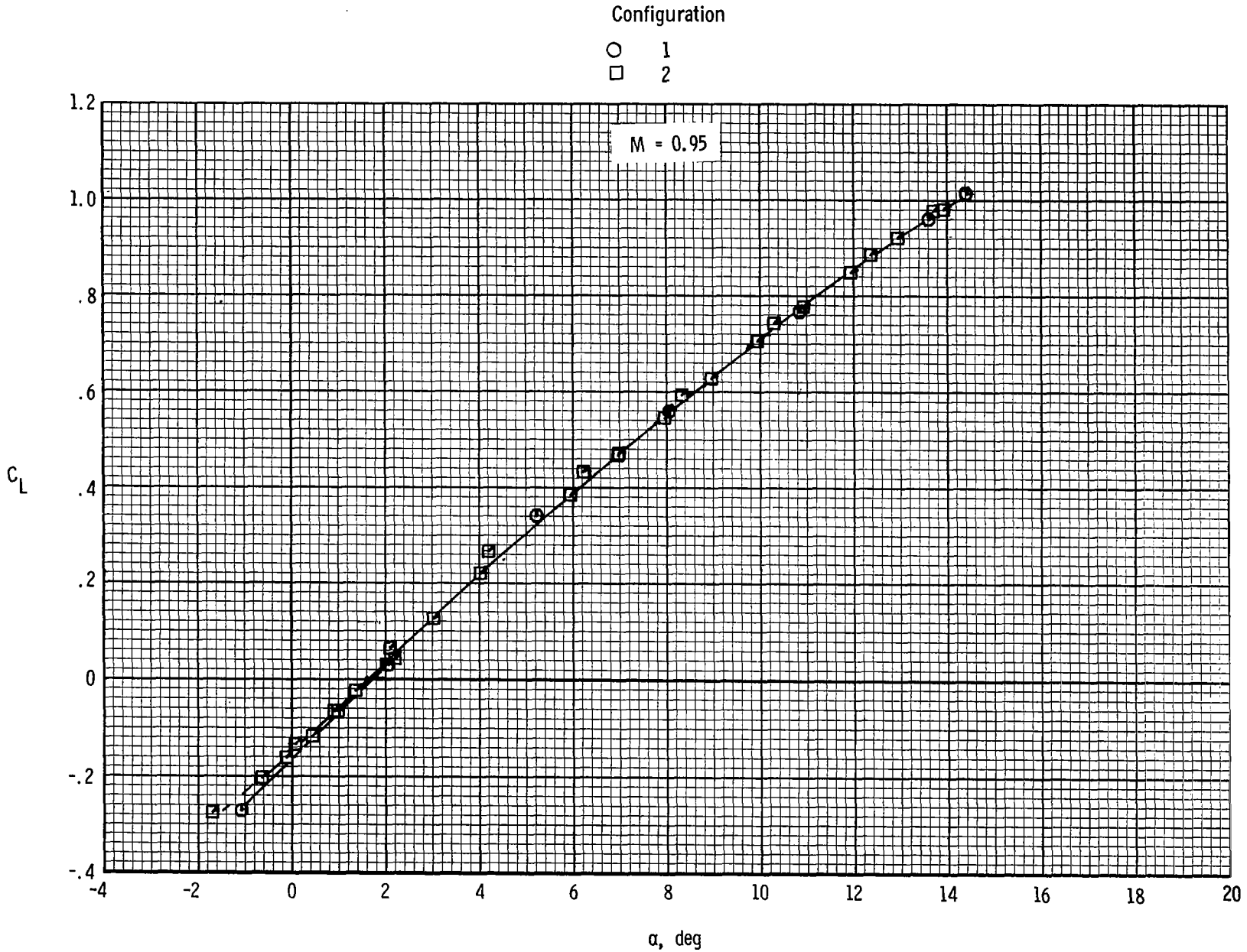

(b) Concluded.

Figure 7.- Continued.

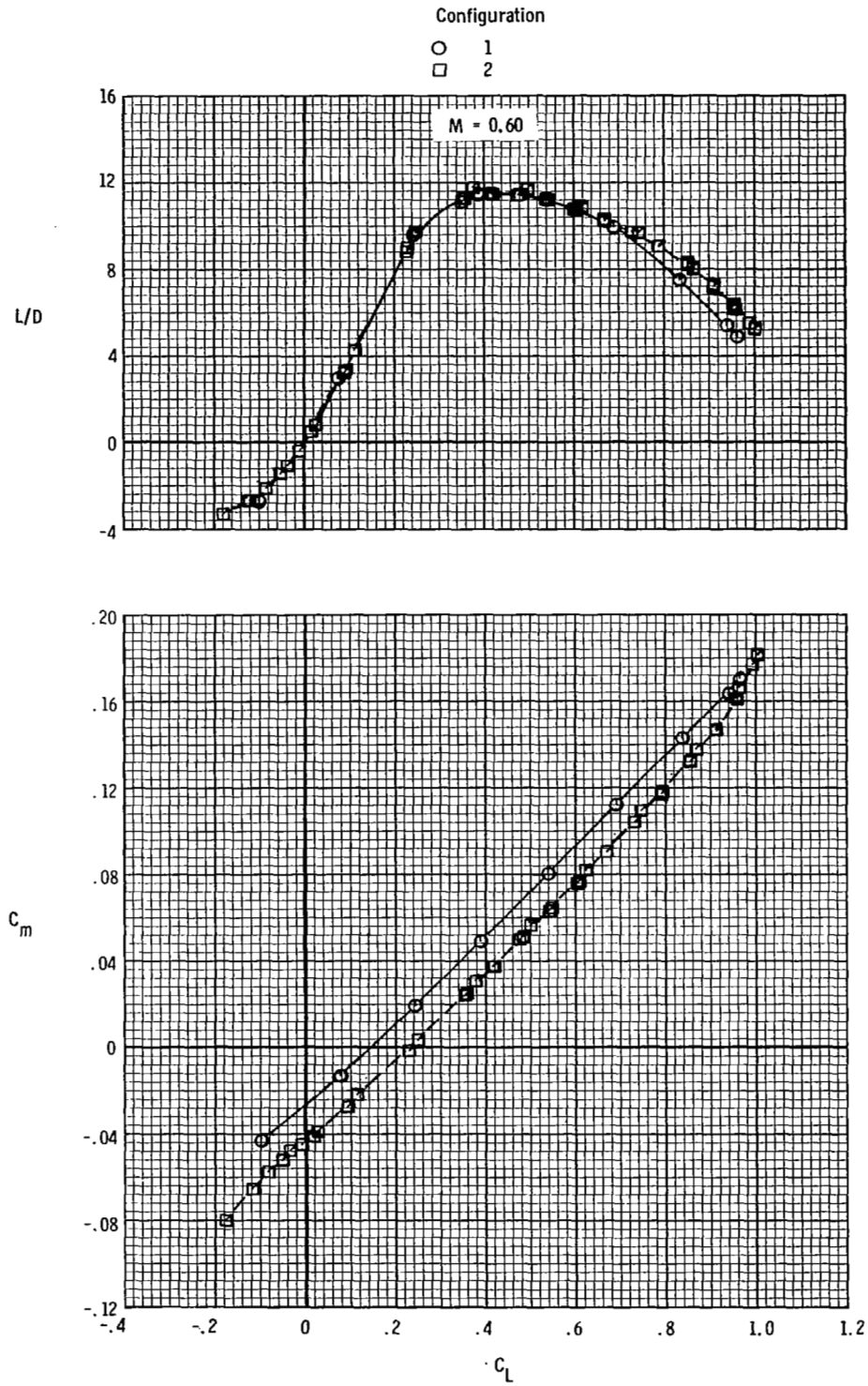

(c) L/D and pitch vs lift.

Figure 7.- Continued.

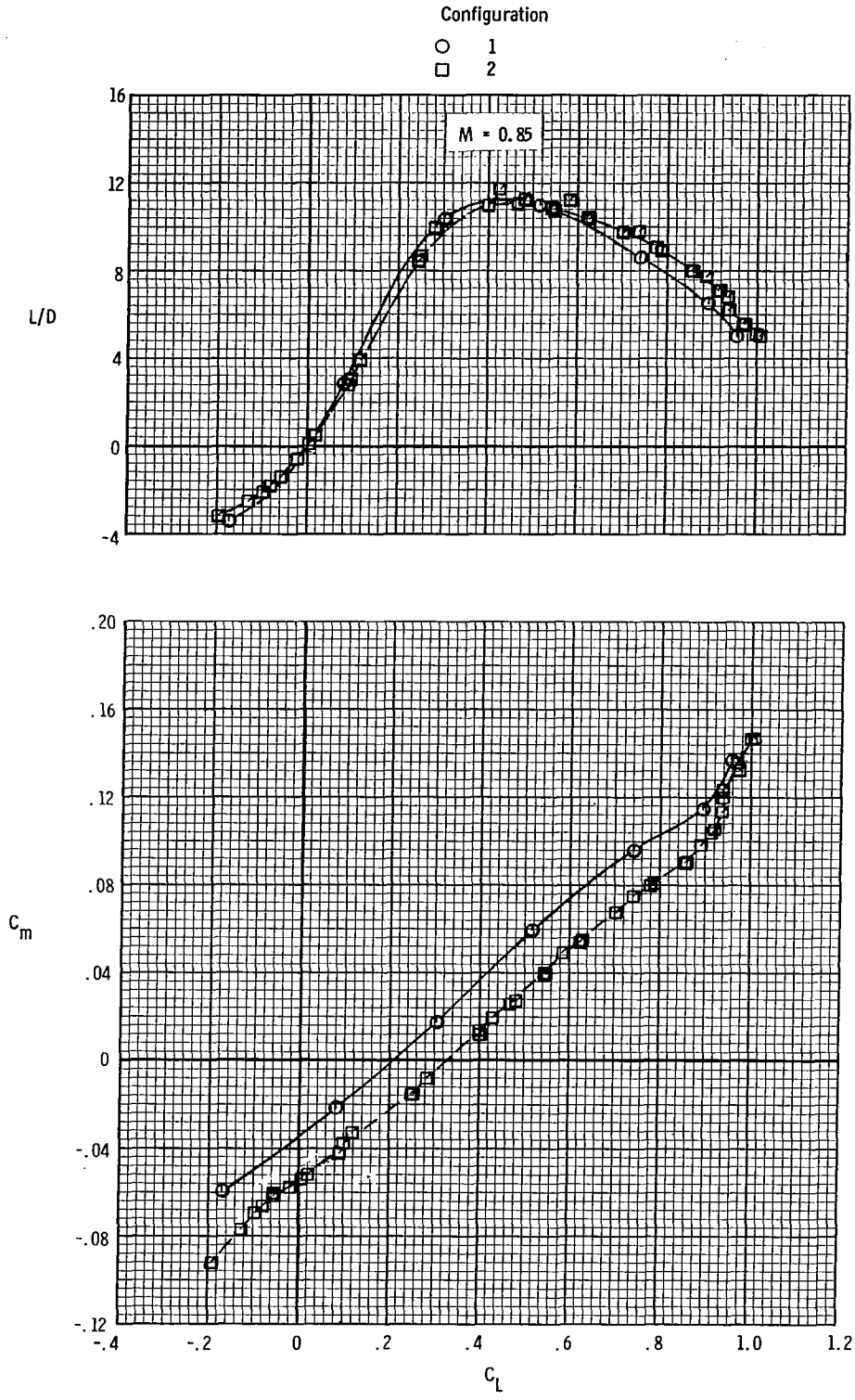

(c) Continued.

Figure 7.- Continued.

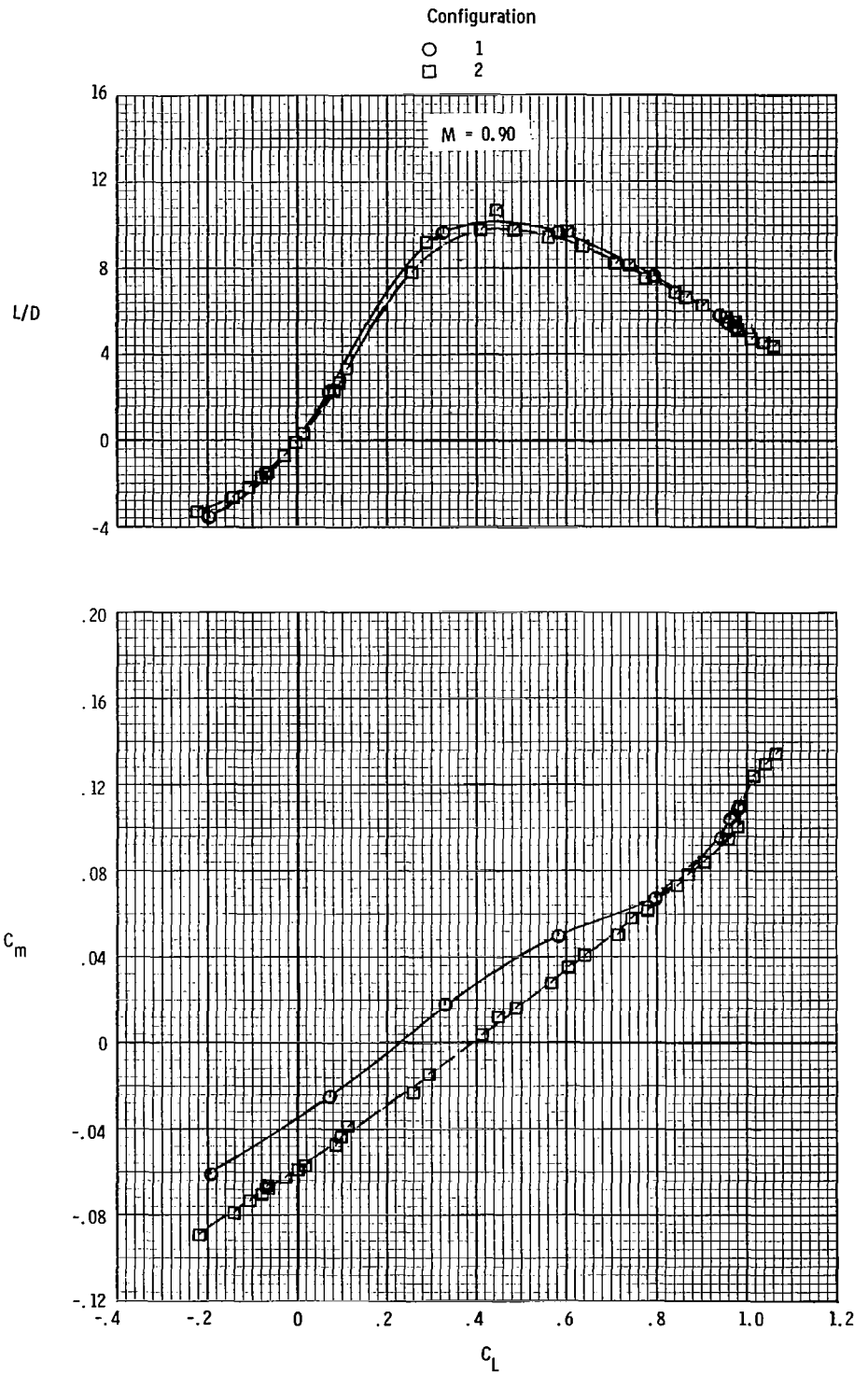

(c) Continued.

Figure 7.- Continued.

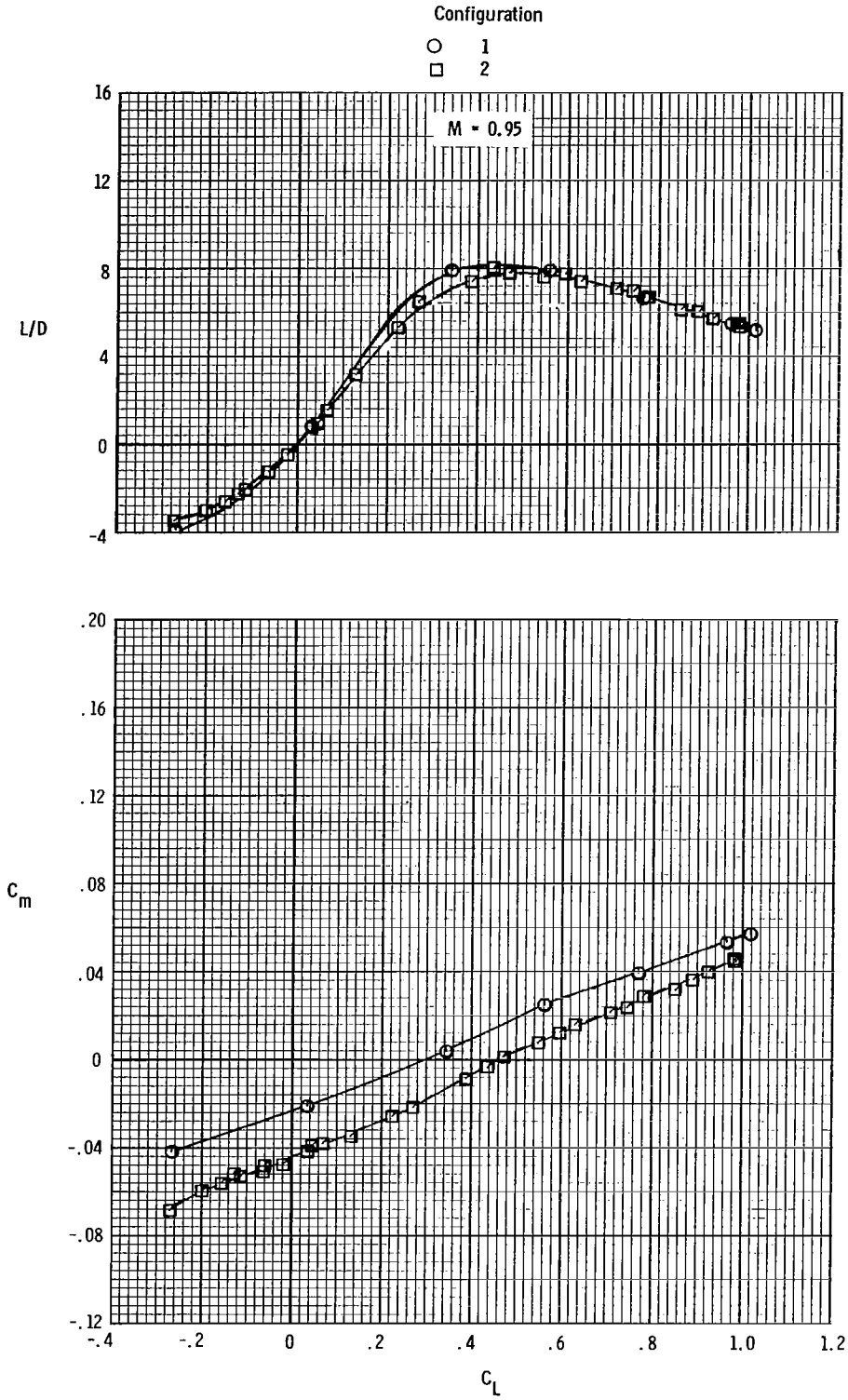

(c) Concluded.

Figure 7.- Concluded.

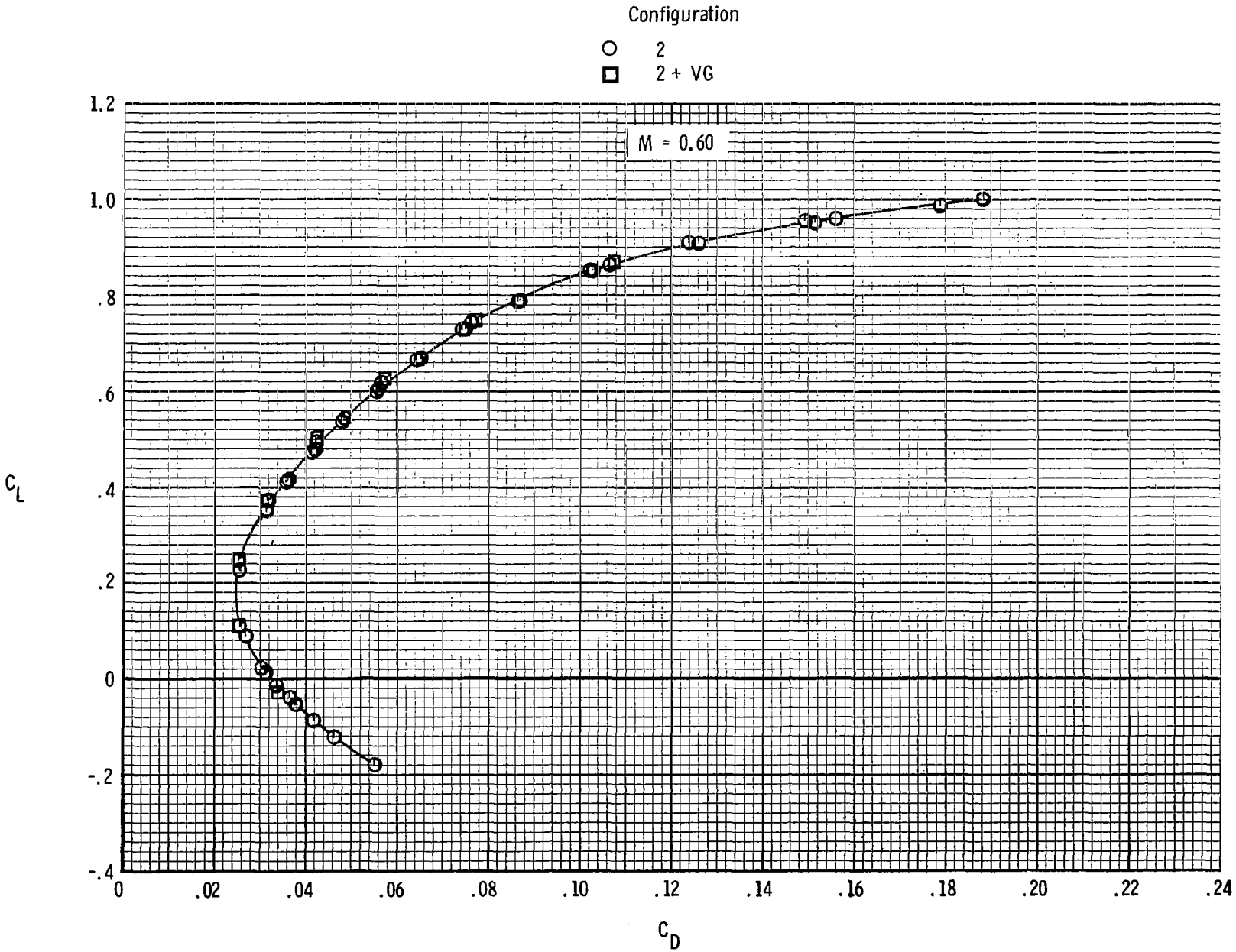

(a) Lift vs drag.

Figure 8.- Effect of wing vortex generators on longitudinal aerodynamic characteristics.

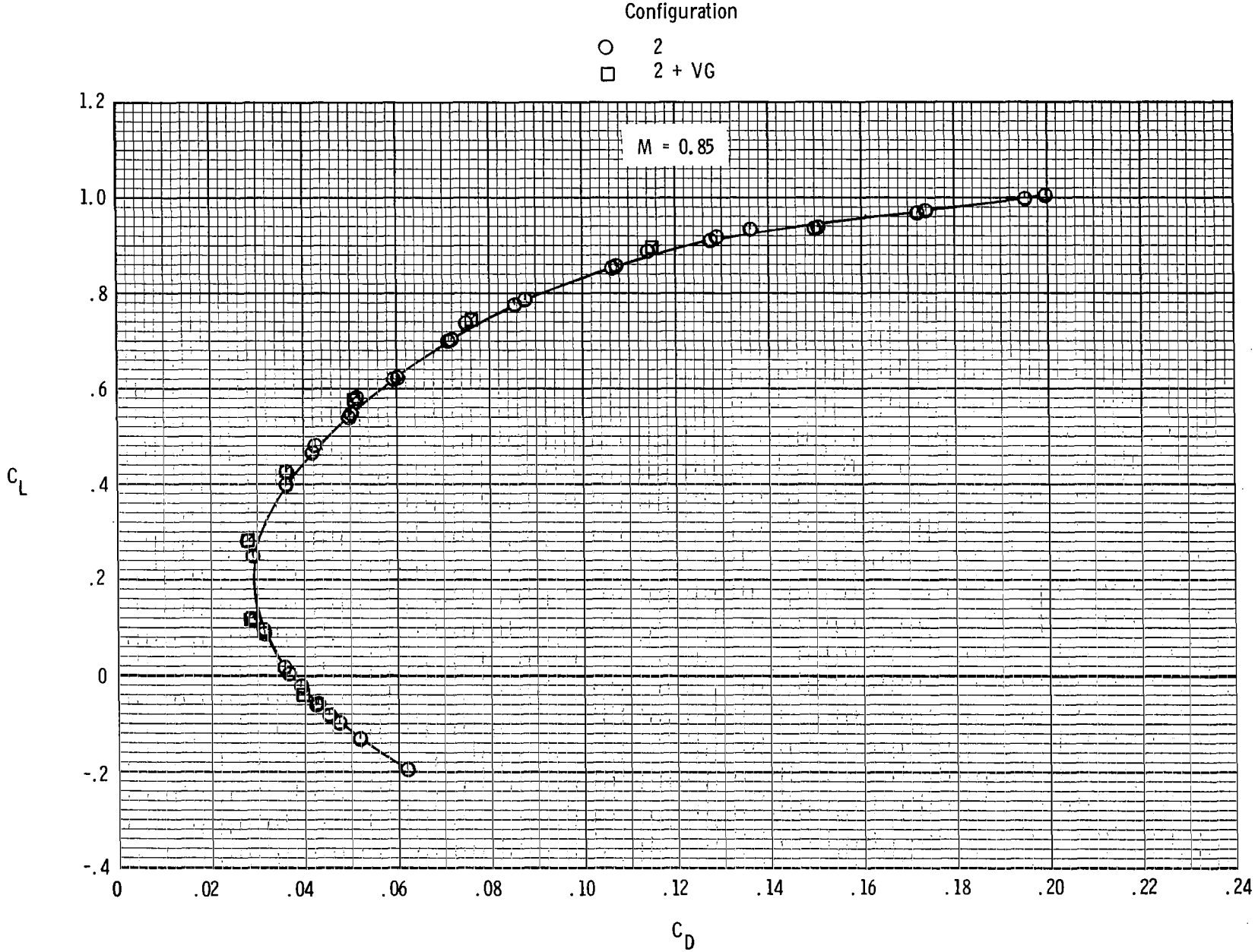

(a) Continued.

Figure 8.- Continued.

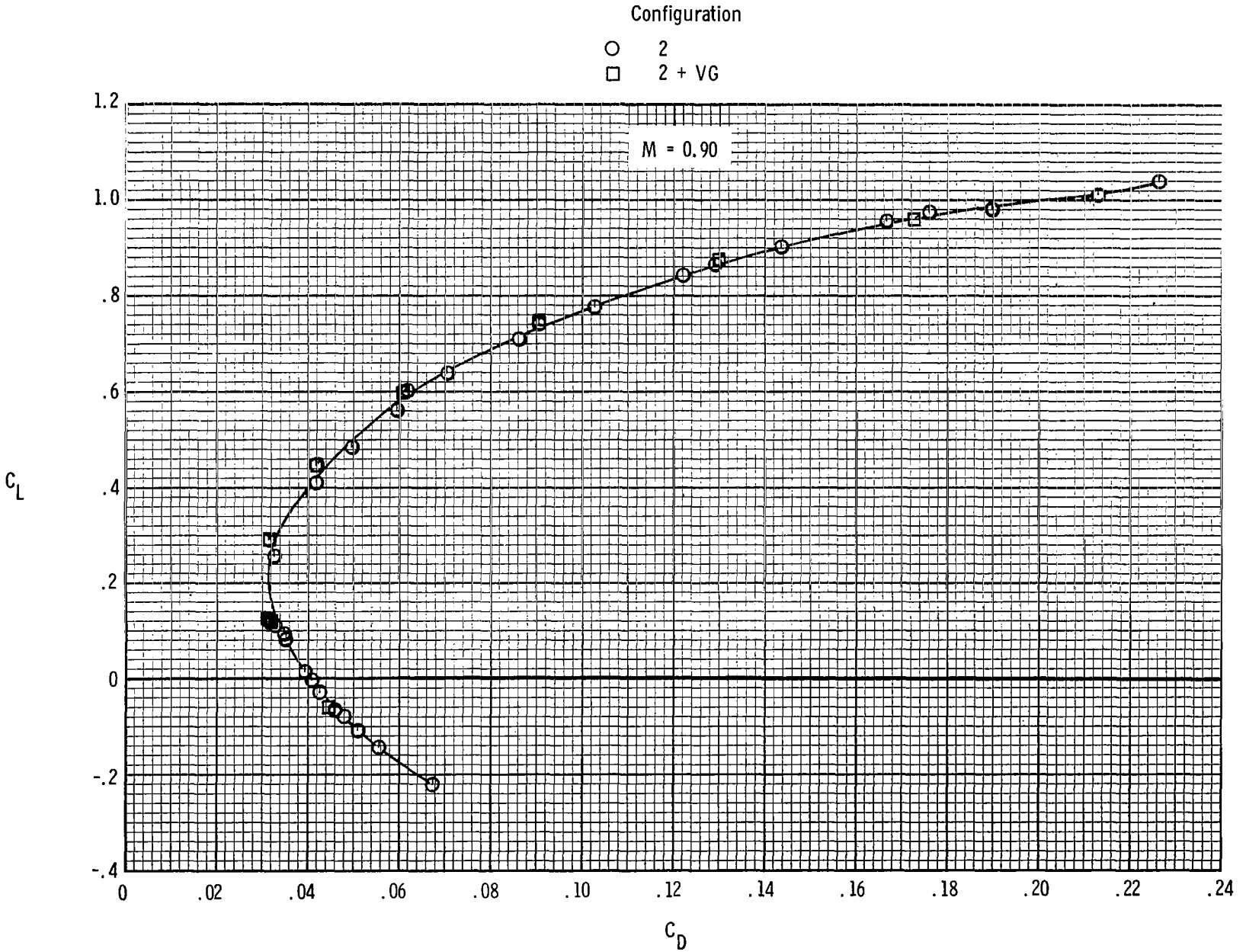

(a) Continued.

Figure 8.- Continued.

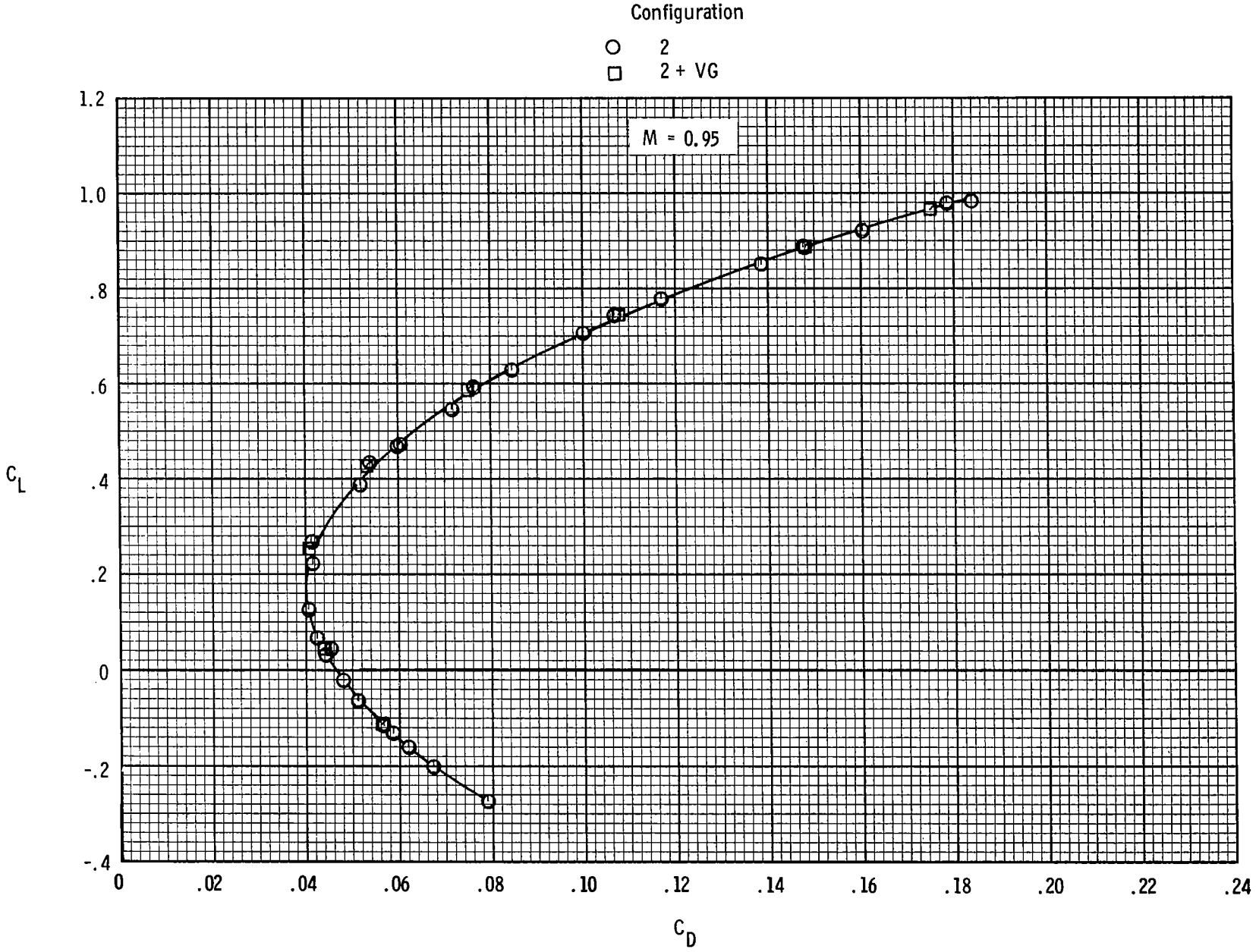

(a) Concluded.

Figure 8.- Continued.

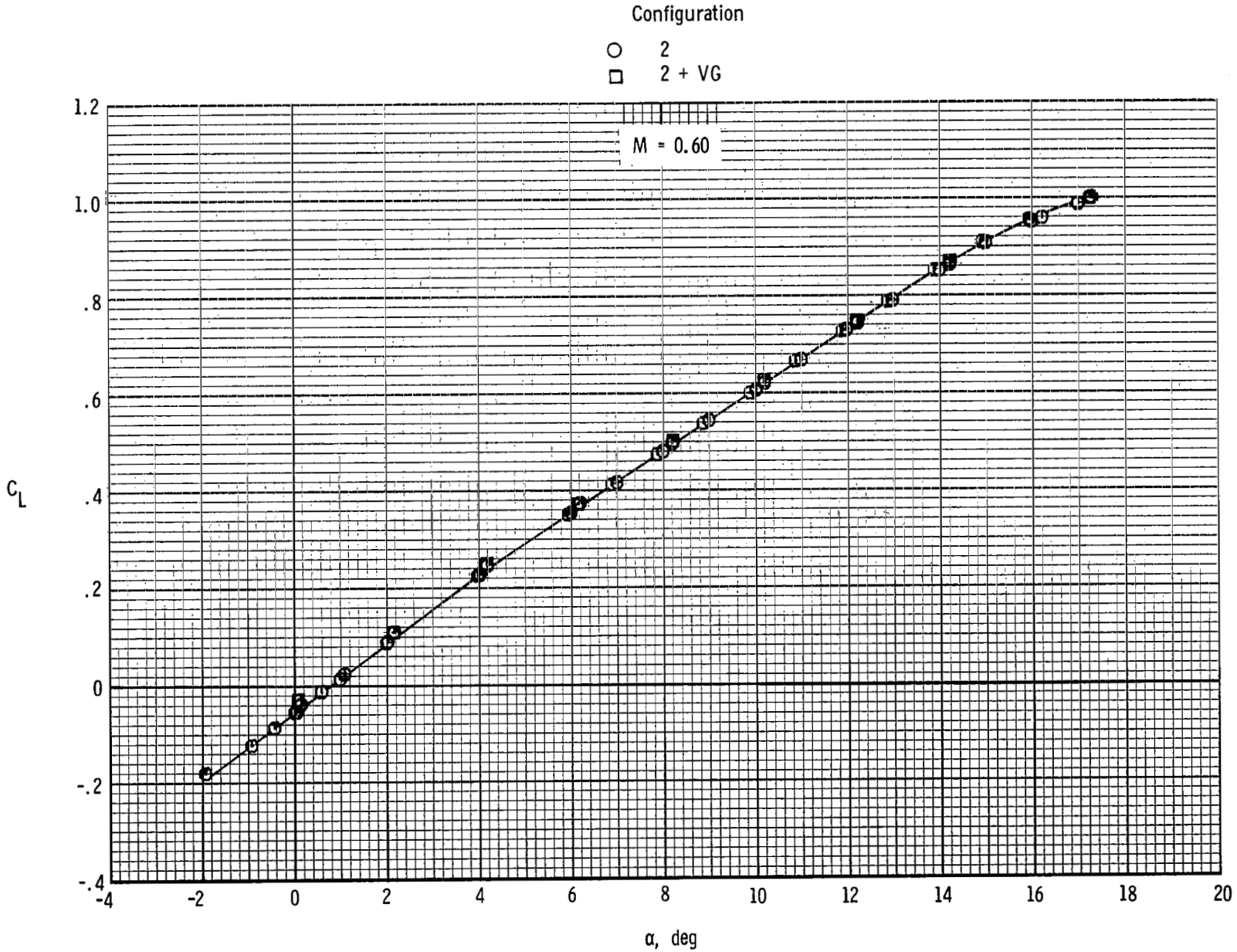

(b) Lift vs angle of attack.

Figure 8.- Continued.

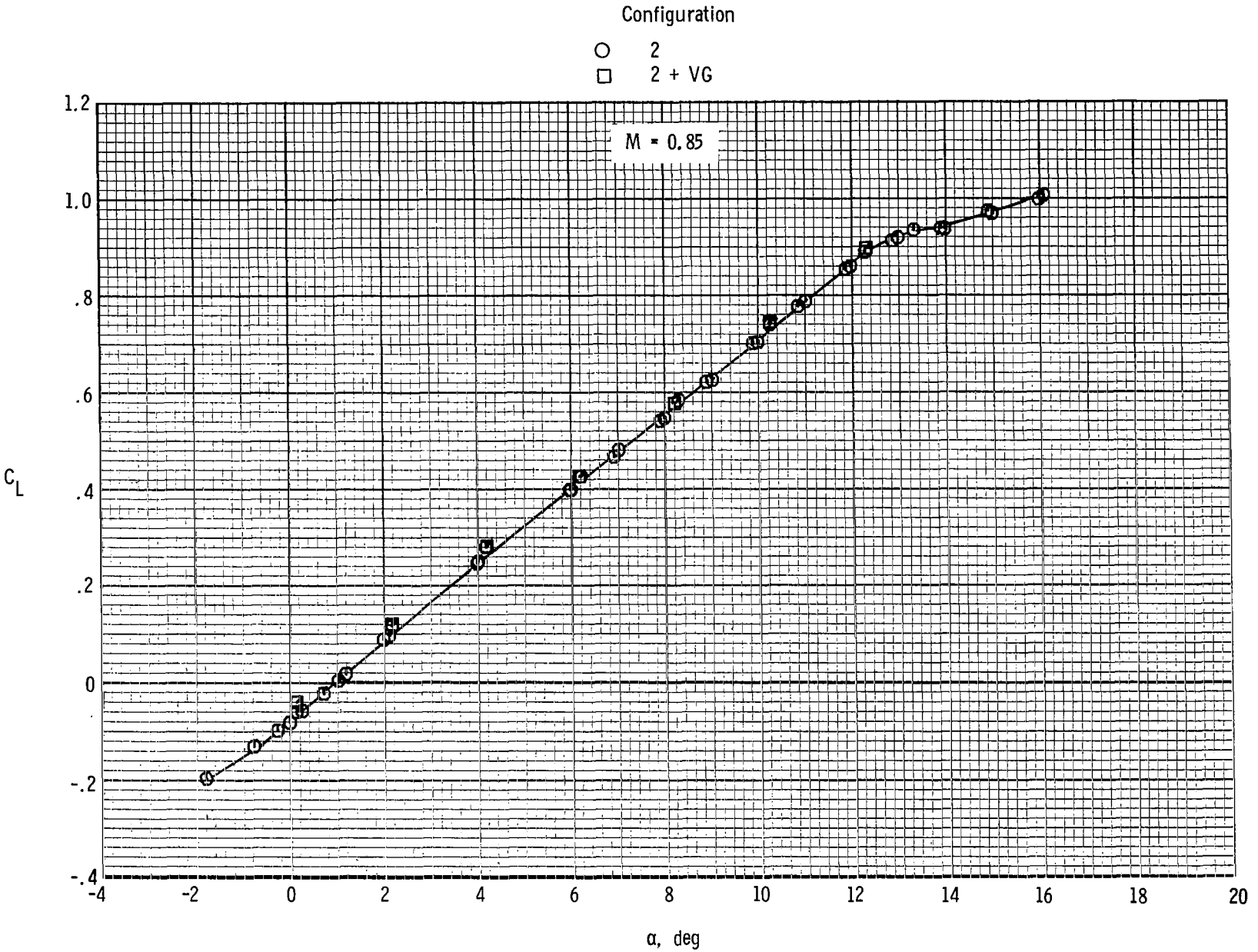

(b) Continued.

Figure 8.- Continued.

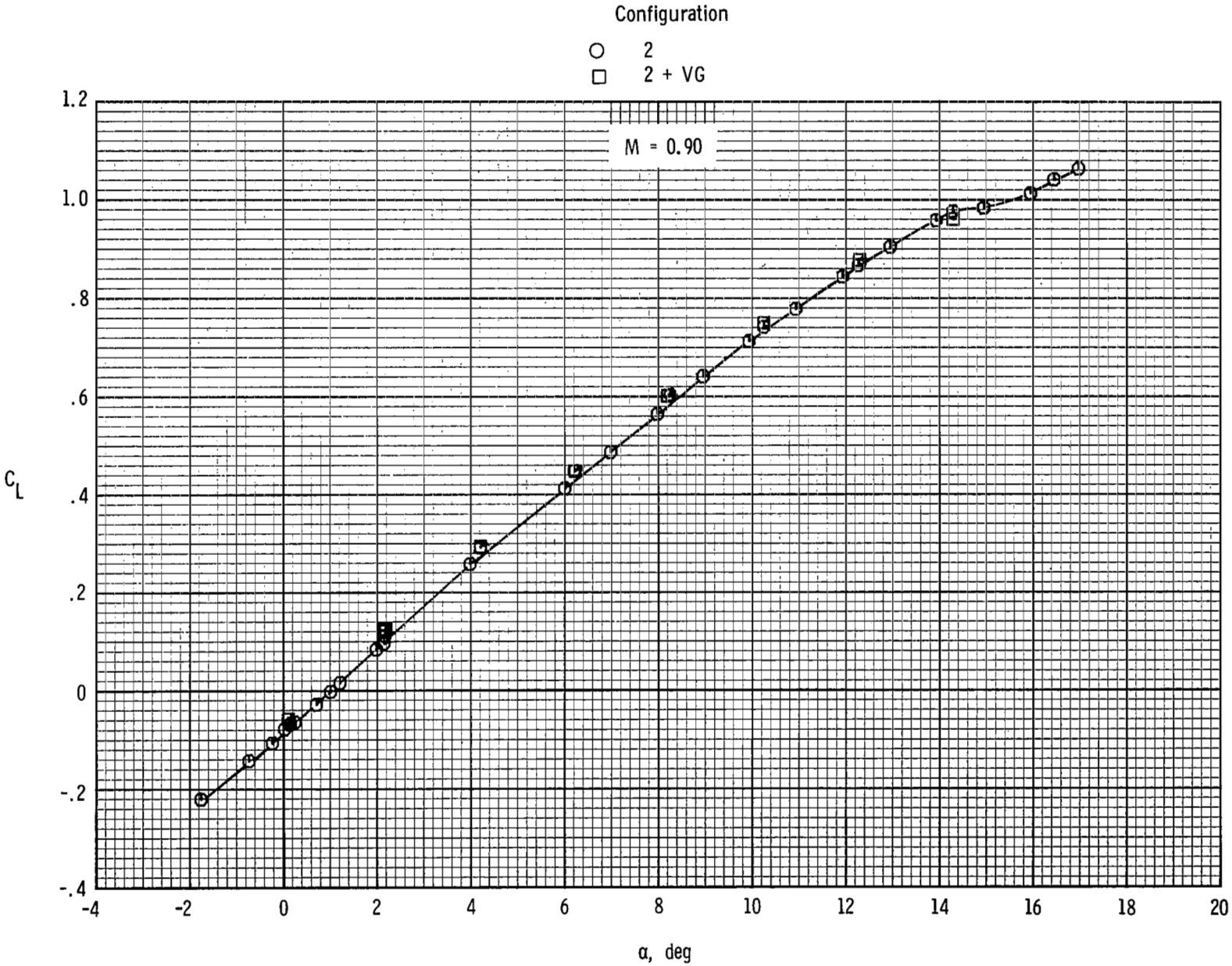

(b) Continued.

Figure 8.- Continued.

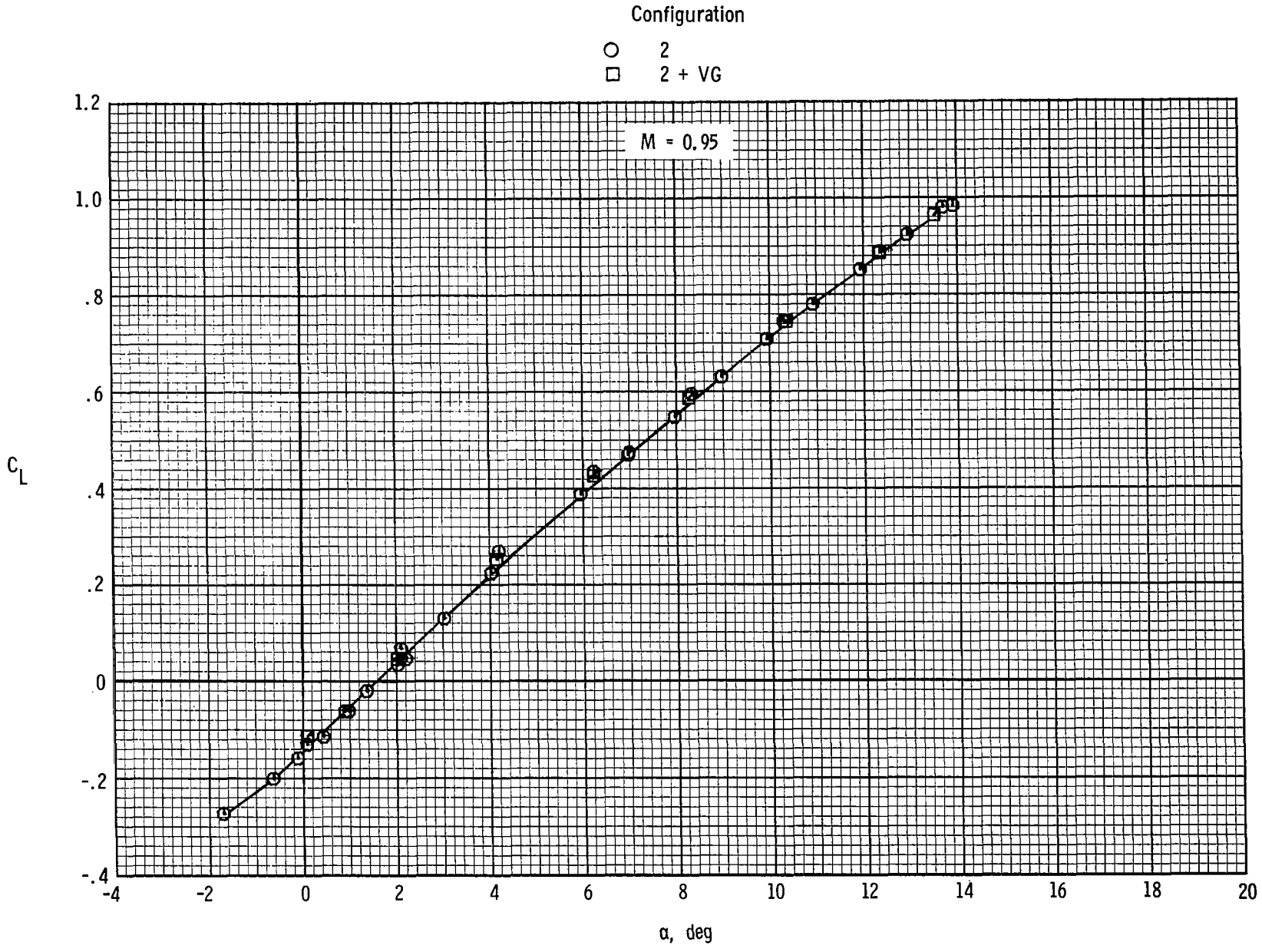

(b) Concluded.

Figure 8.- Continued.

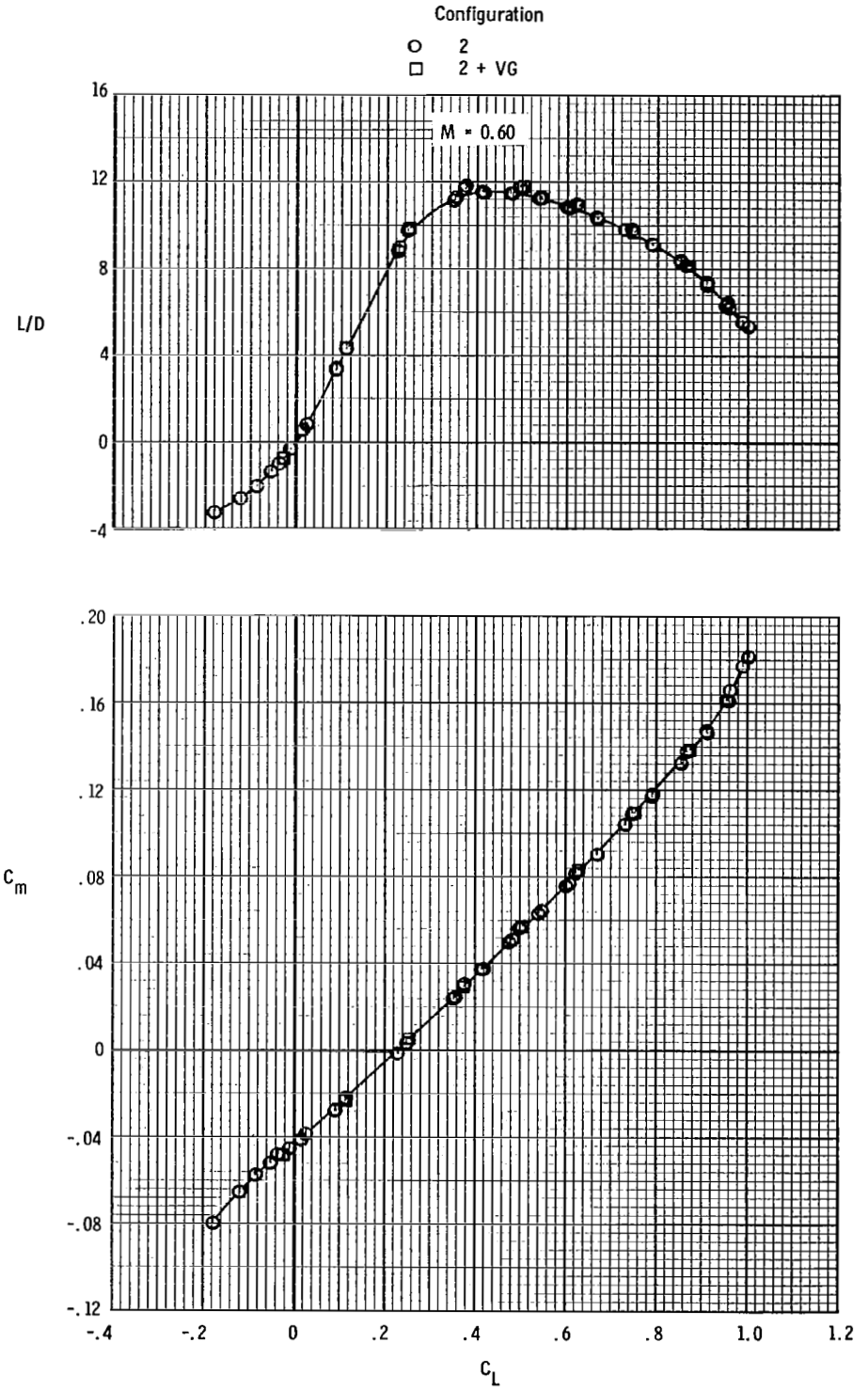

(c) L/D and pitch vs lift.

Figure 8.- Continued.

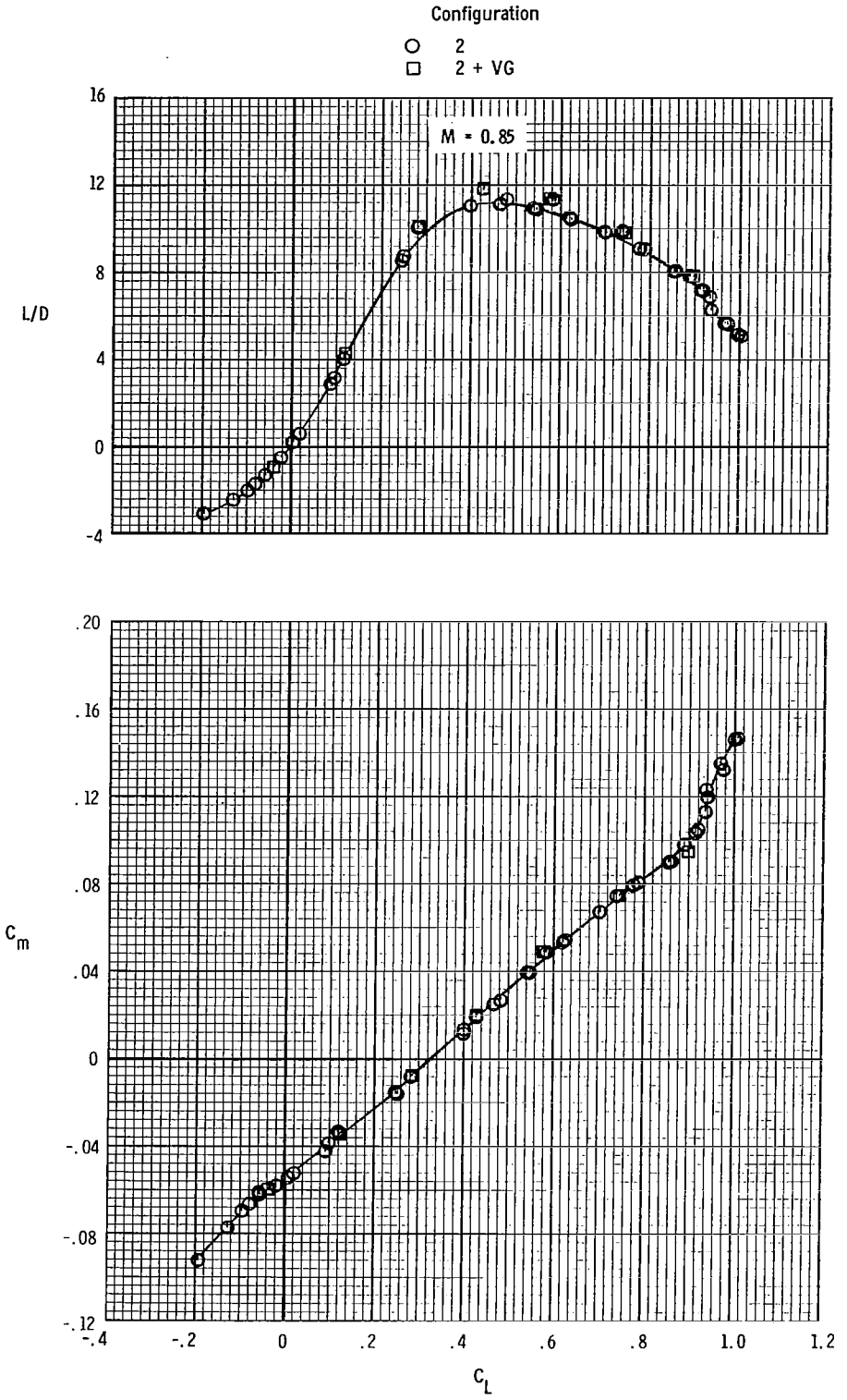

(c) Continued.

Figure 8.- Continued.

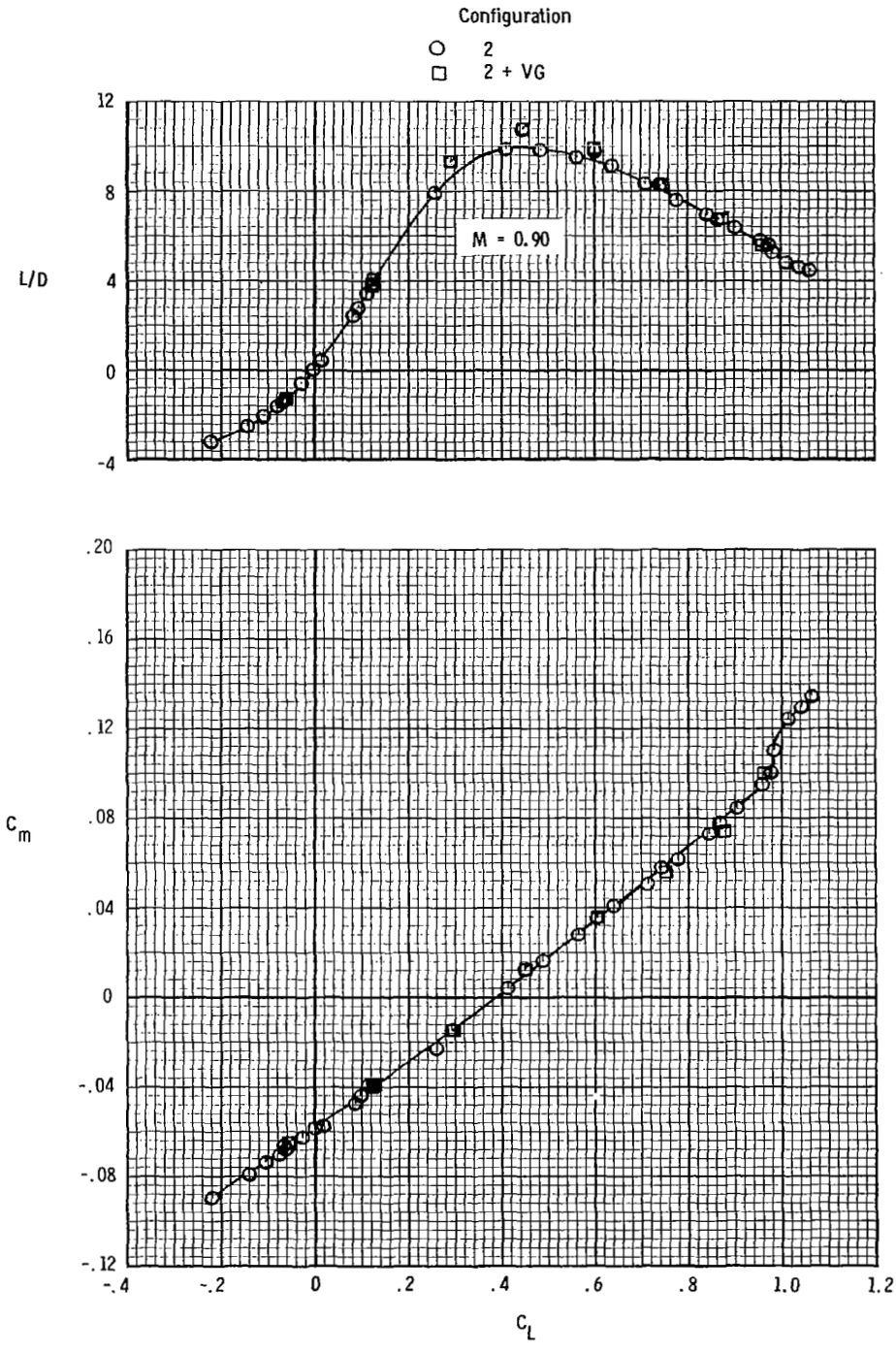

(c) Continued.

Figure 8.- Continued.

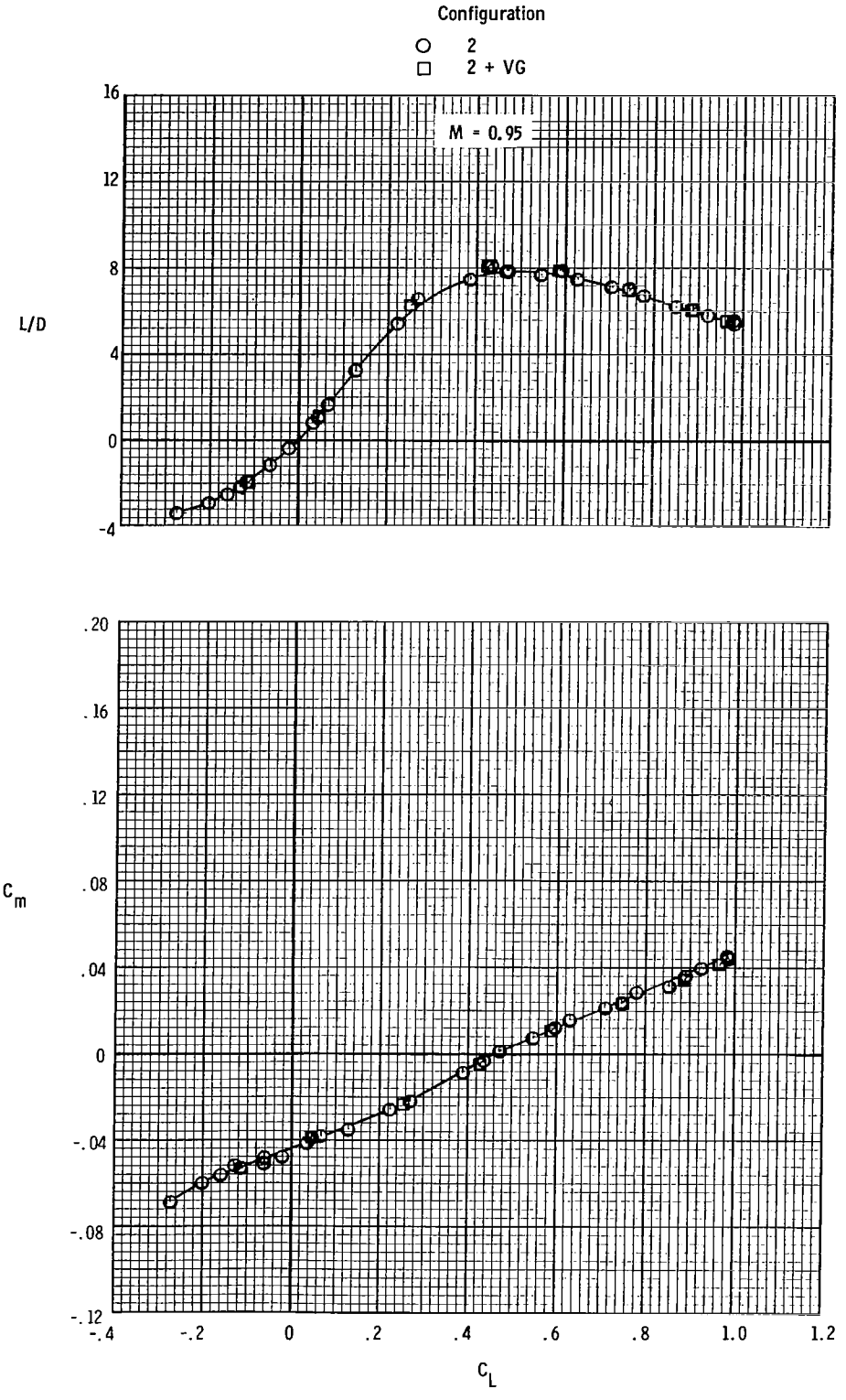

(c) Concluded.

Figure 8.- Concluded.

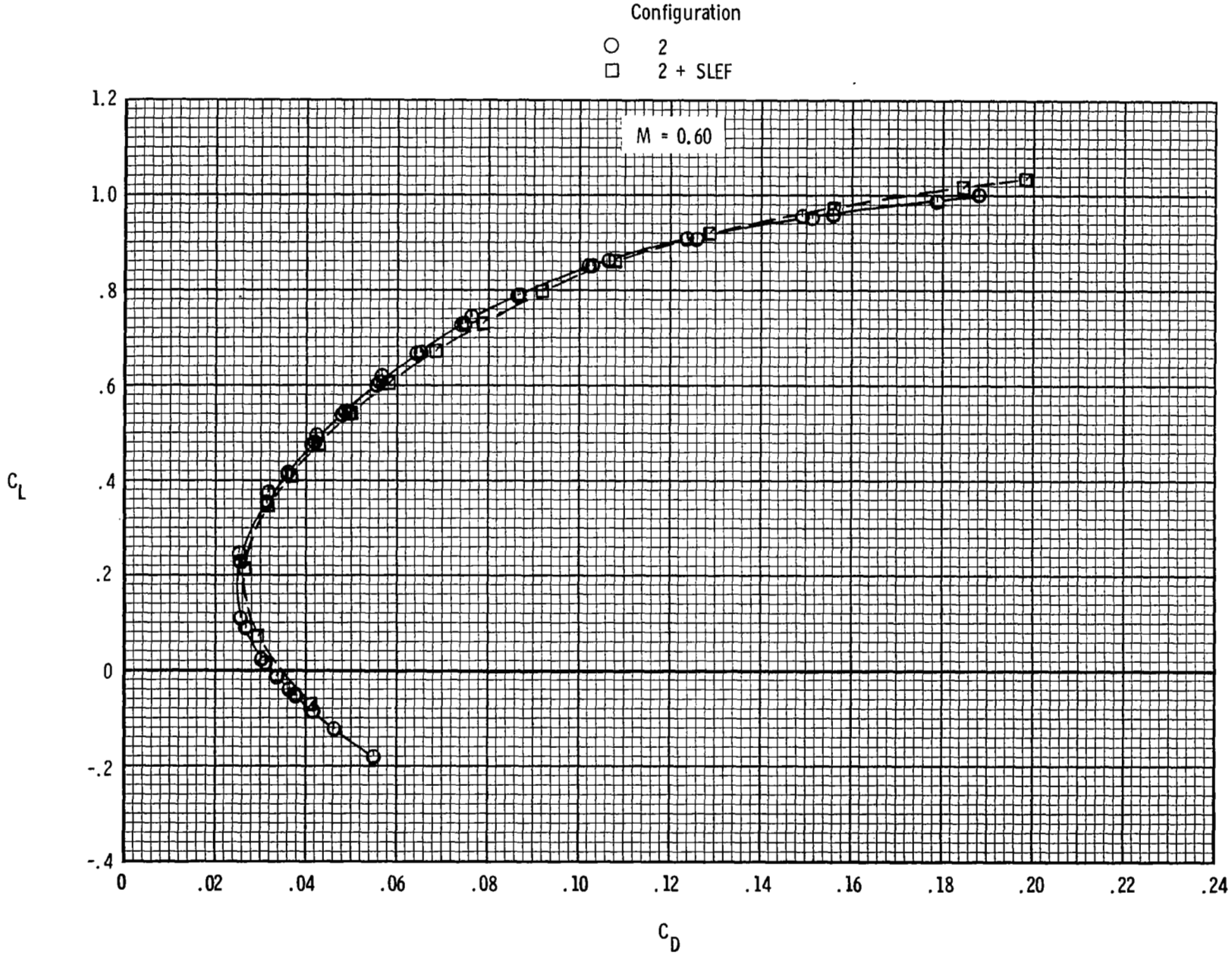

(a) Lift vs drag.

Figure 9.- Effect of wing sharp leading-edge flaps on longitudinal aerodynamic characteristics.

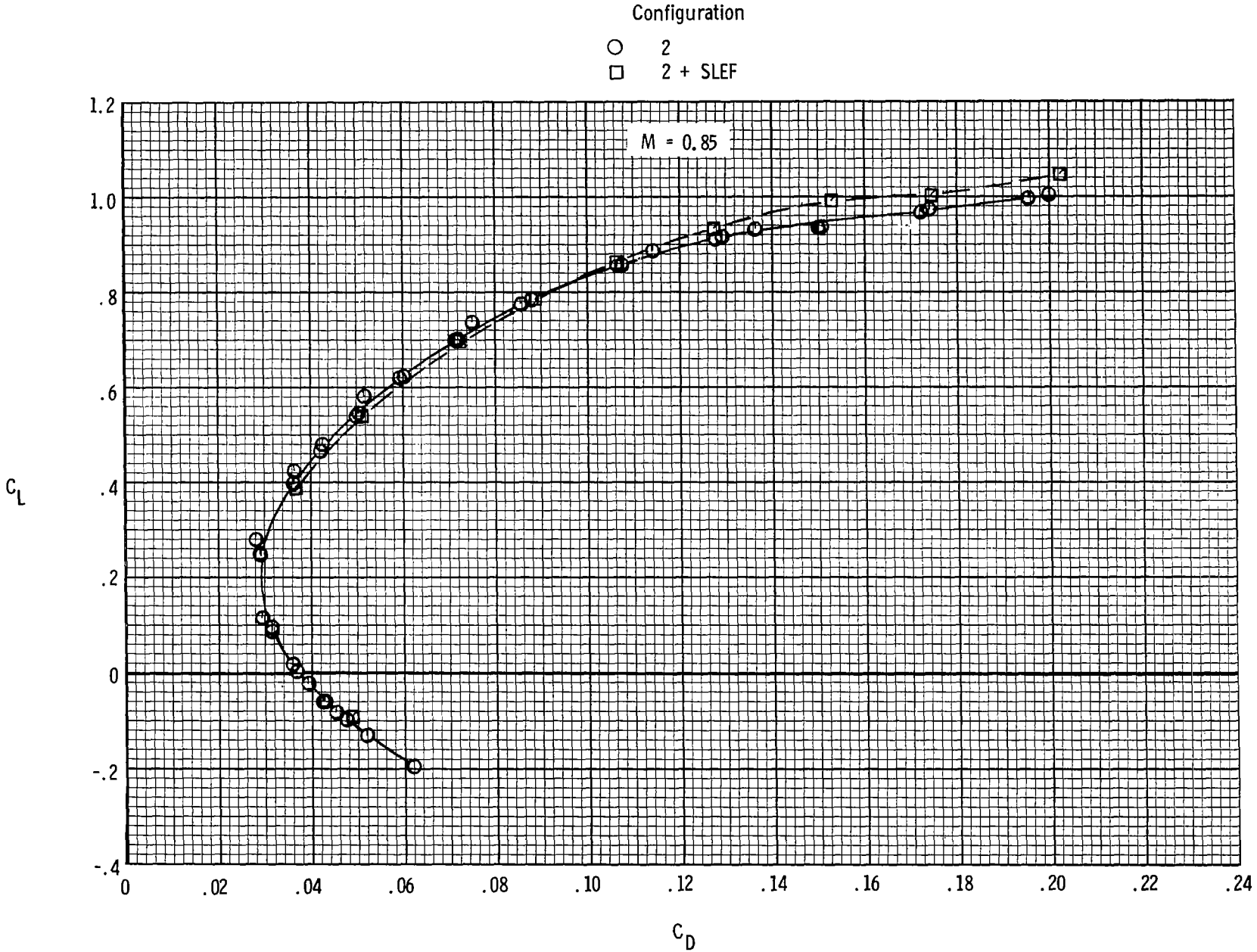

(a) Continued.

Figure 9.- Continued.

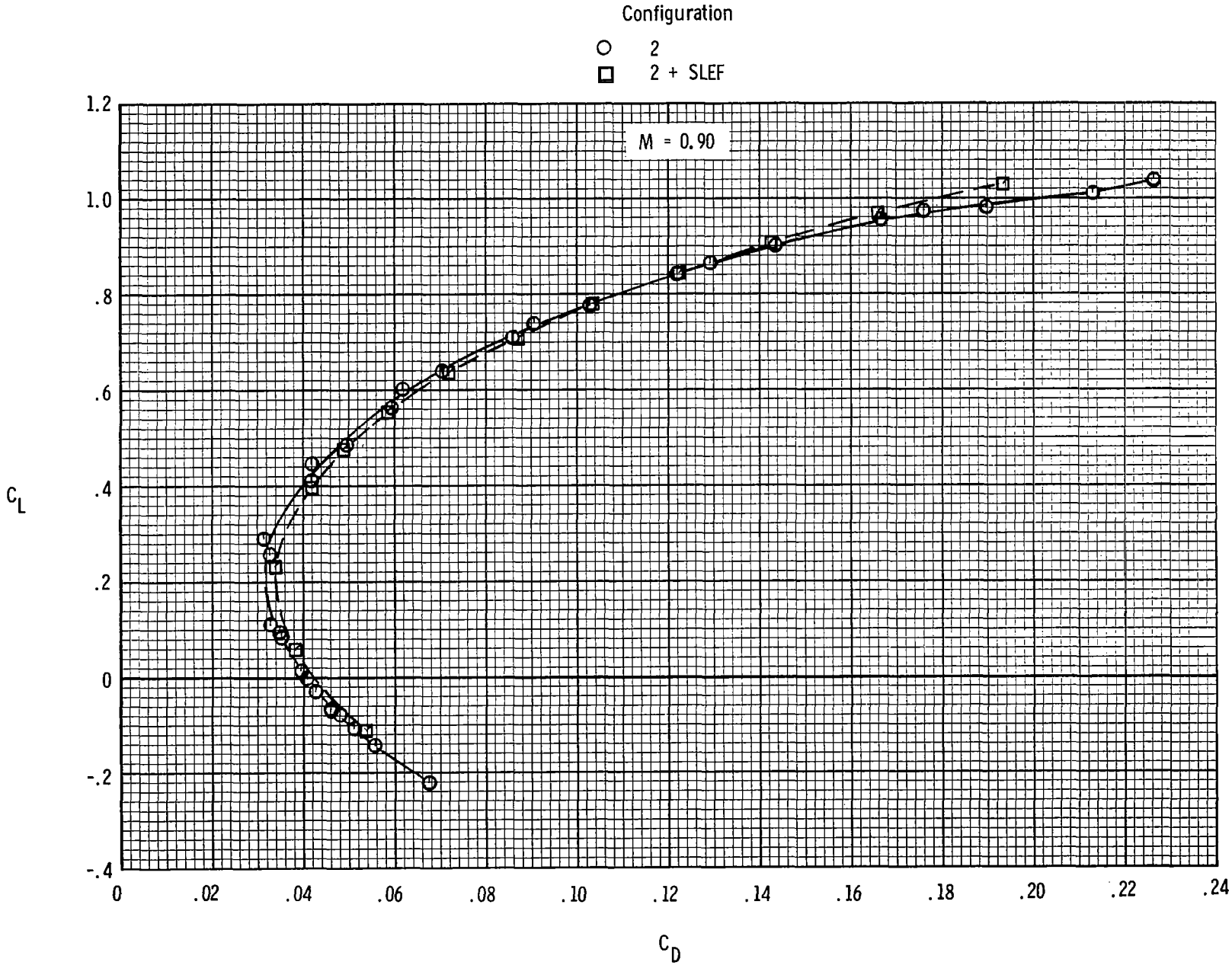

(a) Continued.

Figure 9.- Continued.

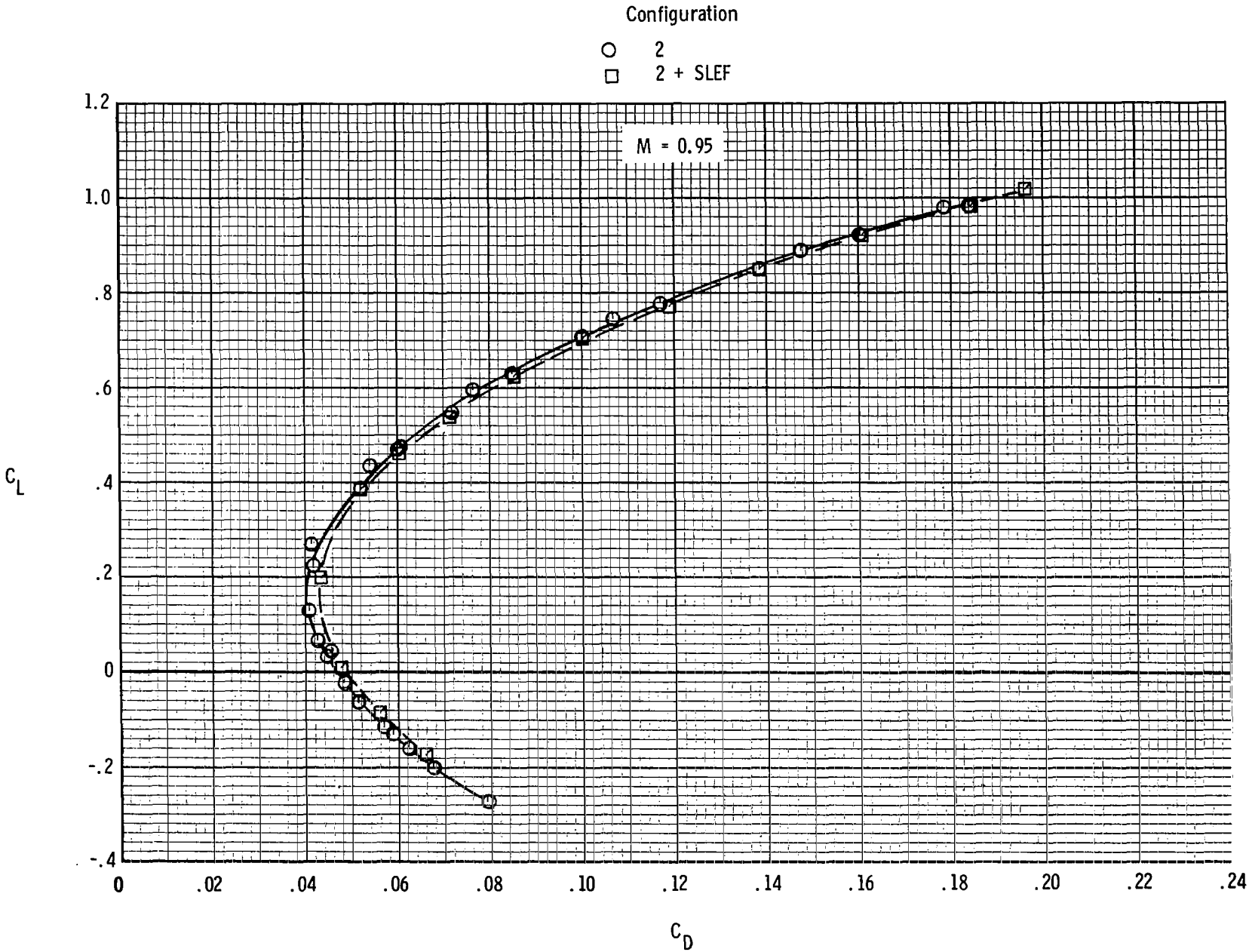

(a) Concluded.

Figure 9.- Continued.

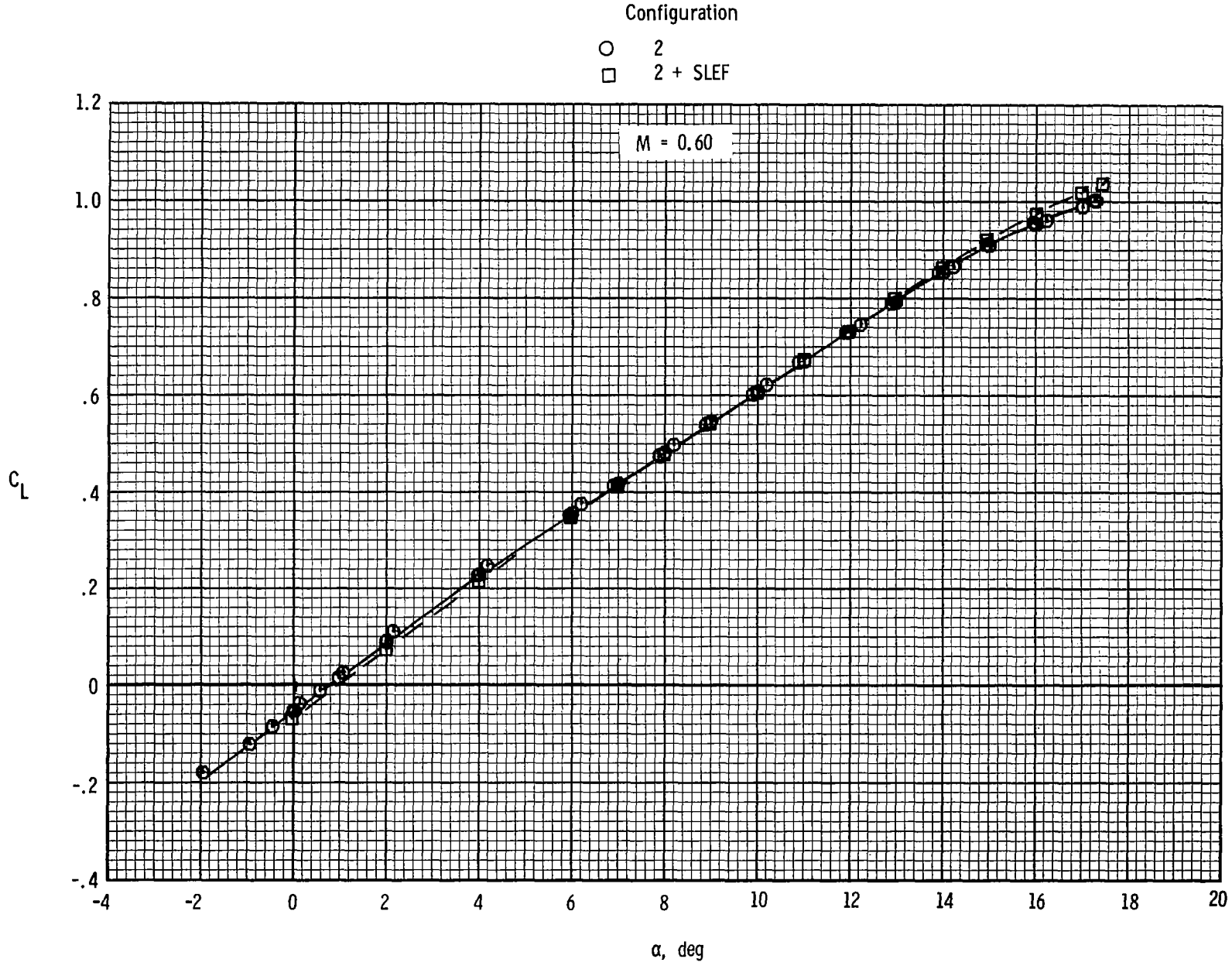

(b) Lift vs angle of attack.

Figure 9.- Continued.

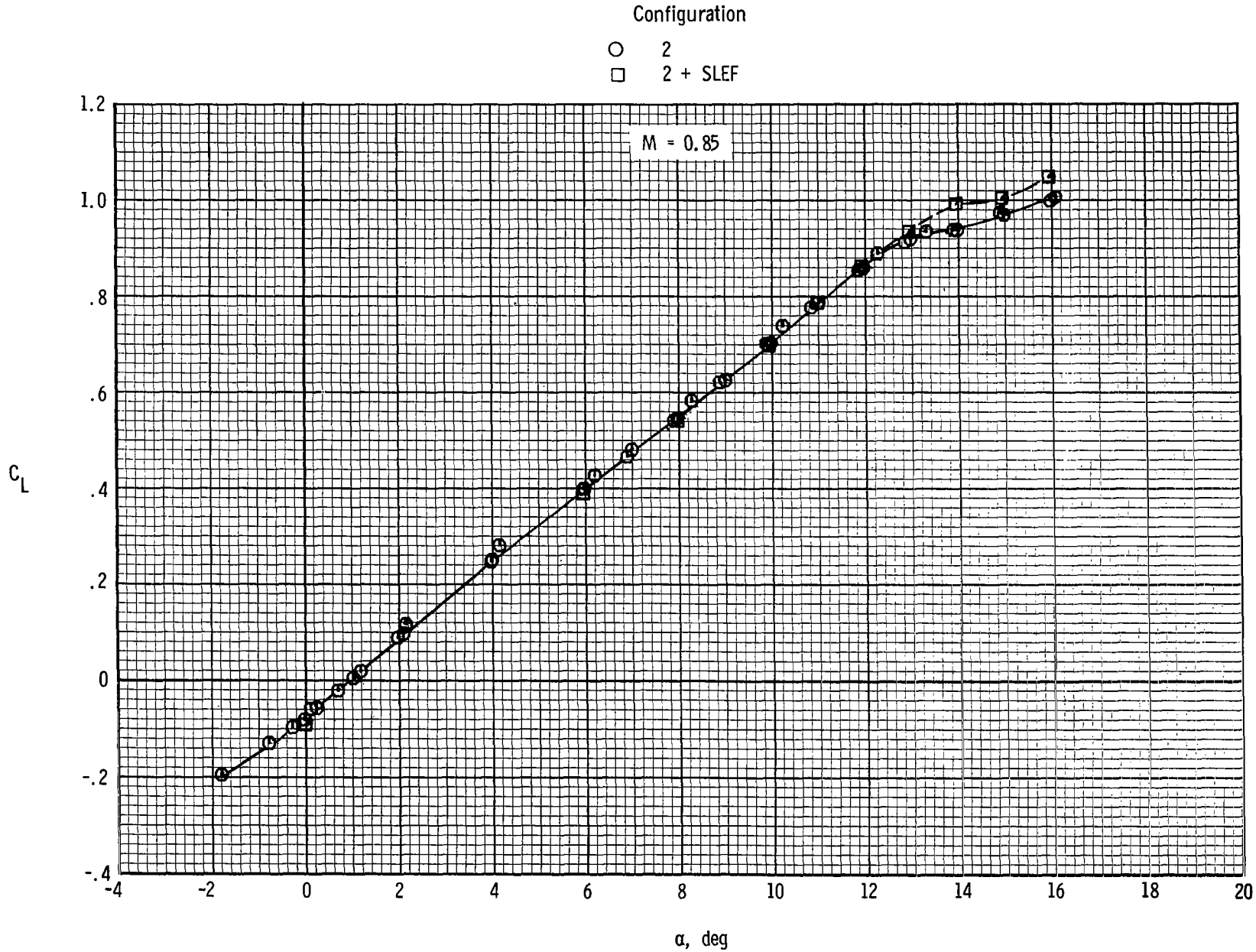

(b) Continued.

Figure 9.- Continued.

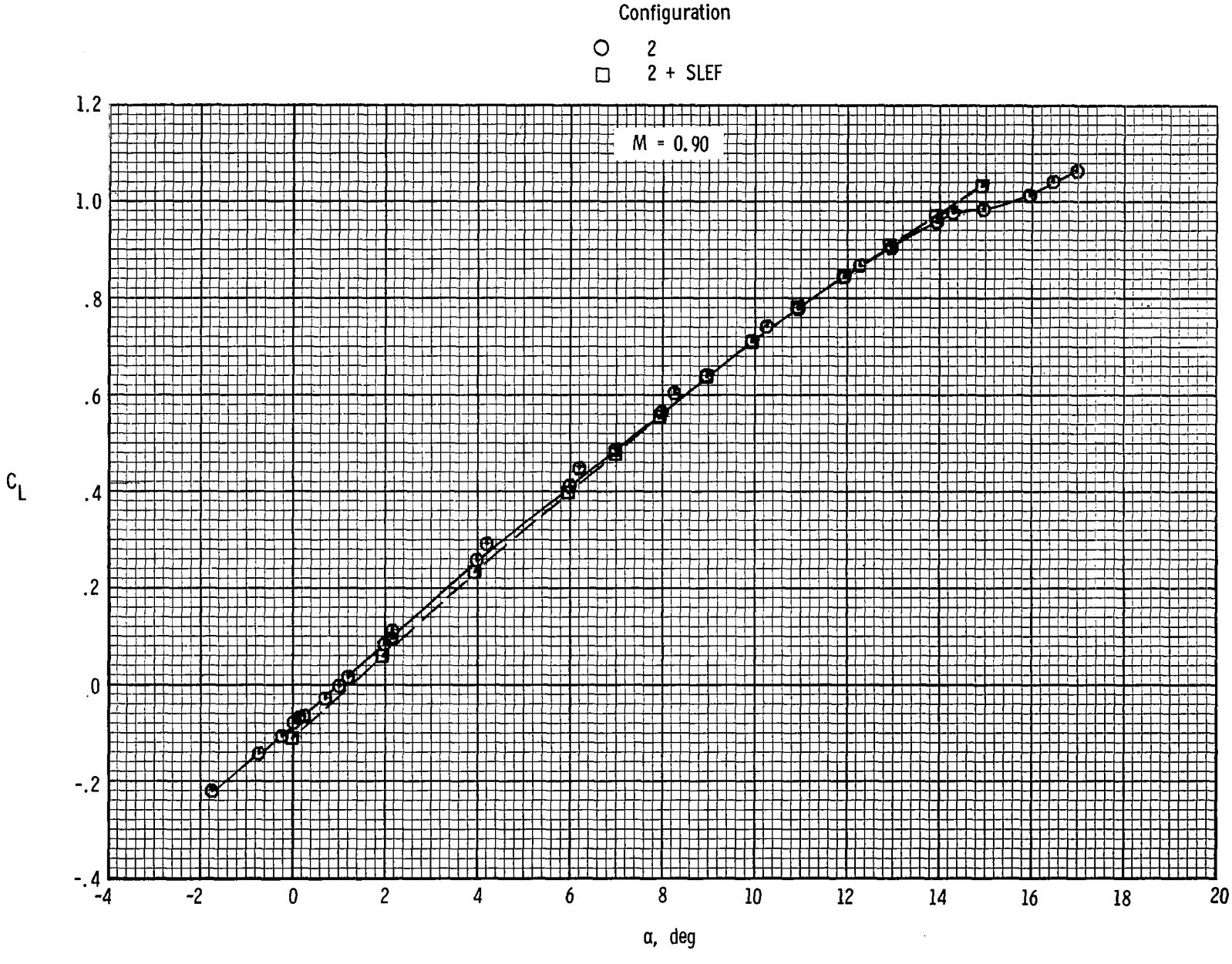

(b) Continued.

Figure 9.- Continued.

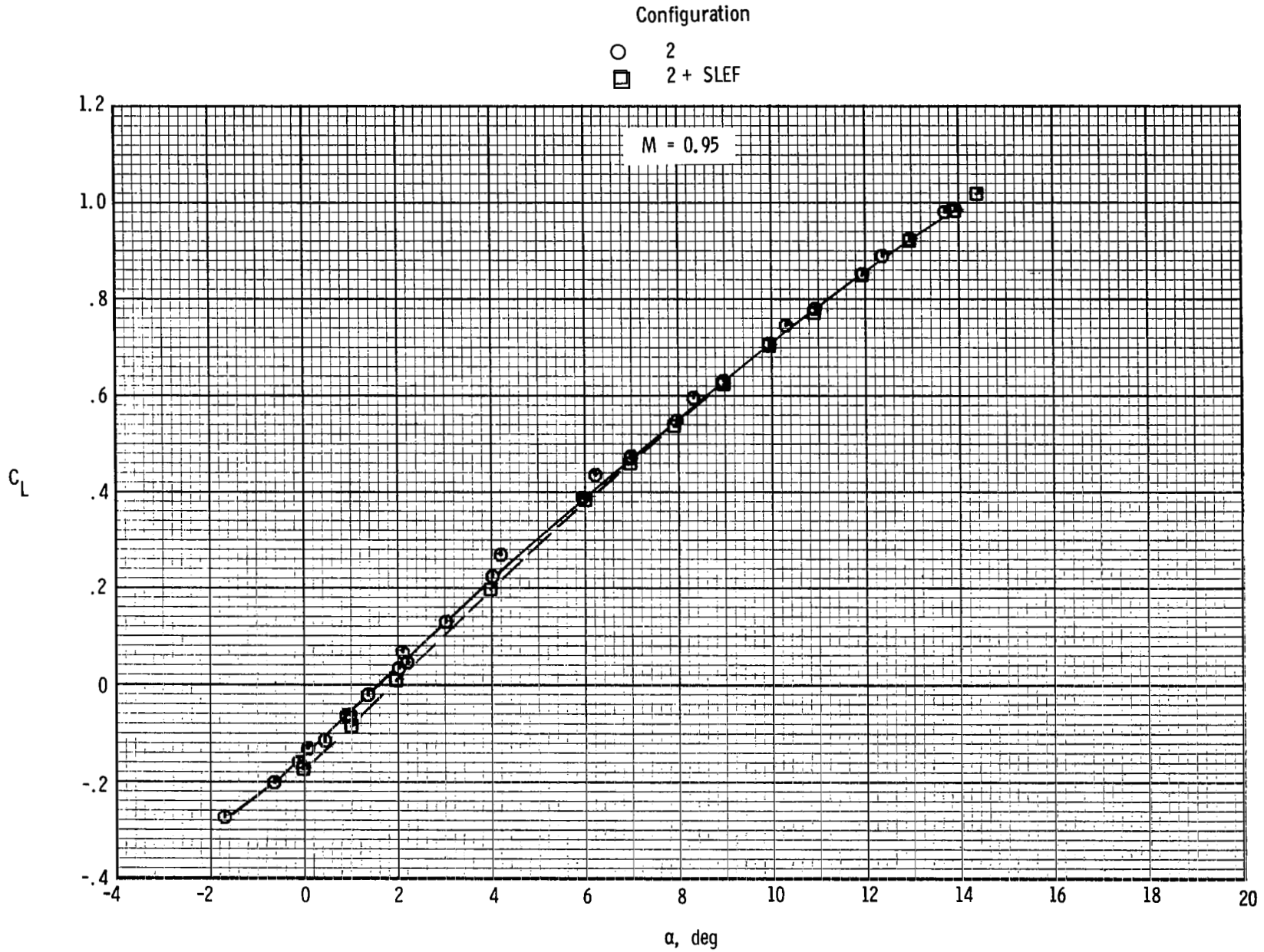

(b) Concluded.

Figure 9.- Continued.

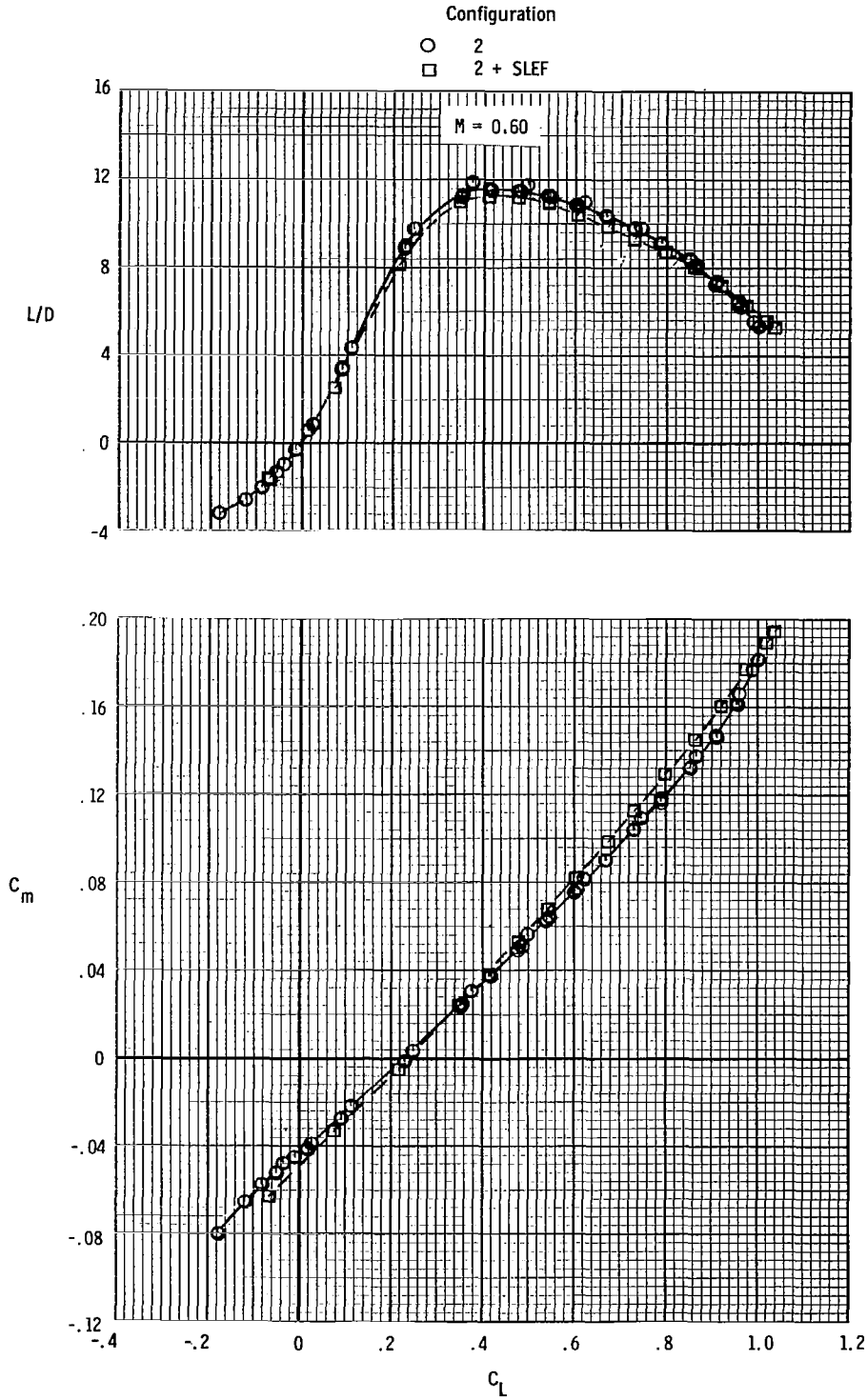

(c) L/D and pitch vs lift.

Figure 9.- Continued.

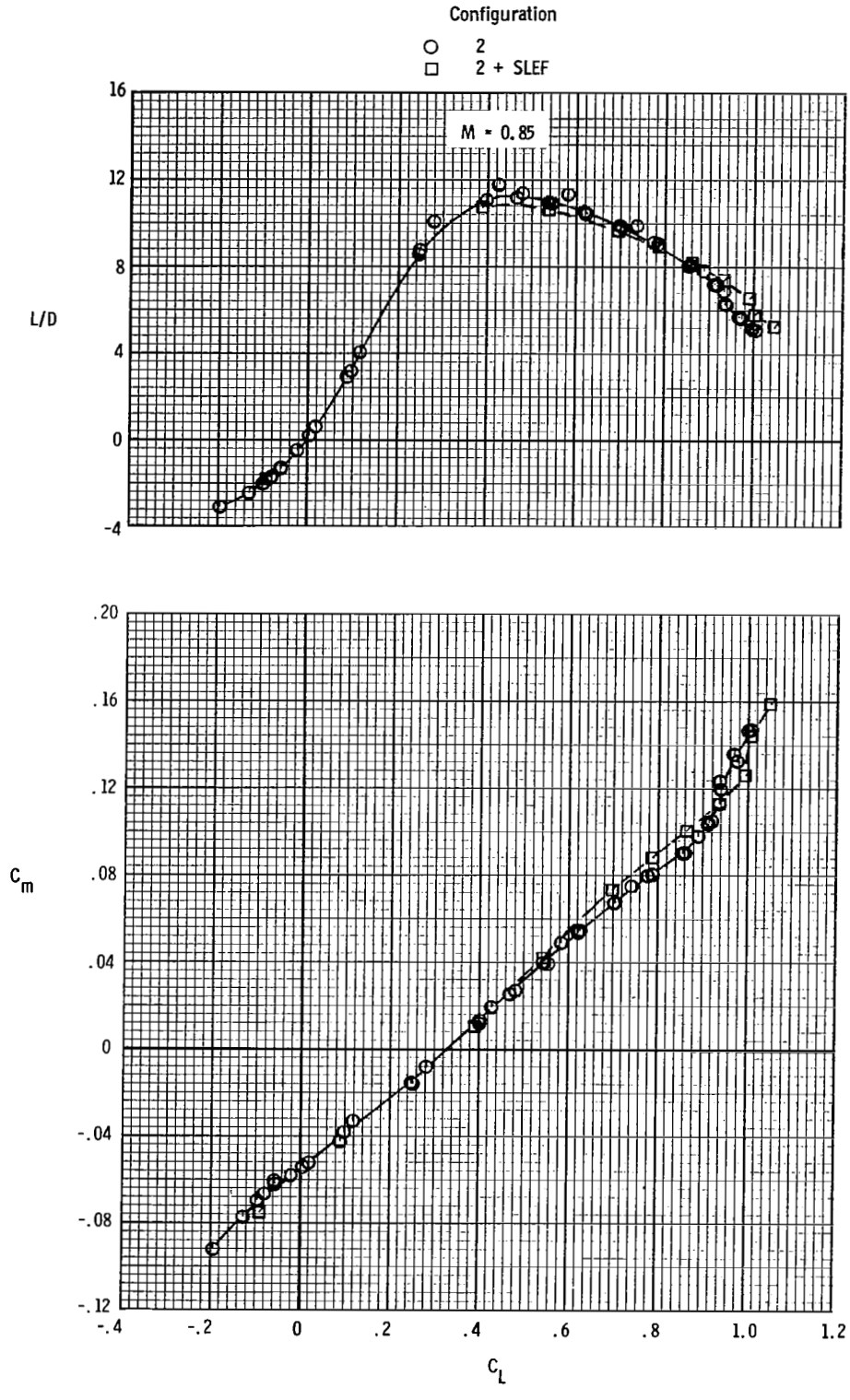

(c) Continued.

Figure 9.- Continued.

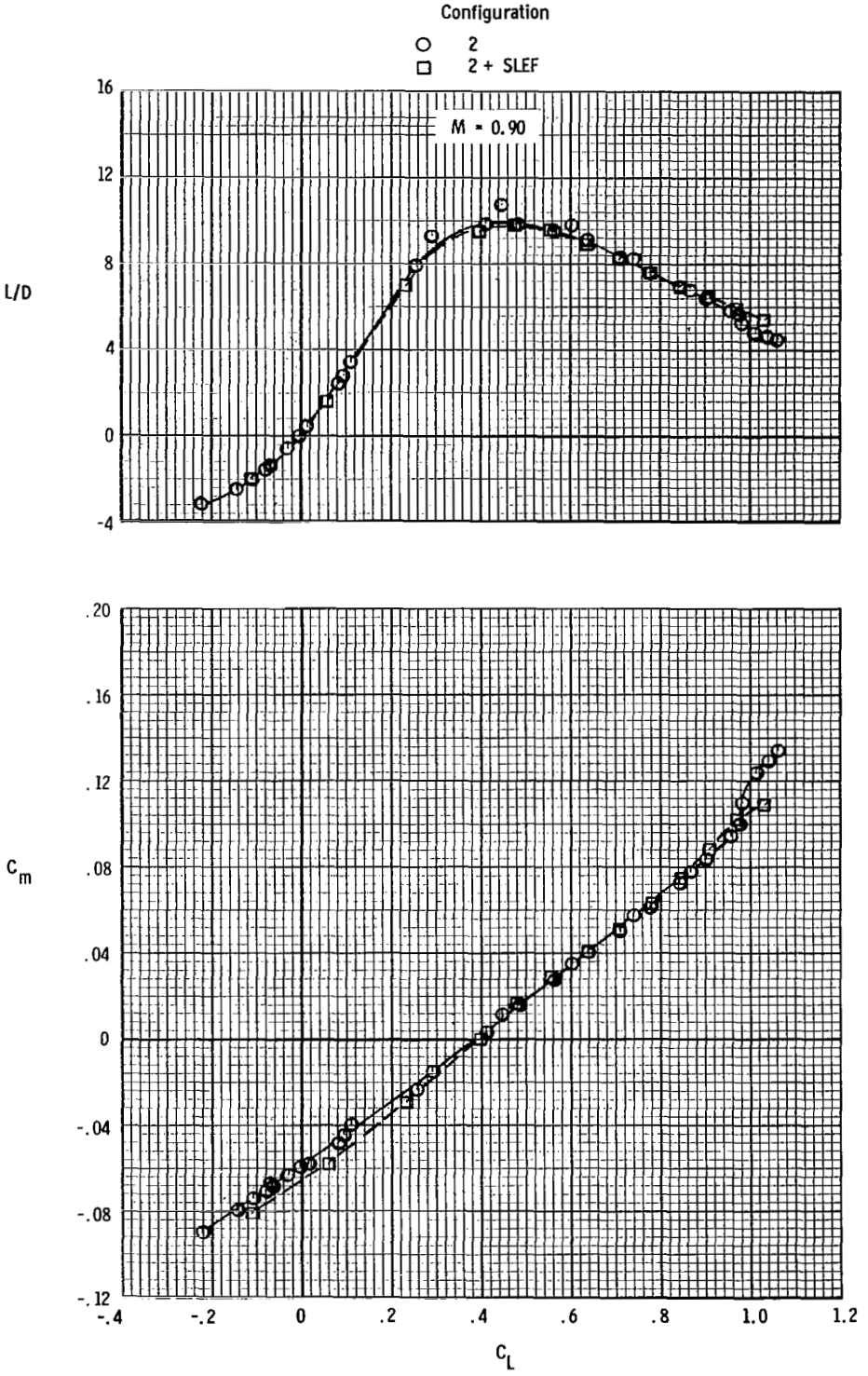

(c) Continued.

Figure 9.- Continued.

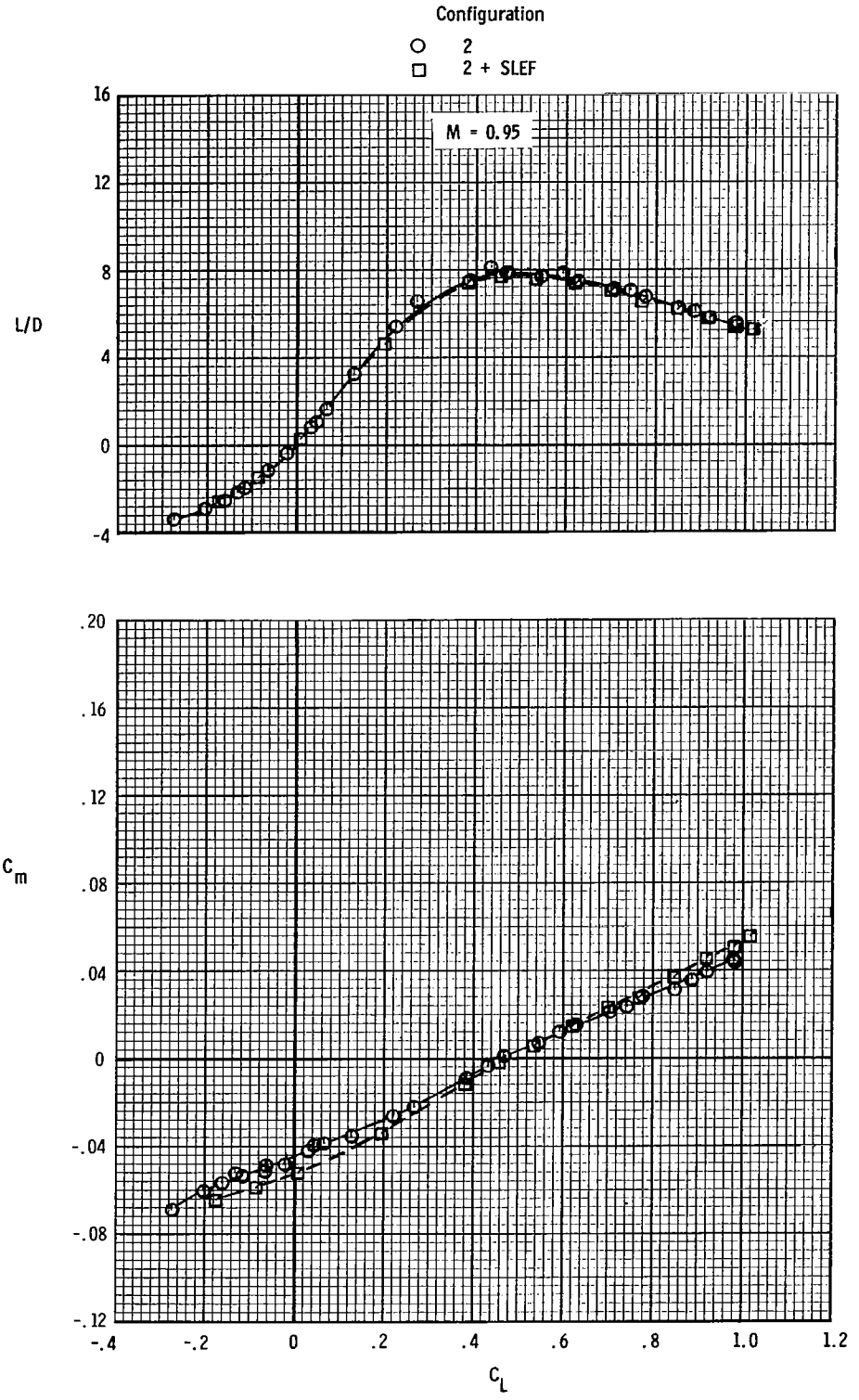

(c) Concluded.

Figure 9.- Concluded.

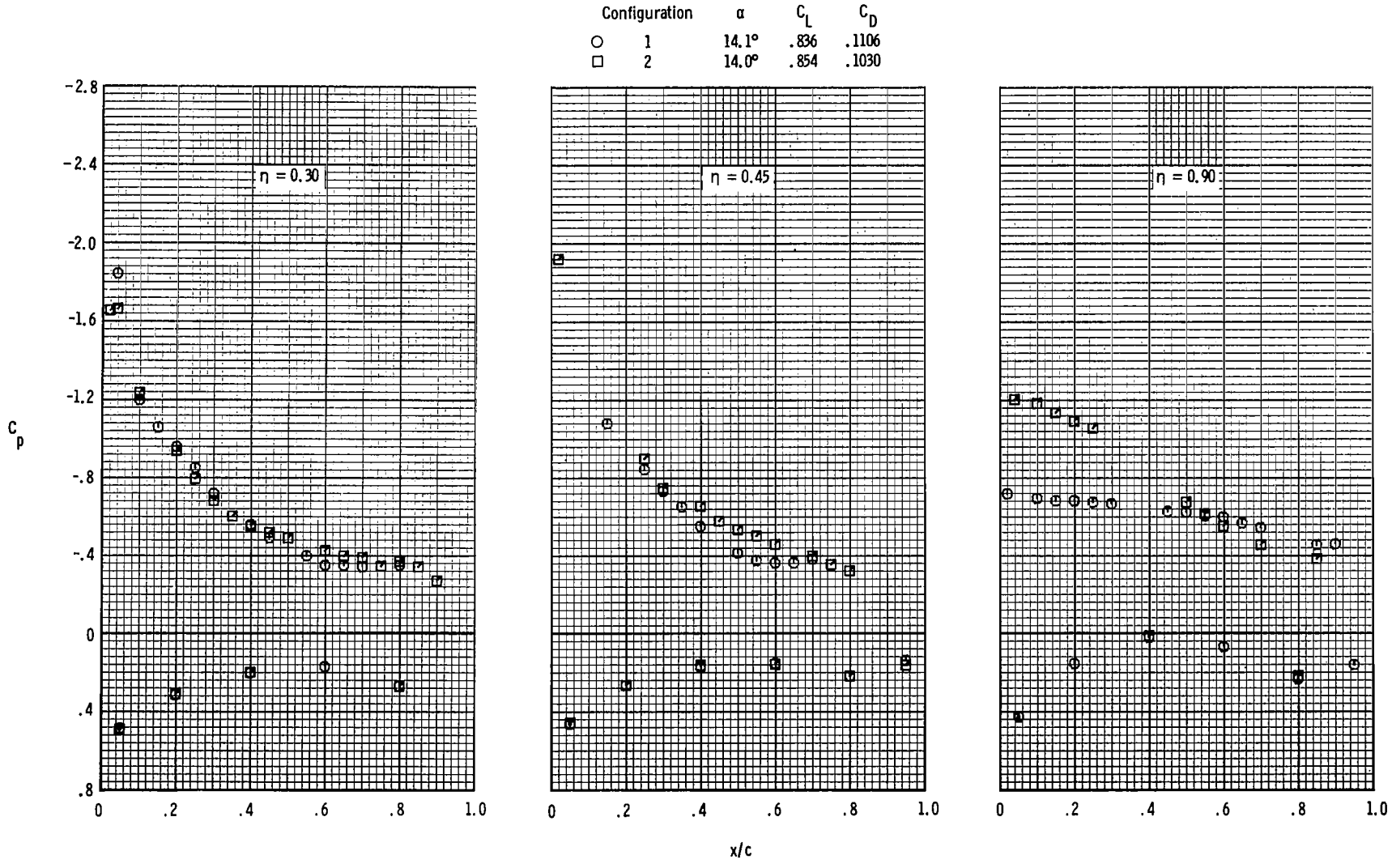

(a) M = 0.60; $\alpha \approx 14°$.

Figure 10.- Effect of wing contouring on wing upper- and lower-surface pressure coefficients.

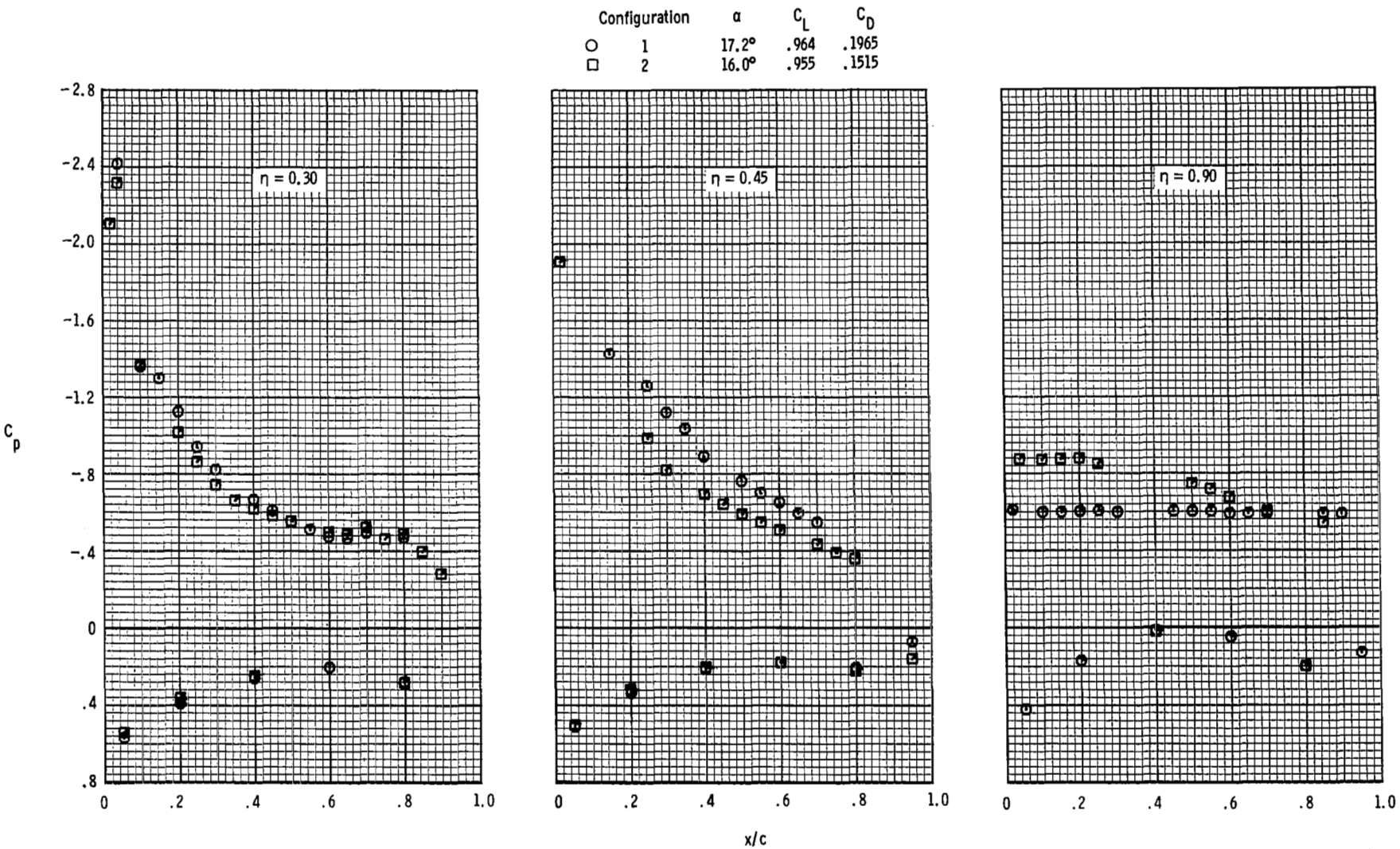

(b) M = 0.60; $\alpha \approx 16°$.

Figure 10.- Continued.

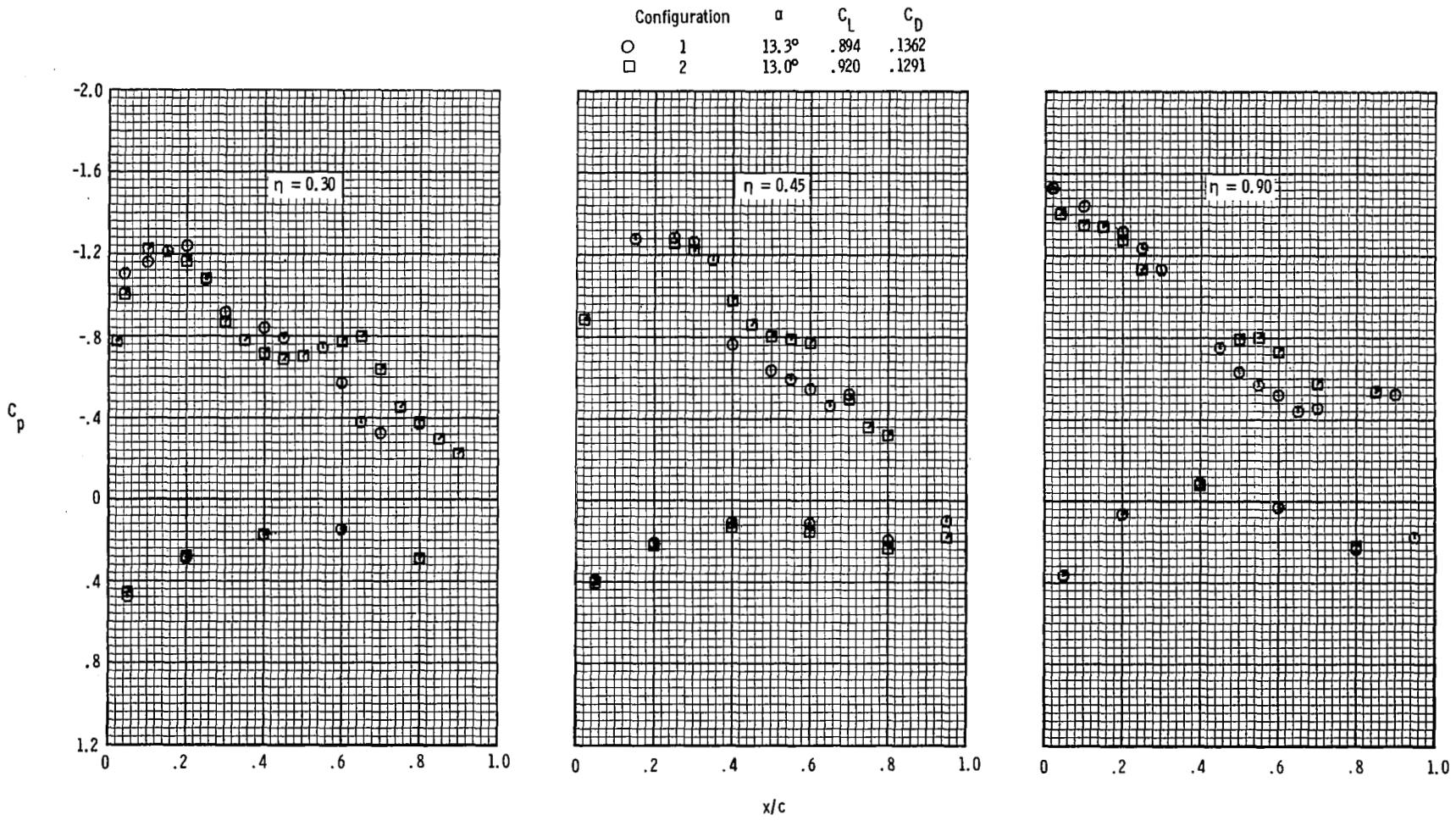

(c) M = 0.85; $\alpha \approx 13°$.

Figure 10.- Continued.

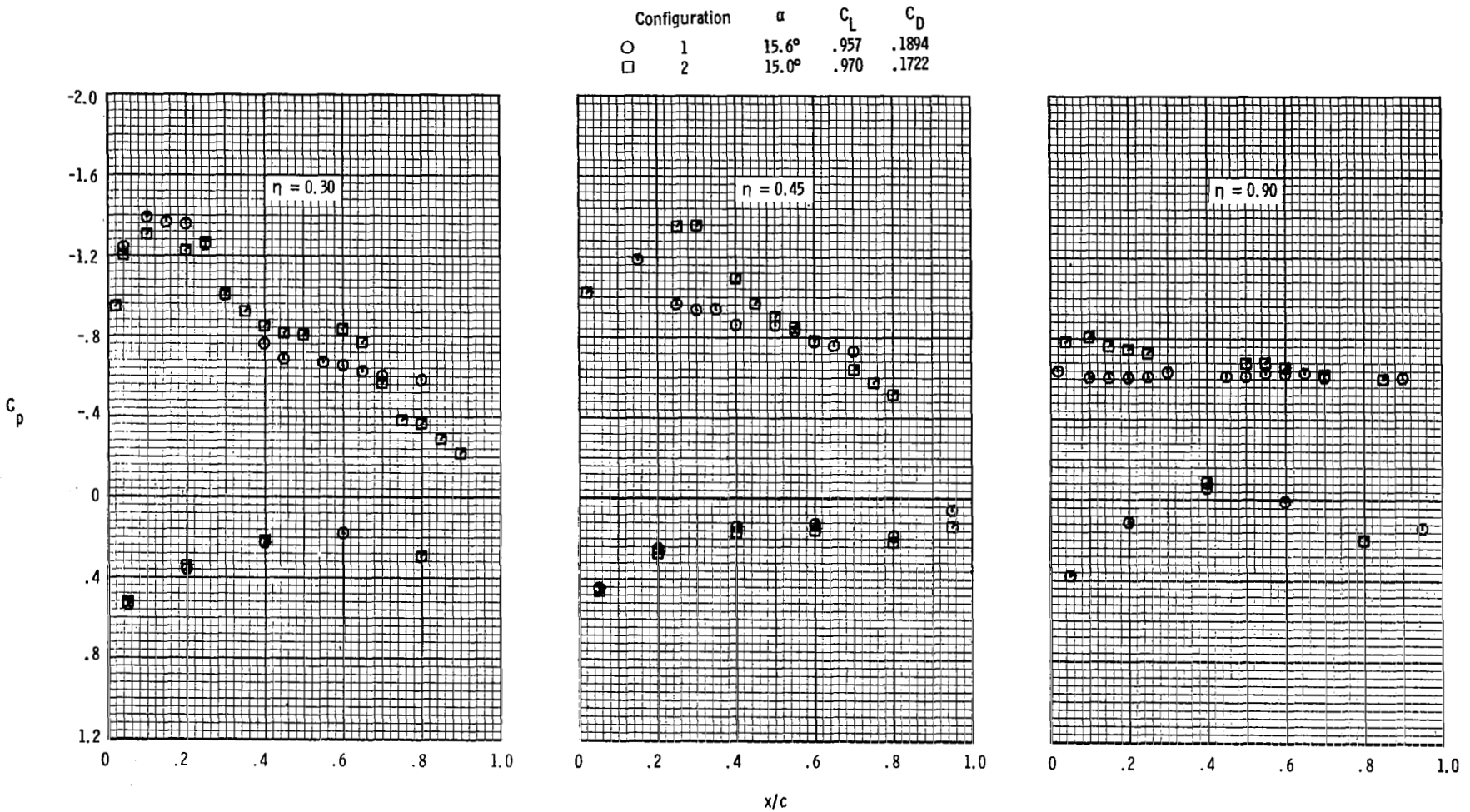

(d) M = 0.85; $\alpha \approx 15°$.

Figure 10.- Continued.

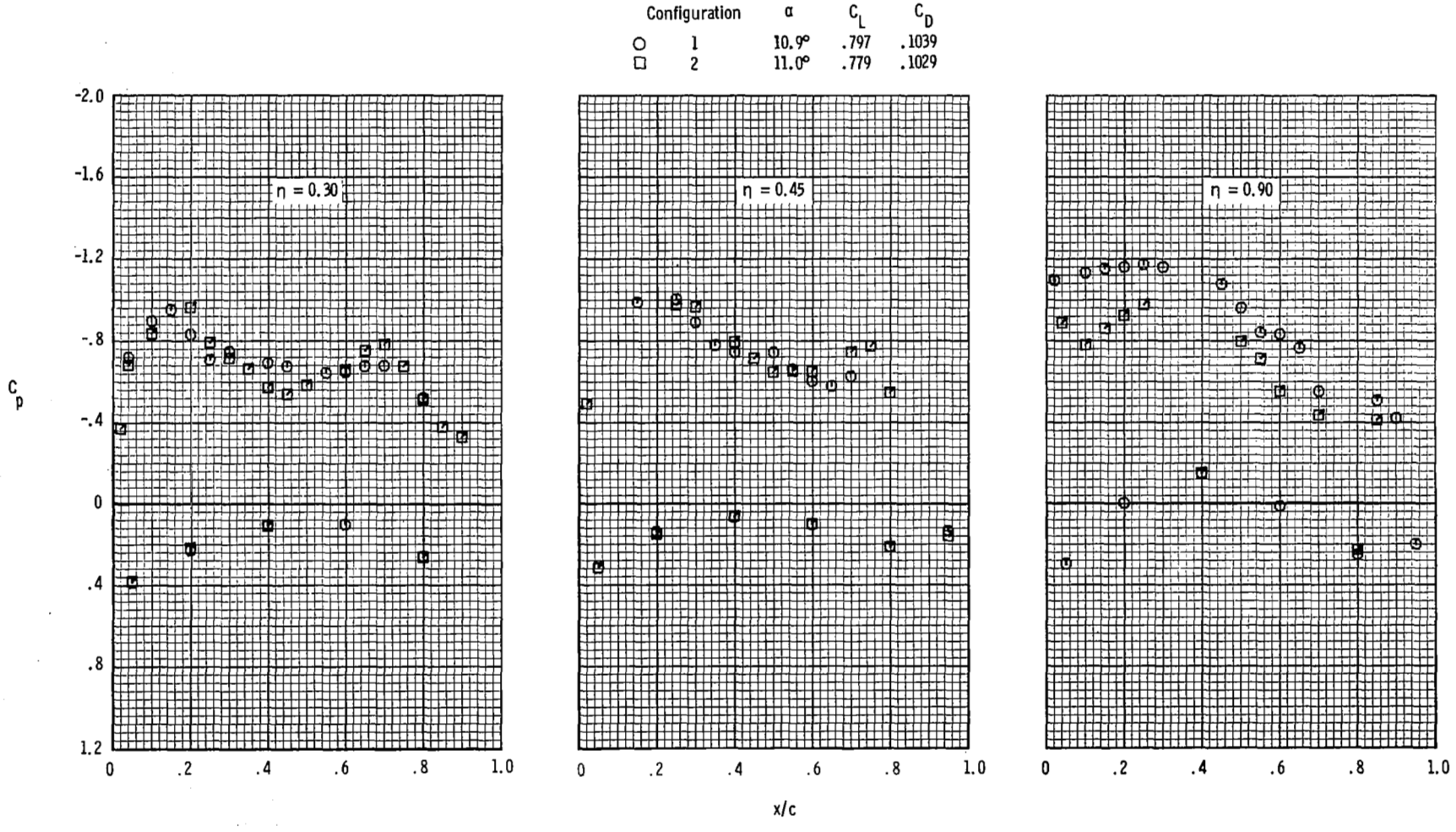

(e) M = 0.90; α ≈ 11°.

Figure 10.- Continued.

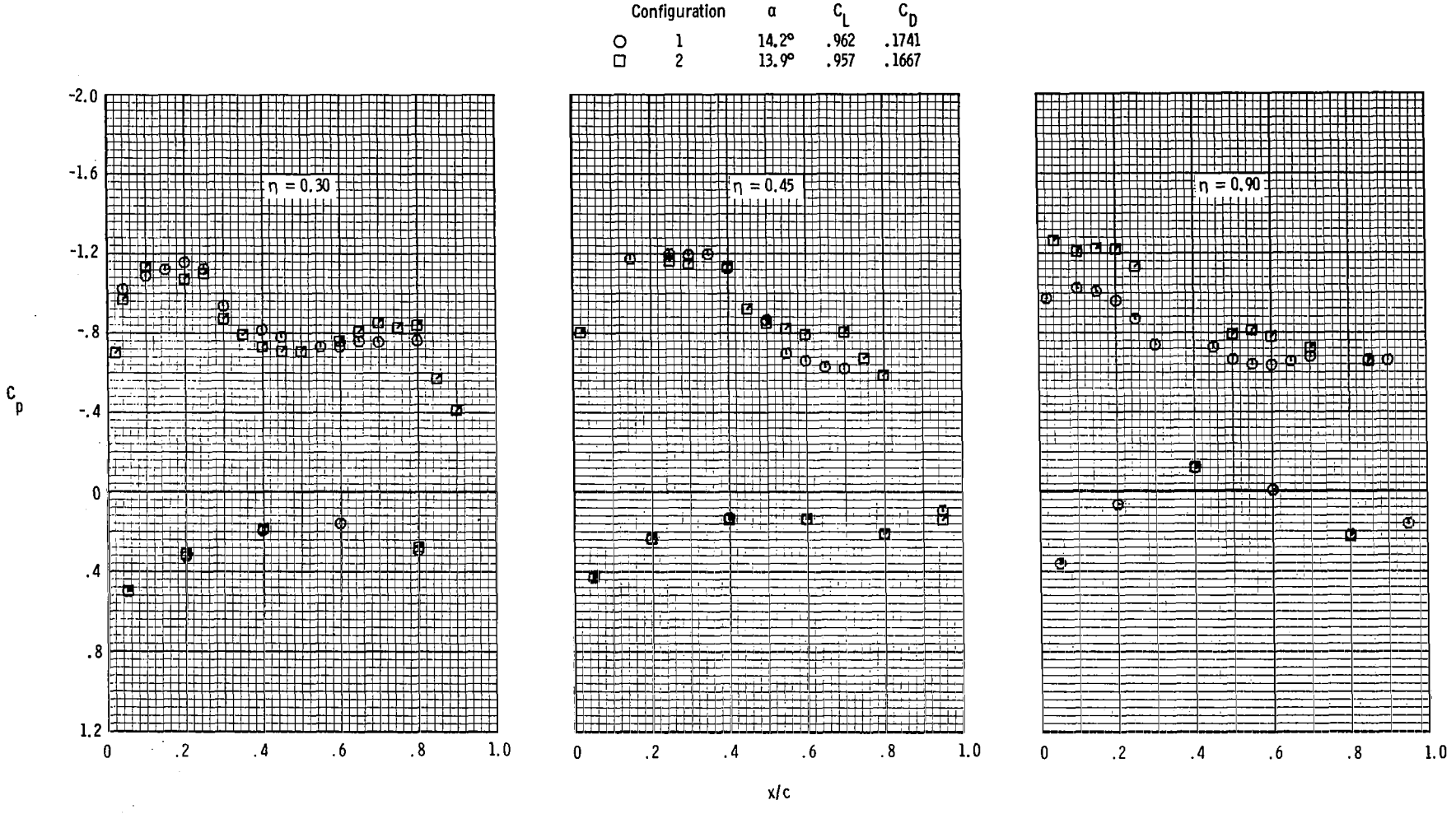

(f) M = 0.90; $\alpha \approx 14°$.

Figure 10.- Concluded.

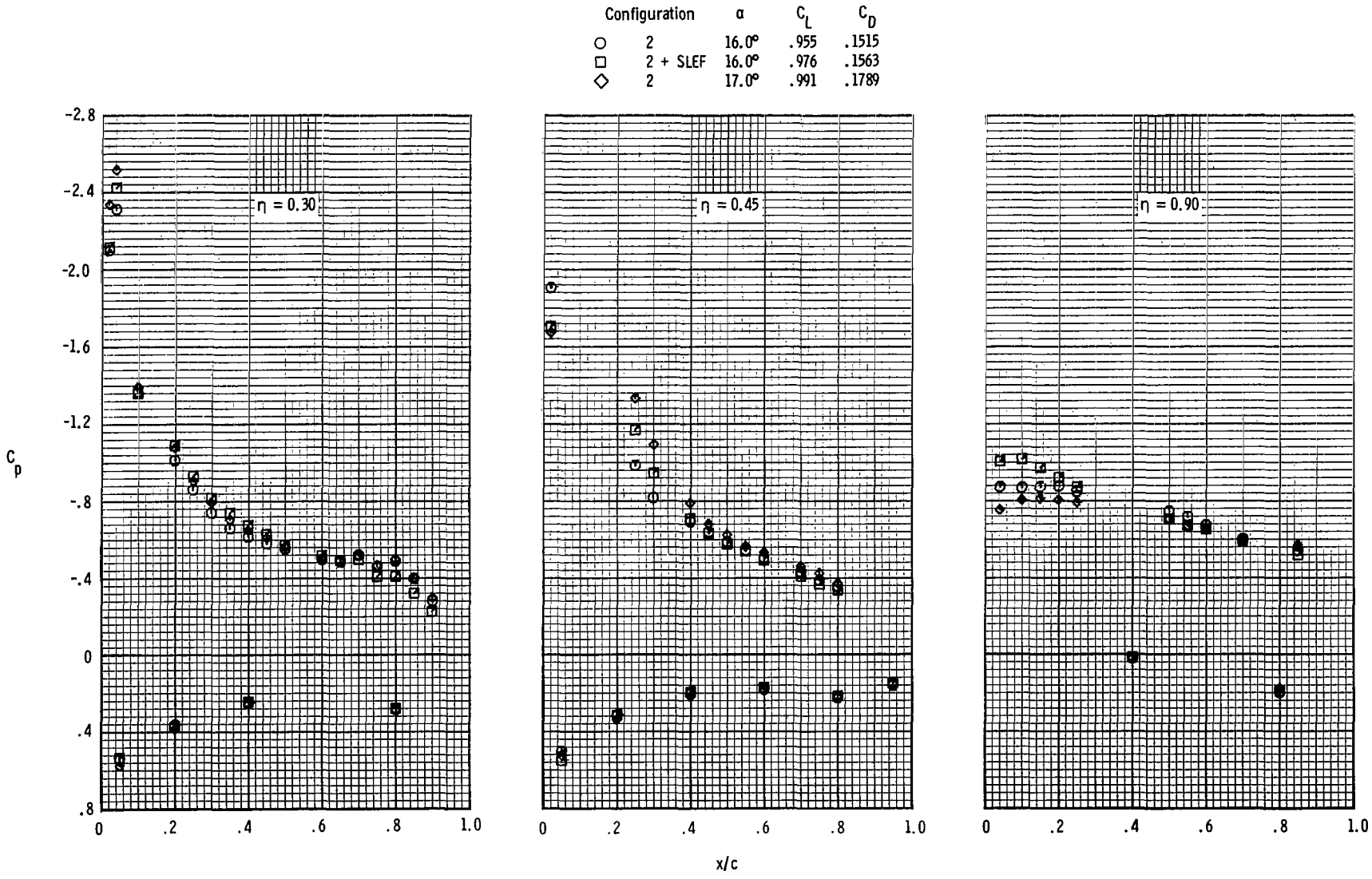

(a) M = 0.60; α ≈ 16°.

Figure 11.- Effect of wing sharp leading-edge flaps on wing upper- and lower-surface pressure coefficients.

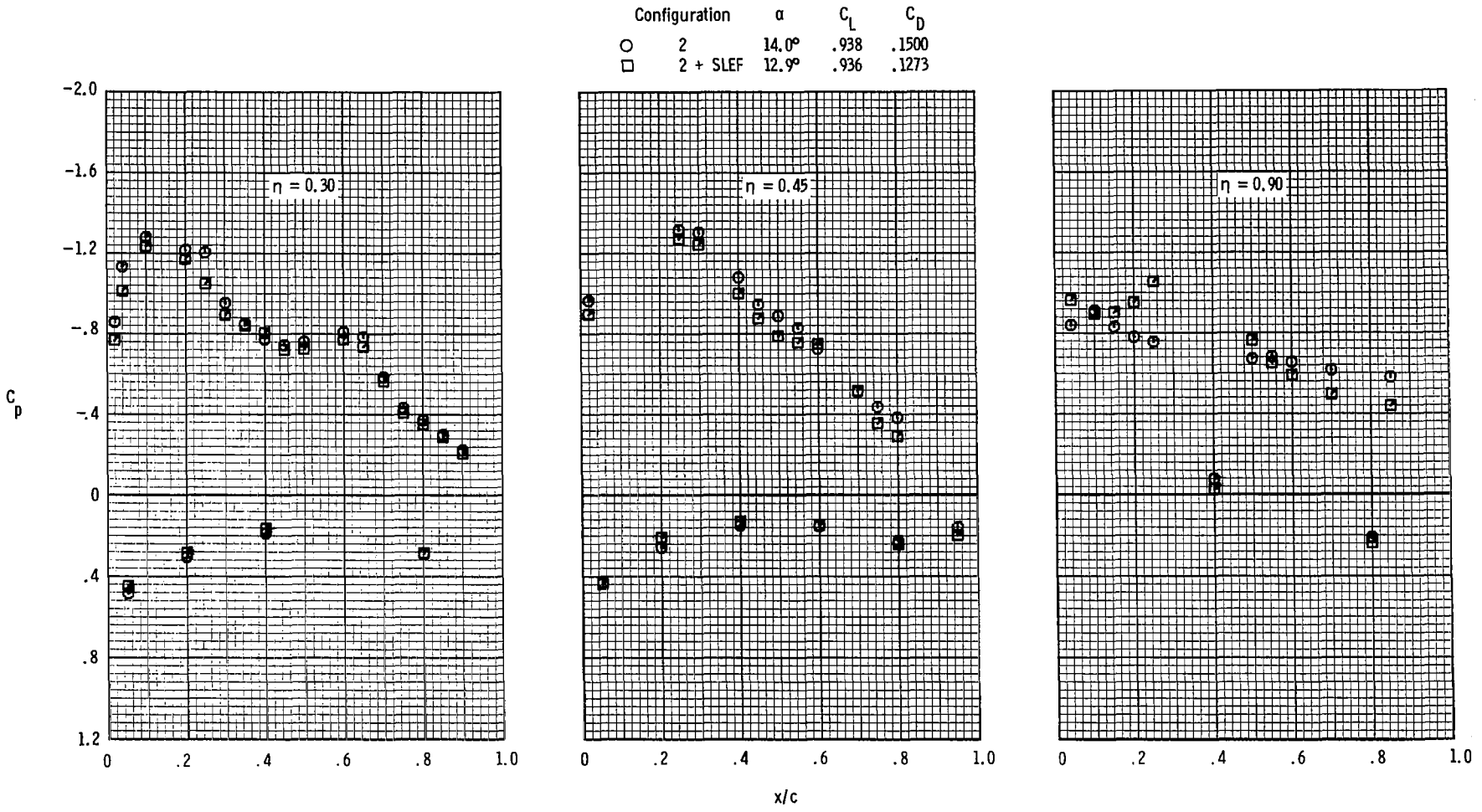

(b) M = 0.85; $\alpha \approx 13°$.

Figure 11.- Continued.

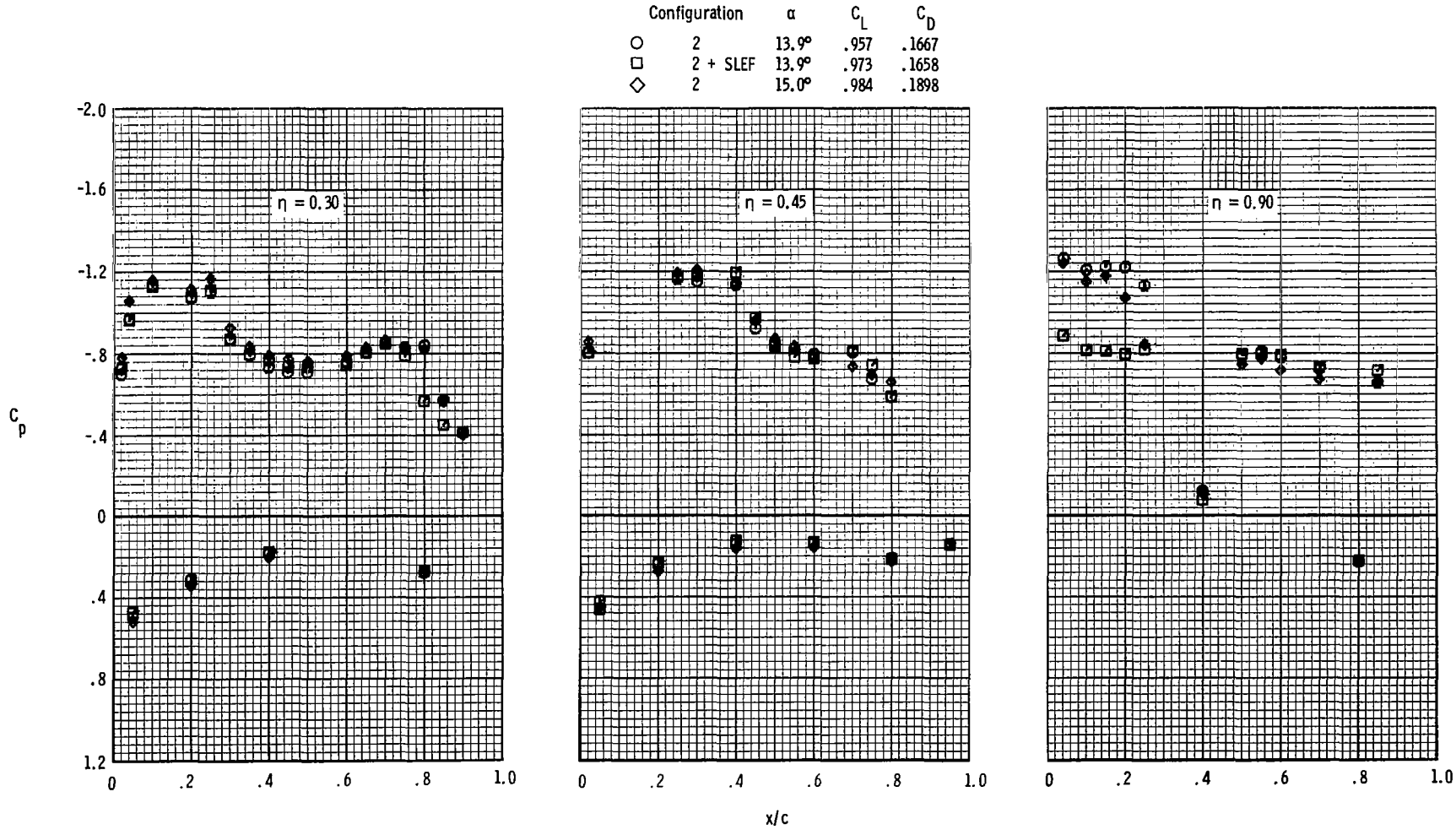

(c) M = 0.90; $\alpha \approx 14°$.

Figure 11.- Continued.

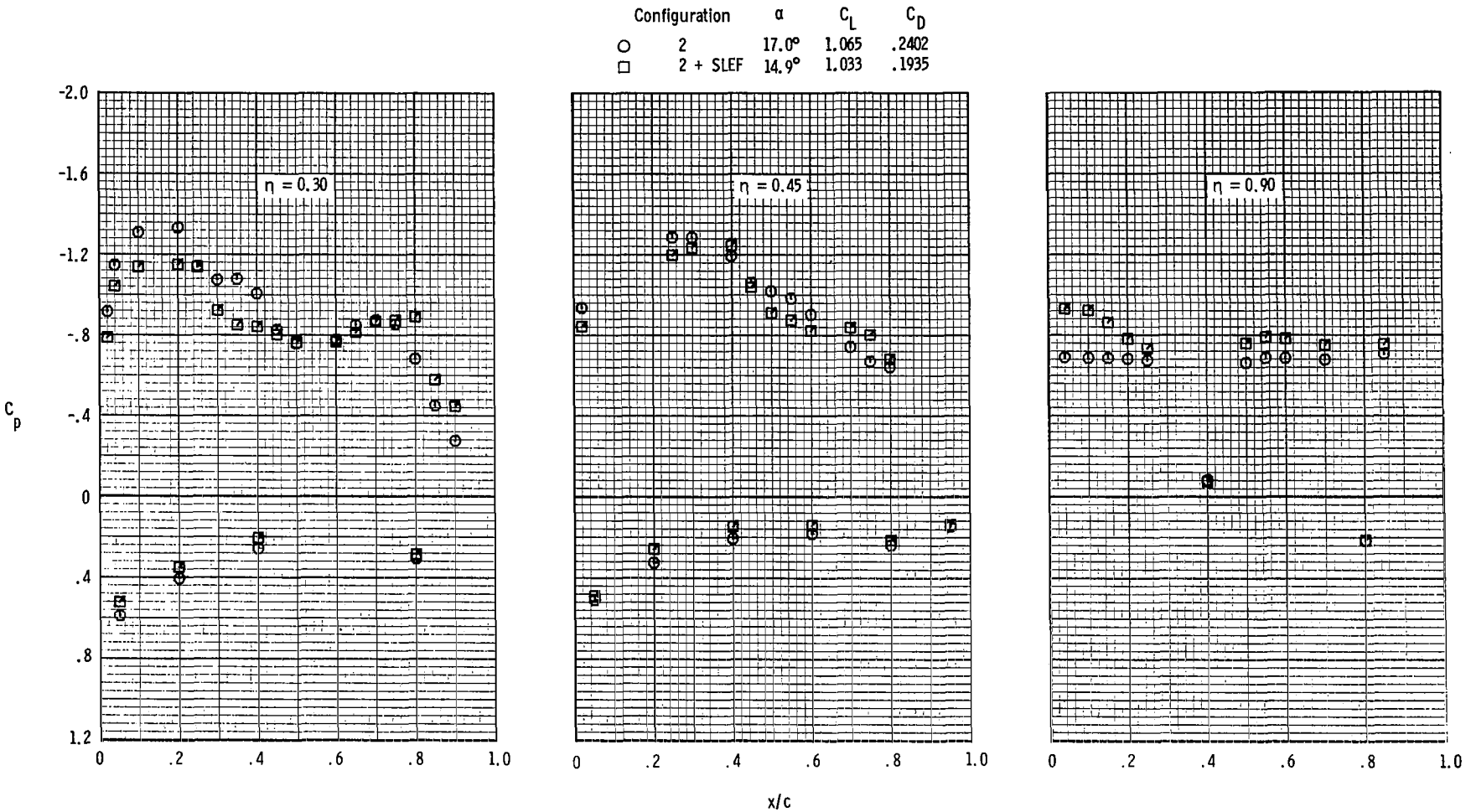

(d) M = 0.90; $\alpha \approx 15°$.

Figure 11.- Concluded.

1. Report No.	2. Government Accession No.	3. Recipient's Catalog No.
NASA TM-84513		

4. Title and Subtitle	5. Report Date
SUPERCRITICAL MANEUVERING FIGHTER CONFIGURATION - WIND-TUNNEL INVESTIGATION AT MACH NUMBERS OF 0.60 to 0.95	September 1982
	6. Performing Organization Code 505-31-13-02
7. Author(s) Michael J. Mann, Charles E. Mercer, and Richard L. Campbell	8. Performing Organization Report No. L-15399
	10. Work Unit No.
9. Performing Organization Name and Address NASA Langley Research Center Hampton, VA 23665	11. Contract or Grant No.
	13. Type of Report and Period Covered Technical Memorandum
12. Sponsoring Agency Name and Address National Aeronautics and Space Administration Washington, DC 20546	14. Sponsoring Agency Code
15. Supplementary Notes	

16. Abstract

A wind-tunnel investigation has been conducted to study the application of supercritical technology to highly maneuverable combat aircraft. The configuration studied has a leading-edge sweep of 45° and an aspect ratio of 3.28. Two supercritical-wing shapes were tested at Mach numbers from 0.60 to 0.95 with angles of attack from -2° to 17°. One supercritical wing was designed to achieve a high level of transonic maneuver performance at a Mach number of 0.90; however, excessive flow separation developed on this wing at a Mach number of 0.85. A second supercritical wing was tested which had significantly reduced flow separation and improved drag characteristics at a Mach number of 0.85 and maintained the performance of the original wing at the higher Mach numbers. Leading-edge vortex generators did not improve the performance of the second wing; however, a sharp leading-edge flap produced sizable drag reductions at Mach numbers from 0.60 to 0.90.

17. Key Words (Suggested by Author(s))	18. Distribution Statement
Transonic aerodynamics Supercritical airfoil application Fighter aircraft Maneuvering aerodynamics Transonic wing design	Unclassified - Unlimited Subject Category 02

19. Security Classif. (of this report)	20. Security Classif. (of this page)	21. No. of Pages	22. Price
Unclassified	Unclassified	67	A04

For sale by the National Technical Information Service, Springfield, Virginia 22161

NASA-Langley, 1982

8 1 1U,A, 820816 S00903DS
DEPT OF THE AIR FORCE
AF WEAPONS LABORATORY
ATTN: TECHNICAL LIBRARY (SUL)
KIRTLAND AFB NM 87117